Susanne Dyrbøl

Heat transfer in Rockwool modelling and method of measurement

Part I:

The effect of natural convection on heat transfer in fibrous materials

DTU

Heat transfer in Rockwool modelling and method of measurement

Part I: The effect of natural convection on heat transfer in fibrous materials

Ph.D. – thesis, May 1998 by Susanne Dyrbøl
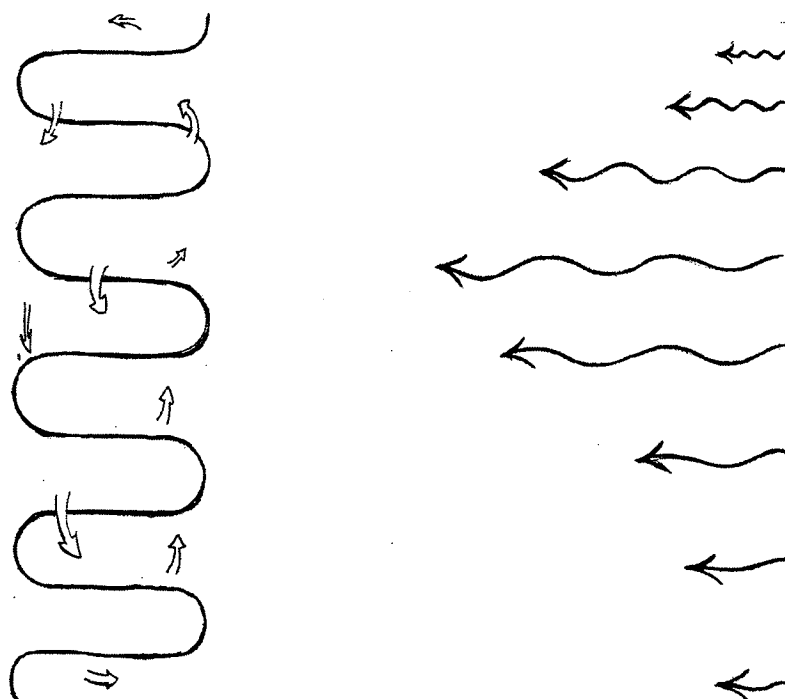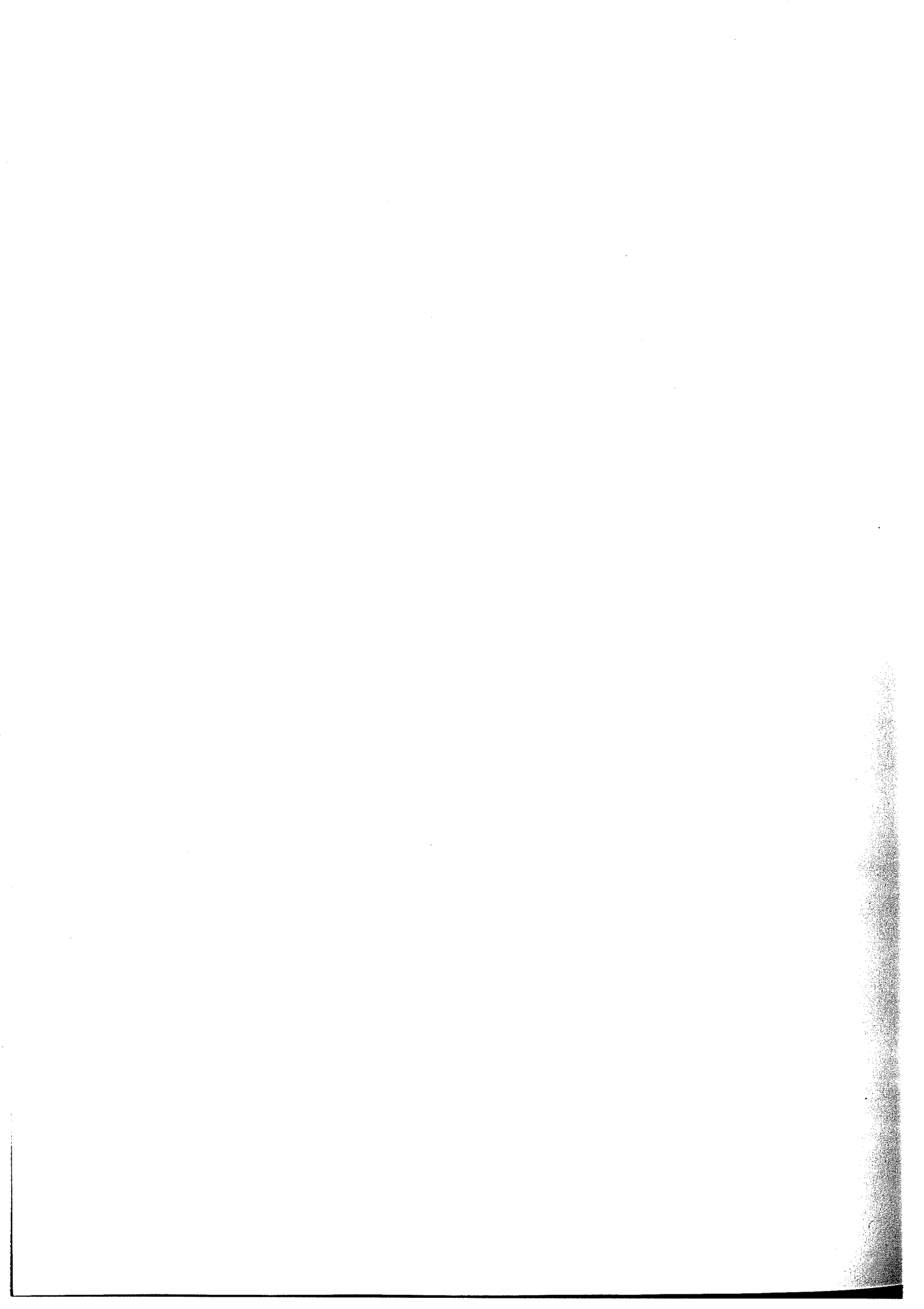
Preface

The Danish Academy of Technical Science, together with Rockwool International A/S and Rockwool A/S, have financed this project, the aim being to support research in the field of building physics in Denmark.

The work was carried out at the Department of Buildings and Energy at the Technical University of Denmark under the supervision of Professor Svend Svendsen and Professor Arne Elmroth from Lund Technical University to whom I owe a great debt of thanks for sharing their views and for helping me during the project.

The analysis of radiative heat transfer models has been carried out in collaboration with Associate Professor Flemming Andersen, Aalborg University. His great engagement and support have been invaluable throughout the entire project.

Special thanks are due to Professor Carl-Erik Hagentoft for sharing his computer code for calculating convection in porous media and for valuable discussions during the project, and to Professor Timothy W. Tong for sharing his computer code for calculating the radiative efficiencies of fibres.

The method of estimating the fibre orientation in fibrous materials has been developed in collaboration with M.Sc. Torben Mandrup Jacobsen, Rockwool International A/S, and with assistance from the Dept. of Mathematical Modelling, Technical University of Denmark.

I extend my sincere gratitude to the many people who have been involved in the project in various ways. Especially to my supervisors Section Leader Erik Rasmussen and Senior Engineer Helge Høyer at Rockwool International A/S, for many valuable discussions, to the laboratory staff at both the University and at Rockwool who provided help with the measurements, to my colleague Jørgen Schultz for assistance with data recording and for many valuable hours and discussions together with Lise Boye-Hansen, Kirsten Engelund Thomsen and Finn Kristiansen over the past three years, to Gitte Nellemose for making the drawings in the report and to Solvej Allen, Gyda Metz and Maj Britt Højgaard for linguistic help.

Copenhagen, May 1998

Susanne Dyrbøl

Part I   Effect of natural convection on heat transfer in fibrous materials

Contents

Summary

Preconditions

Fibrous materials are some of the most widely used materials for thermal insulation. In this project the focus of interest has been on fibrous materials for building application. Interest in improving the thermal properties of insulation materials is increasing as legislation is being tightened to reduce the overall energy consumption. A knowledge of the individual heat transfer mechanisms – whereby heat is transferred within a particular material is an essential tool to improve continuously the thermal properties of the material.

Heat is transferred in fibrous materials by four different transfer mechanisms: conduction through air, conduction through fibres, thermal radiation and convection. In a particular temperature range the conduction through air can be regarded as a constant, and conduction through fibres is an insignificant part of the total heat transfer. Radiation, however, constitutes 25-40% of the total heat transfer in light fibrous materials. In Denmark and a number of other countries convection in fibrous materials is considered as non-existent when calculating heat transmission as well as when designing building structures.

Two heat transfer mechanisms have been the focus of the current project: radiation heat transfer and convection.

The radiation analysis serves to develop a model that can be used in further work to gain a wider knowledge of the way in which the morphology of the fibrous material, i.e. fibre diameter distribution, fibre orientation distribution etc., influences the radiation heat transfer under different conditions.

The convection investigation serves to examine whether considering convection as non-existent is a fair assumption to use in present and future building structures. The assumption applied in practically is that convection makes a notable difference only in very thick insulation, at external temperatures below -20°C, and at very low densities. For large thickness dimensions the resulting heat transfer through the fibrous material will be relatively small, which means that a relatively small increase in heat loss by convection may counterbalance part of the savings achieved by increasing the thickness.

Heat radiation analysis – method - delimitation

A literature study has been carried out, primarily in regard to the theoretical modelling of radiation heat transfer in fibrous materials. This study has led to the overall conclusion that there are two important aspects within thermal radiation.

- One aspect is the radiation heat transfer itself, in which the mathematical model describing the radiation heat transfer in fibrous materials cannot be solved analytically. In the literature there are several different approximation methods for solving the radiative transport equation, the two-flux method being that most commonly used for fibrous materials, due to its simplicity. It has not been possible to assess the significance of the simplification for the calculated radiation heat transfer within the temperature range relevant to building insulation.

- The other aspect is the determination of the radiative properties of the fibrous material which are part of the radiation transport equation. In the literature these are used partly on a spectral basis, and partly as weighted values with a consequent high degree of simplification of the equation systems to be solved. Neither in this case has it been possible to find an assessment of the significance of using weighted values rather than spectral values when calculating radiation heat transfer in the specific temperature range. The radiative properties depend on the morphology of the fibrous material, the only parameter that cannot be determined experimentally being the fibre orientation distribution.

There are many aspects to the field "radiation transfer in fibrous materials", and it has therefore been necessary to limit the extent of the project. The delimitation has been based on the considerations identified from the literature survey and the shortness of time allocated to the project.

The radiation analysis has been delimited to include:

- a theoretical examination of the precision achieved when applying the two-flux model as an approximation for the radiative transport equation, compared with the spherical harmonics method, which has proved to give high precision in earlier cases of radiation problems with an analytical solution; in order to simplify the equation systems when comparing the two approximation methods, the Planck-weighted radiative properties have been used in the radiation transport equation;

- a theoretical examination of the precision achieved when applying the Planck-weighted radiative properties as opposed to a spectral solution when the two-flux model is used for approximating the radiation transport equation;

- developing a method that can be used to determine an estimate of the fibre orientation distribution.

The concepts of thermal radiation introduced in this project can well be applied to other thermal radiation problems arising when the radiative properties of the material depend on the wavelength of the radiation. In the present project the focus has been on fibrous materials for building insulation, which has determined the geometry and the conditions applied in the investigations, i.e. steady-state one-dimensional heat flow at a mean temperature of 10°C.

Heat radiation analysis – main results

A computer model for the heat transfer in fibrous materials has been developed. The model includes conduction in air and fibres, heat exchange between the two phases, and radiative heat transfer. As an approximation to the radiation transport equation, the two-flux model and the spherical harmonics method with an arbitrary high approximation order have been applied. In the computer code using the two-flux model a spectral solution of the radiation transport equation can be obtained.

Comparison of the two approximation methods shows that:

- the two-flux model underpredicts the radiative heat flux by approximately 15%, whereas the spherical harmonics method is more exact;

- considering only the computed total radiative heat flux, the same result is achieved with the simplest spherical harmonics method (P-1) as with a higher approximation order;

- the air and the fibre temperature are the same at the applied temperature level.

Comparison of the radiative heat flux obtained using the Planck-weighted radiative properties as opposed to the spectral solution led to the following conclusions:

- using the Planck-weighted properties underpredicts the radiative heat flux in the centre of the fibrous materials by approximately 15% compared to the spectral solution;

- it is not possible to determine a suitable weighting function for the radiation constants without first knowing the spectral solution.

The radiation properties in fibrous materials are determined by the morphology of the material; hitherto it has not been possible to measure the distribution of fibre orientation in the material. In connection with the project, a method for characterising the macro texture in fibrous materials has been developed. The dominant direction in the macro texture is measured by means of image analysis performed on partial images of the texture. By assuming that the macro texture reflects the fibre structure within the material, an estimate of the fibre orientation distribution can be approximated on the basis of the distribution of the dominant directions measured on the macro texture.

Convection investigation – method - delimitation

Convection may be divided into two fields: natural convection and forced convection. The overall delimitation for this project is natural convection.

The literature on performed theoretical and experimental research concerning natural convection has been studied. The literature survey can be summarised as follows.

- The mathematical models describing convection can be approximated using a series of dimensionless numbers. Depending on the geometry of the structure, a critical limit value of the Rayleigh number, Ra_{cr}, exists for the point at which the convection starts to influence the total heat transfer in the material. This critical value is theoretically and experimentally well defined for horizontal structures, whereas for vertical structures it is empirically determined but not clearly defined in the literature. For fibrous materials the permeability and the heat conductivity are the main parameters determining the effect of convection.

- Most examinations have been concentrated on determining the influence on the total heat transfer in the material. Introducing permeable borders or insulation error into the material increases the influence of convection, which becomes obvious at an earlier stage.

In order to be able to assess the convection conditions when the material is placed in a real structure it is necessary to know the convection conditions in the material itself. To facilitate the experimental work, a convection apparatus with a measuring field of 3·1 m² was designed, within which it is possible to measure a specimen thickness ranging from 0.1 m – 0.5 m. The boundary conditions are achieved immediately in the apparatus design. To support the interpretation of the measurements, the experimental work has been supplemented with numerical calculations.

The project was limited to an experimental search for the occurrence of natural convection in fibrous materials of different permeability under the following conditions:

- "perfectly" installed materials
- impermeable and isothermal boundaries
- measuring of fibrous materials with dimensions similar to those applied in building structures.

The effect of building physics strain in connection with convection, such as comfort and moisture transfer, has not been examined in the project.

Convection investigation – main results

The contribution of natural convection to the total heat transfer has been experimentally examined for two fibrous materials of different permeability and heat conductivity. The measurements performed have been supported by numerical calculations.

Both the measurements and the concurrent computations show a clear convection-induced redistribution of the heat flow in the material in the form of an increased heat flow primarily through the lower part of the vertical structure, and a decreased heat flow primarily through the upper part.

- The redistribution of the convection-induced heat flow is distinct, even at a material thickness as low as 0.2 m and at a temperature gradient of 20°C across the material.

- In the low permeable material the redistribution of the heat flow has no influence on the total heat flow through the material.

- In the highly permeable material the convection caused an increase in the total heat flow through the material.

Establishing that convection occurs even in "perfectly" installed materials with low permeability, impermeable boundaries and at small temperature differences means that the assumption that convection is non-existent, which has been the basis of the common practice, is invalid even under the most ideal conditions.

The measuring principle of the convection apparatus in which a three-dimensional guard system is used was found suitable for measuring one-dimensional heat flows at thick specimen dimensions. The measuring properties of the convection apparatus were verified on an impermeable material at a thickness of 0.5 m, in which good agreement with laboratory measurements on 0.1 m thick samples was found.

When performance-testing the apparatus, problems were found in a few of the guard sections. The chosen solution to this problem proved to be less optimal during the measuring. How this problem may have influenced the measurements is analysed and discussed in the report.

Resumé

Forudsætninger

Fibermaterialer hører til blandt de dominerende materialer indenfor termisk isolering. I dette projekt er fokuseret på fibermaterialer til bygningsisolering, hvor interessen for at forbedre materialernes termiske egenskaber hele tiden øges i takt med, at lovgivningen skærpes for at reducere det totale energiforbrug. Her er kendskabet til de enkelte transportmekanismer, hvorved varme transporteres i materialet, et væsentligt og nødvendigt værktøj for fortsat at kunne forbedre materialets termiske egenskaber.

Varmetransporten i fibermaterialer foregår ved fire forskellige transportmekanismer: Ledning i luft, ledning i fibre, varmestråling samt konvektion. Ledning i luften kan indenfor det aktuelle temperaturområde betragtes som værende af en konstant størrelse, og ledning i fibrene udgør en forsvindende lille del af den samlede varmetransport. Varmestrålingen udgør derimod mellem 25 - 40% af den samlede varmetransport ved lette fibermaterialer. I Danmark og en lang række andre lande betragtes konvektion i fibermaterialer som et ikke-forekommende fænomen såvel i varmetabsberegninger som ved design af bygningskonstruktioner.

I det udførte projekt er der fokuseret på to af varmetransportmekanismerne: varmestråling og konvektion.

Varmestrålingsanalysen har som formål at udarbejde en model, der kan anvendes i det videre arbejde med at opnå et større kendskab til, hvordan fibermaterialets morfologi (fiber diameter fordeling, fiber orientering, etc.) påvirker strålingsvarmetransporten under forskellige betingelser.

Konvektionsundersøgelsen har til formål at undersøge eksperimentelt om den i praksis anvendte antagelse, at konvektion kun har nævneværdig betydning ved meget store isoleringstykkelser, udvendige temperaturer lavere end -20°C, samt ved meget lave densiteter, er en rimelig antagelse i forbindelse med nutidens og fremtidens byggeri. Ved store isoleringstykkelser vil den resulterende varmetransport gennem materialet være relativ lille, og derfor vil en relativ lille forøgelse i varmetabet på grund af konvektion kunne modsvare en del af den opnåede energibesparelse ved en forøget isoleringstykkelse.

Varmestrålingsanalyse - metodik – afgrænsning

Der er her udført et litteratur studie, primært indenfor teoretisk arbejde med at modellere strålingsvarmetransport i fibermaterialer. Studiet har ført til den overordnede konklusion, at der er to vigtige aspekter inden for termisk stråling i forbindelse med fibermaterialer.

- Det ene aspekt er selve strålingsvarmetransporten, hvor den matematiske model, der beskriver strålingsvarmetransporten i fibermaterialer, ikke kan løses analytisk men ved flere forskellige approksimative løsningsmetoder, hvor two-flux metoden på grund af sin enkelhed er den hyppigst anvendte approksimation ved fibermaterialer. Det har ikke været muligt, at finde en vurdering af hvad forenklingen betyder for den beregnede varmestråling indenfor det temperaturområde, der er aktuelt for bygningsisolering.

vi

- Det andet aspekt er bestemmelse af fibermaterialets strålingsegenskaber, der indgår i strålingstransportligningen. I litteraturen anvendes disse dels på spektral basis og dels som vægtede værdier med en deraf følgende stor forenklingsgrad af de ligningssystemer, der skal løses. Det har ikke været muligt at finde en vurdering af, hvilken betydning anvendelsen af vægtede værdier frem for spektrale værdier har for den beregnede varmestråling i det aktuelle temperaturområde og for fibermaterialets morfologi. Strålingsegenskaberne afhænger af fibermaterialets morfologi, hvor den eneste parameter, der ikke kan bestemmes eksperimentelt, er fiberorienteringen.

Der er mange aspekter indenfor emnet "varmestråling i fibermaterialer", og det har derfor været nødvendigt at afgrænse udstrækningen af opgaven. Den valgte afgrænsning er foretaget med udgangspunkt i problemstillingen fra litteraturstudiet samt den begrænsede projekttid.

Varmestrålingsanalysen er afgrænset til at omfatte:

- en teoretisk undersøgelse af den opnåede nøjagtighed ved at anvende two-flux modellen som approksimation til strålingstransportligningen sammenlignet med spherical harmonics metode der ved stålingsproblemer med en analytisk løsning tidligere har vist at give en høj præcision. For at simplificere ligningssystemerne ved sammenligningen af de to approksimationsmetoder er Planck-vægtede strålingskoefficienter anvendt ved sammenligningen

- en teoretisk undersøgelse af den opnåede nøjagtighed ved at anvende Planck-vægtede strålingskoefficienter i forhold til en spektral løsning. Two-flux modellen er her anvendt som approksimation til strålingstransportligningen

- udvikling af en metode, der kan anvendes til at estimere en fiber-orienteringsfordeling.

De udførte betragtninger i projektet vedrørende varmestråling kan umiddelbart overføres på mange andre termiske strålingsproblemer, hvor materialets strålingsegenskaber afhænger af strålingens bølgelængde. I det udførte projekt er der fokuseret på fibermaterialer til bygningsisolering, hvilket har bestemt geometrien og forholdene, der er anvendt i de udførte undersøgelser; en-dimesional stationær varmestrøm ved en middeltemperatur på 10°C.

Varmestrålingsanalyse - hovedresultater

Der er udviklet en computermodel til beregning af varmetransporten i fibermaterialer. Modellen inkluderer ledning i luft og fibre, varmeoverføring mellem luft og fibre, samt termisk strålingstransport. Som approksimation til strålingstransportligningen er anvendt two-flux modellen og spherical harmonics metoden med en vilkårlig høj approksimationsorden. I computermodellen, hvor two-flux modellen anvendes, kan der bestemmes en spektral løsning af strålingstransportligningen.

Den udførte sammenligning af de to approksimationsmetoder viser at:

• Two-flux modellen underbestemmer strålingseffekten med ca. 15% sammenlignet med den mere præcise spherical harmonics metode

• betragtes kun den beregnede resulterende strålingseffekt, opnås samme resultat med den mest simple spherical harmonics metode (P-1) som ved anvendelse af en højere approksimationsorden

• luft og fibre har samme temperatur ved det anvendte temperaturniveau.

Sammenligningen af strålingseffekten beregnet med Planck-vægtede strålingskonstanter i forhold til den spektrale løsning førte til følgende konklusioner:

• anvendelsen af Planck-vægtede strålingskonstanter giver en strålingseffekt, der er ca. 15% lavere i forhold til den spektrale løsning i fiber materialer

• det er ikke muligt at bestemme en passende vægtningsfunktion for strålingskonstanterne uden først at kende den spektrale løsning.

Strålingskonstanterne i fibermaterialer bestemmes af materialets morfologi, hvor vi hidtil ikke har været i stand til at måle fordelingen af fiberorienteringer i materialet. Der er i forbindelse med projektet udviklet en metode til karakterisering af makrostrukturen i fibermaterialer. Den foretrukne retning i makrostrukturen måles ved hjælp af billedanalyse udført på delbilleder af strukturen. Ved at antage, at makrostrukturen afspejler materialets fiberstruktur, kan et estimat for fiberorienteringsfordelingen approksimeres med fordelingen af de fremtrædende retninger i makrostrukturen.

Konvektionsundersøgelse - metodik - afgrænsning

Konvektion inddeles i to områder: Naturlig konvektion og tvungen konvektion. Dette projekt er overordnet afgrænset til kun at omfatte naturlig konvektion.

Der er udført et litteraturstudie over udført teoretisk og eksperimentelt arbejde indenfor naturlig konvektion. Litteraturstudiet kan summarisk sammenfattes i nedenstående.

• De matematiske modeller, der beskriver konvektion, kan approksimeres med en række dimensionsløse tal. Afhængig af konstruktionens geometri eksisterer der en kritisk grænseværdi for Rayleigh tallet Ra_{cr}, for hvornår konvektionen påvirker varmetransporten i materialet. Den kritiske værdi er både teoretisk og eksperimentelt veldefineret for horisontale konstruktioner, hvorimod den for vertikale konstruktioner er empirisk fastlagt og ikke helt entydigt bestemt i litteraturen. For fibermaterialer er permeabiliteten og varmeledningsevnen de væsentligste parametre for effekten af konvektion.

• De fleste undersøgelser er koncentreret om at bestemme den resulterende effekt på varmetransporten i materialet. Ved at introducere permeable grænser eller isoleringsfejl i materialet øges effekten af konvektion og konvektionen bliver tydelig på et tidligere tidspunkt.

For at være i stand til at vurdere konvektionsforholdene når materialet anbringes i en virkelig konstruktion er det nødvendigt også at kende konvektionsforholdene i selve materialet. Til det eksperimentelle arbejde er opbygget et konvektionsapparat med et målefelt på 3·1 m², hvor det er muligt at måle materialetykkelser i intervallet 0.1 m - 0.5 m. Grænsebetingelserne er tilnærmet gennem apparatdesignet. Som hjælp til fortolkningen af de udførte målinger er det eksperimentelle arbejde understøttet af numeriske beregninger.

Projektet er afgrænset til eksperimentelt at undersøge forekomsten af naturlig konvektion i fibermaterialer med forskellig permeabilitet under følgende betingelser:

- "perfekt" installerede materialer
- impermeable og isoterme grænser
- måling på materialet i samme dimensioner som det forekommer indenfor bygningsisolering.

Effekten af bygningsfysiske belastninger i forbindelse med konvektion herunder komfort og fugt transport er ikke undersøgt.

Konvektionsundersøgelse - hovedresultater

Betydningen af naturlig konvektion for det totale varmetab er eksperimentalt undersøgt for to fibermaterialer med forskellig permeabilitet og varmeledningsevne. De udførte målinger er understøttet af numeriske beregninger.

Både målinger og de tilhørende beregninger viser en tydelig omfordeling af materialets varmetab på grund af konvektion i form af et forøget varmetab primært gennem den nederste del i den vertikale konstruktion og en reduktion af varmetabet primært gennem den øverste del i konstruktionen.

- Omfordelingen af materialets varmetab på grund af konvektion ses tydeligt, selv ved en materiale tykkelse på 0.2 m og helt ned til en temperaturgradient over materialet på 20°C.

- Ved materialet med lav permeabilitet påvirker omfordelingen af varmetabet i materialet ikke det totale varmetab.

- Ved materialet med høj permeabilitet medførte konvektionen at det totale varmetab gennem materialet blev forøget.

Konstateringen af, at der forekommer konvektion selv i "perfekt" installerede materialer med lav permeabilitet, impermeable grænser og ved selv små temperaturforskelle betyder, at forudsætningen for den hidtil anvendte praksis, hvor konvektion negligeres ikke er tilstede selv under de mest ideelle betingelser.

Måleprincippet i konvektionsapparatet, hvor der anvendes et tre-dimensionelt guardsystem, er fundet velegnet til måling af en-dimensionale varmestrømme ved store isoleringstykkelser. Konvektionsapparatets måleegenskaber er verificeret på et impermeabelt materiale, hvor der ved en prøvetykkelse på 0.5 m blev fundet fin overensstemmelse med laboratoriemålinger udført på prøvetykkelser af 0.1m.

ix

Ved apparattesten blev der konstateret problemer med enkelte guardsektioner. Den valgte løsning på problemet har i målingerne vist sig at kunne forbedres. Hvorledes de udførte målinger er påvirket af dette er analyseret og kommenteret i rapporten.

Nomenclature

Latin letters

a	thermal diffusivity [m^2/s]
a_w	non-dimensional wavenumber
c_p	specific heat capacity at constant pressure [$J/kg \cdot K$]
d	thickness [m]
Da	Darcy number [-]
g	gravitational acceleration: 9,81 m/s^2
Gr	Grashof number [-]
h	height of vertical space [m]
K	permeability of porous medium [m^2]
L	non-dimensional width/depth ratio of a convection cell [-]
Nu	Nusselt number [-]
$\dot{m}$	mass flow rate [$kg/m^2 \cdot s$]
p	pressure [Pa]
Pr	Prandtl number [-]
q	density of heat flow rate [W/m^2]
u	flow rate [m/s]
Ra	Rayleigh number [-]
T	temperature [K]
x, y, z	positions coordinates [m]

Greek letters

β	thermal expansions coefficient [K^{-1}]
Δ	difference
Φ	heat flow rate [W]
η	dynamic viscosity [$Pa \cdot s$]
∇	gradient
λ	thermal conductivity [$W/m \cdot K$]
λ_w	non-dimensional wavelength [-]
Λ	conductivity ratio (λ_f/λ_m) [-]
ρ	mass density [kg/m^3]
ν	kinematic viscosity [m^2/s]

Subscripts

a	air
cd	conduction
cr	critical
cv	convection
f	fluid
H	horizontal
m	porous material, modified
r	radiation
tot	total
V	vertical
0	reference
x, y, z	direction coordinates
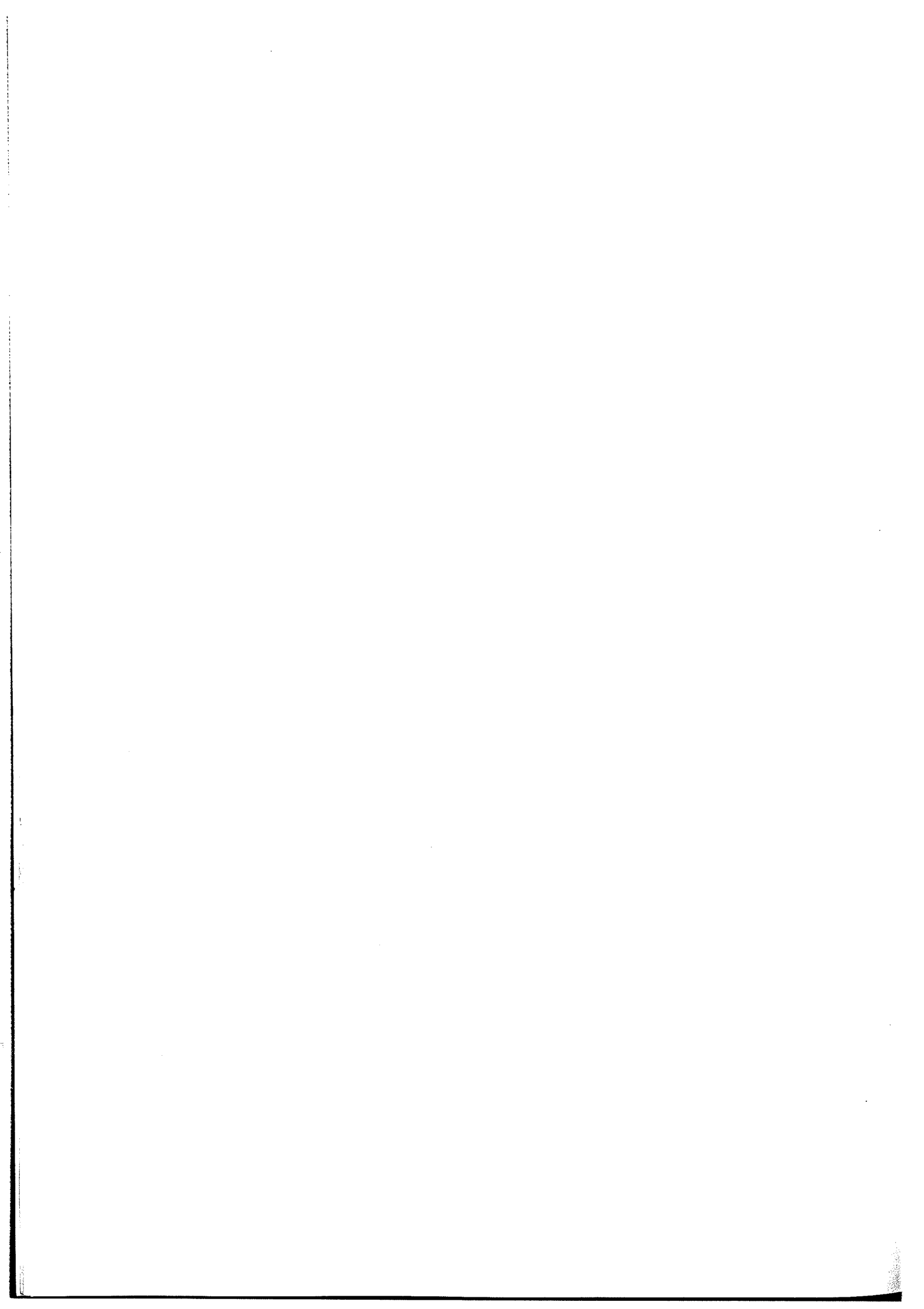
1.   Introduction

1.1   Background

Fibrous material is one of the most frequently used materials for building insulation. The demands for the thermal performance of both the building as a whole as well as the individual building elements are currently intensified in order to reduce the overall heat loss. This project has therefore focused on the thermal performance of fibrous materials. To be able to improve the performance of these materials in the long term, it is important to know the influence of various parameters on the thermal performance.

Fibrous materials are heterogeneous and consist of two phases; a gas phase (air) and a solid matrix (fibres). In such a material, heat is transmitted in three physically different ways: by conduction in fibres and gas, by radiation, and by convection.

In heat conduction, the energy is transmitted through lattice vibration in the solid and by random collision of molecules in the gas.

Transfer of energy by radiation takes place through electromagnetic waves between the fibres while the air does not interact with radiation.

Natural convection is caused by temperature-induced density differences in the gas phase which generate an airflow in the material.

Assuming little or no interaction between the different heat transfer mechanisms, the total heat transfer across the fibrous material is described by eq. (1.1):

$$\overline{q}_{tot} = \overline{q}_{cd} + \overline{q}_{r} + \overline{q}_{cv} \tag{1.1}$$

from which the thermal conductivity of the fibrous material is obtained by using Fourier's law:

$$\overline{q}_{tot} = -\lambda_{tot} \cdot \nabla T \tag{1.2}$$

In practice, the effect of convection is usually disregarded, and a semi-empirical relation, where the apparent thermal conductivity is a function of the density of the fibrous material, can be expressed according to Bomberg and Klarsfeld [1983], eq.(1.3):

$$\lambda_{tot} = A + B \cdot \rho + \frac{C}{\rho} \tag{1.3}$$

in which the constant A is the air conduction term λ_{air}, $B \cdot \rho$ is the conduction in the fibres λ_{fibre}, and C/ρ is the radiative term λ_{r}. The constants B and C must be determined by measurements, and are related to the specific material while the air conduction term is a constant at constant temperatures $\lambda_{air,10°C} \sim 0.0249$ W/m·K (Pitts and Sissom, 1997). The solid conduction term is insignificant in low-density materials $\lambda_{fibre} \sim 0.001$-$0.002$W/mK, whereas the radiation part represents approximately 0.008-0.020 W/m·K at room temperature when dealing with low-density materials, e.g. in the interval 10-40 kg/m^3. These models are able to predict the apparent thermal conductivity when only the density is changed but they are not

detailed enough in many other cases. For example, when the distribution of fibre diameters or fibre orientations in the fibrous material is changed, eq. (1.3) cannot be used to predict the change in thermal conductivity.

Figure 1.1 shows an example of the contribution by conduction in air, in fibres, and by radiation to the total thermal conductivity in a typical fibrous material for building application, the convection part being disregarded.
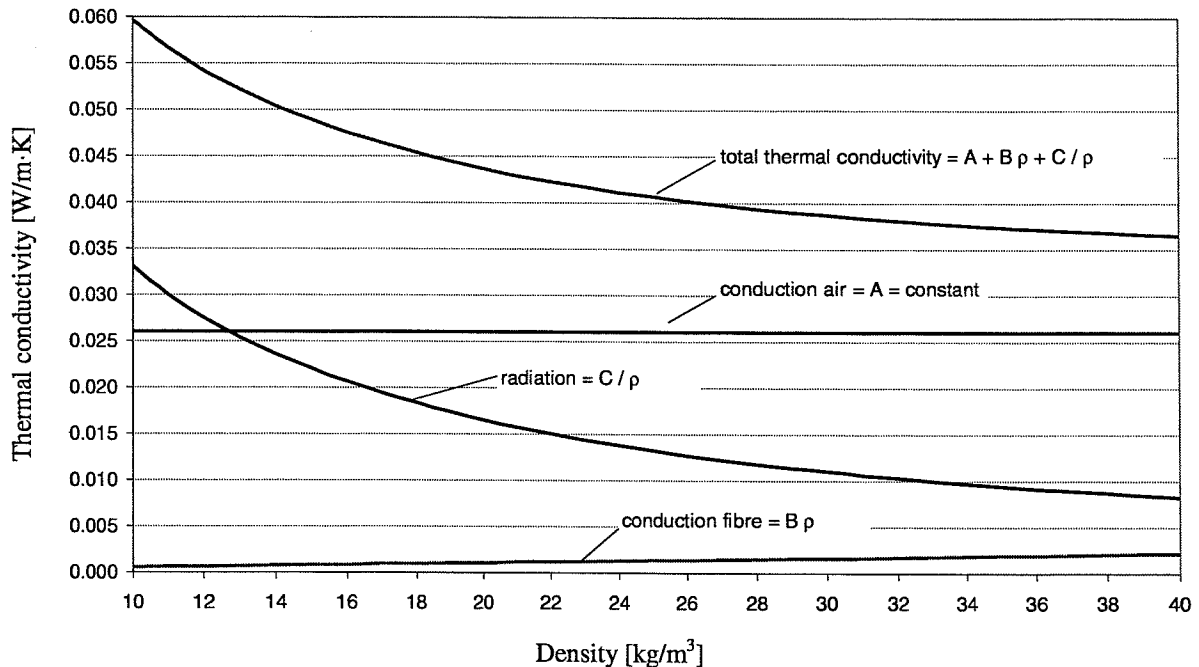
Figure 1.1: Contributions from conduction in air, conduction in fibres and radiation to the total thermal conductivity in a mineral fibre insulation for building application according to Kumaran [1996] in which the constants A = 0.02606 W/m·K, B = 5.48·10^{-5} W·m^2/K·kg and C = 0.331 W·kg/K·m^4 are used at a temperature of 10°C in eq. (1.3). However, minor variations in the constants will exist when comparing with the work of other authors.

The air conduction must be considered as a part of the total thermal conductivity which cannot be influenced unless the fibrous material is in vacuum or the air is replaced by an inert gas; the conduction due to the fibres is negligible when considering low-density materials. On this background, attention in the current project has been centred on two subjects:

• examining whether disregarding natural convection in fibrous materials is an acceptable assumption when dealing with thick dimensions (Part I)

• studying the modelling of radiative transfer in fibrous materials (Part II)

The present report (Part I) includes only the examination of natural convection in fibrous materials. Forced convection has not been treated in the project.

1.2 Purpose and limitations of the study in part I

In the main part of previous work considering the effect of natural convection, only a limited thickness has been studied, and primarily the increase in the overall heat transfer is regarded. From this perception natural convection is not expected to occur in fibrous materials, except at very low densities which signifies a very permeable material, and when big temperature differences exist across the material. In the last two decades, the different properties of the products have currently been optimised in order to fulfil various demands – which in some cases may has caused the permeability to increase, and the applied thickness of the fibrous materials has been increased in order to reduce the overall heat loss.

Therefore, the purpose of this work was to investigate experimentally:

- *whether convection takes place in fibrous materials*

- *and if convection occurs - how it affects the heat flow in the material*

when the fibrous materials have various properties, a thick dimension, and when various temperature differences are applied.

Generally, when measuring steady-state thermal resistance the limit in the specimen thickness is within 0.1-0.15 m, depending on the size of the measuring area, in order to achieve a one-dimensional heat flow. The experimental investigation in this project is carried out in a new designed convection apparatus in which it is possible to measure the effect of convection when the height of the specimen is 3 m, and the thickness within 0.1 – 0.5 m. When the specimen thickness increases the measured heat flow decreases and it becomes more difficult to measure the heat flow precisely.

Furthermore, the purpose was:

- *to evaluate the ability of the convection apparatus for measuring on big specimen thickness*

It is important to know how convection takes place in the fibrous material itself when containing inhomogenities and joints, in order to be able to analyse the effect of convection when the materials are applied at real conditions. This project only concerns the convection in the fibrous materials.

Therefore, the following test conditions have been applied in the experimental investigation:

- "perfectly" installed material (i.e. without known imperfections in the material)
- impermeable and isothermal boundaries
- both horizontal and vertical structures are measured.

1.3 Structure of the thesis

The thesis consists of two separate reports which treats the subjects:

- Part I: "Effect of natural convection on heat transfer in fibrous material"
- Part II: "Modelling radiative heat transfer in fibrous material"

The two reports can be read independently, and only the structure of part I will be presented in the following. The structure of part II is described in part II.

1.3.1 Structure of part I

Chapter 2 contains a review of previous theoretical and experimental results concerning heat transfer by natural convection. The literature survey presents the basic equations theoretically describing the problem natural convection in fibrous materials with impermeable boundaries, and presents the onset criteria for natural convection when the space is either horizontal or vertical.

Chapter 3 describes the computer calculations performed on a model similar to the convection apparatus. From the computer calculations an impression is obtained of the natural convection effect which should be detected in the measurements, if the specimen complies with the assumption made; directionally homogeneous properties, and perfectly installed in the apparatus. A brief description is given of the computer program applied. The chapter ends with a brief summary.

Chapter 4 describes the convection apparatus applied to detect the effect of natural convection in the specimens. A brief description is presented of the performance test which has been completed before the measurements started. An estimate of the maximum error when performing absolute measurements in the apparatus is given in a separate appendix.

In chapter 5 the test specimens and performed measurements are described. The results of the experimental investigations are presented and commented in relation to error detected in the apparatus, and to the computer calculations presented in chapter 3. The chapter ends with a brief summary.

Chapter 6 contains the conclusion, which gives a brief summary of the experimental work and recommendations for further work.

The summary of the reports, parts I and part II, is placed as the first part in both reports.

The literature to which references have been made in this report is described in the bibliography.

To the extent possible, symbols according to ISO have been used. Any other symbols are explained in the text. SI units are used throughout the entire thesis.

2. Studies of literature

2.1 Introduction

The following section outlines the theoretical relationship describing heat transfer by combined fluid conduction/convection through an air-permeable insulation. The equations, which describe the heat transfer in porous media with natural convection (the porous-medium analog of the Rayleigh-Bérnard problem) were first examined by Horton and Rogers [1945] and independently by Lapwood [1948]. More recent work, after 1967, improved the equations, and comparisons of theoretical calculations with experimental work proved acceptable for the last one obtained (Fournier and Klarsfeld, 1974). The physical problem of a fluid space (the Rayleigh-Bérnard problem) can be found in many textbooks and is treated in connection with convection in porous media by several authors, e.g. Bankvall [1972] and Serkitjis [1995]. This problem will not be discussed in detail here.

2.2 Theoretical description - Classic Darcy Approximation

The basic equations describing natural convection in a porous layer are presented in eq. (2.1-2.3). The equations describe the conservation of mass, momentum equilibrium, and conservation of energy in the porous layer. The Classic Darcy approximation only considers the porous layer in which the boundary conditions are assumed to be known (impermeable and isothermal). In cases where an air space is in contact with the porous layer, the Darcy-Brinkmann model should be considered.

The basic equations are derived from the study of a unit volume and describe the conditions in the general case of an *isotropic* material based on the following assumptions:

- the flow is steady and within the laminar Darcy region
- the fluid is incompressible
- all fluid properties are assumed to be constant, except the fluid density the temperature dependency of which causes the convection to take place
- the boundaries are impermeable and isothermal

The continuity equation:

Describes the conservation of mass for incompressible fluids i.e. the same amount of mass flows out as into the control volume.

$$\nabla \bar{u} = 0 \qquad (2.1)$$

The moment equation (force balance equation):

Describes that the acceleration of a unit volume of air carried along in the current equals all external forces affecting the volume.

$$-\frac{\eta_f}{K_m} \cdot \bar{u} - \nabla p + \rho_f \bar{g} = \rho_f \cdot \bar{u} \cdot \nabla \bar{u} \qquad (2.2)$$

in which

$$\rho_f \cdot \overline{u} \cdot \nabla \overline{u}$$

describes the acceleration of the unit volume of fluid due to the total force acting on it.

$$\frac{\eta_f}{K_m} \cdot \overline{u}$$

describes the resistance of the porous material against air movements

$$\nabla p$$

describes the driving force due to pressure differences and

$$\rho_f \cdot \overline{g}$$

describes the gravitation acting on the fluid.

The energy equation:

Describes the change in energy content at steady-state conditions in a unit volume i.e. in this case, the change in temperature equals the heat conducted into it by air flow.

$$\nabla \cdot (\lambda_m \cdot \nabla T) - (\rho c_p)_f \overline{u} \cdot \nabla T = 0 \tag{2.3}$$

In order for the thermal convection to occur, the air density must be a function of the temperature. The Boussinesq approximation eq. (2.4) is normally used to describe the temperature dependence of the air density:

$$\rho_f = \rho_0 (1 - \beta \cdot (T - T_0)) \tag{2.4}$$

in which T_0 is a reference temperature for which $\rho_f = \rho_0$. The Boussinesq approximation is valid provided that the changes in density remain small compared to ρ_0 throughout the flow region; and provided that the temperature variations are incapable of causing the various properties of the fluid to vary significantly from their mean values (Nield & Bejan, 1992).

Equations (2.1-2.4) are given in many textbooks on heat transfer together with their references e.g. in Nield and Bejan [1992] and Claesson and Hagentoft [1994].

2.2.1 Non-dimensional numbers in the general case

In the last three decades, a lot of experimental work has been done in the field of convective heat transfer resulting in empirically derived equations which contain non-dimensional numbers e.g. Wolf [1966], Klarsfeld [1970], Bankvall [1972], Fournier & Klarsfeld [1974], Langlais et al. [1990] and Silberstein et al. [1990]. The advantage is that a large number of

variables can be combined in a few non-dimensional numbers containing the properties of the fluid and the porous material, the height and thickness of the space, as well as the temperature difference throughout the material.

The following non-dimensional numbers are normally used to characterise the convection process in an air space. The corresponding non-dimensional numbers when the space is filled with a homogeneous material are analogical with the air space.

The Prandtl number
The Prandtl number Pr characterises the fluid and is the ratio of the kinematic viscosity v to the thermal diffusivity a_f of the fluid:

$$Pr = \frac{v}{a_f}; \qquad a_f = \frac{\lambda_f}{(\rho c_p)_f} \tag{2.5}$$

The kinematic and the dynamic viscosity of the fluid are related through the density:

$$v = \frac{\eta}{\rho_f} \tag{2.6}$$

In the case of air, Pr can be considered constant over a broad temperature interval with the value 0.73 (Serkitjis, 1995).

The Grashof number
The ratio between the thermal forces, caused by differences in density, and viscose forces in the fluid is expressed in the Grashof number. The Grashof number is used to define the flow field in natural convection, in which the temperature difference in the air initiates the flow, and is defined by:

$$Gr = \frac{g \cdot \beta \cdot d_f^3 \cdot \Delta T}{v^2} \tag{2.7}$$

d_f is the vertical height of the air space and is shown in figure 2.1 for a horizontal and a vertical air space.
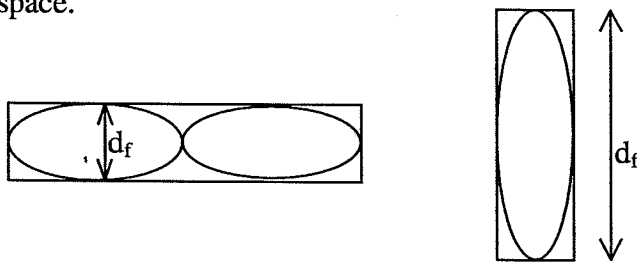
Figure 2.1: The vertical height d_f in the Grashof number in case of a horizontal and vertical space containing one or two convection cells.

The thermal expansion coefficient β of an ideal gas is given by:

$$\beta = \frac{1}{T} \tag{2.8}$$

in which T is the absolute temperature.

The Rayleigh number
The product of the Prandtl number and the Grashof number is called the Rayleigh number and expresses the ratio between released energy, due to difference in density, and energy used in conduction and friction:

$$Ra = Pr \cdot Gr = \frac{(\rho c_p)_f}{\lambda_f} \cdot \frac{g \cdot \beta \cdot d_f^3 \cdot \Delta T}{\nu}$$ (2.9)

The Nusselt number
The Nusselt number Nu is defined as the ratio between heat transfer with convection and heat transfer without convection.

$$Nu = \frac{\Phi_{\text{with convection}}}{\Phi_{\text{without convection}}}$$ (2.10)

If no convection occurs, Nu becomes "1.00"; otherwise the value of Nu will exceed unity.

The non-dimensional numbers, describing the air space, are modified to describe the convection in a homogeneous material. For this purpose, the Darcy number and the thermal conductivity ratio are introduced.

The Darcy number
The Darcy number Da is the ratio between the permeability and the square of the vertical height of the space.

$$Da = \frac{K_m}{d_m^2}$$ (2.11)

The thermal conductivity ratio
Is the ratio between the thermal conductivity of the fluid λ_f and the thermal conductivity of the porous material λ_m.

$$\Lambda = \frac{\lambda_f}{\lambda_m}$$ (2.12)

According to the definition of the air space eqs. (2.5 and 2.9), the modified Rayleigh number and Prandtl number describing natural convection in the homogeneous porous material are:

$$Ra_m = Ra \cdot Da \cdot \Lambda, \qquad Pr_m = Pr \cdot \Lambda$$ (2.13)

2.3   Horizontal space: Onset criteria for natural convection

In a horizontal space filled with a homogeneous porous material, in which the boundaries are impermeable, the Rayleigh number from eq. (2.13) becomes:

$$Ra_m = \frac{g \cdot \beta \cdot (\rho c_p)_f}{\nu} \cdot \frac{d_m \cdot K_m \cdot \Delta T}{\lambda_m} \qquad (2.14)$$

in which d_m is the vertical height of the permeable material and equals d_f defined in figure 2.1.

Nield [1968] studied the onset of convection in a homogeneous porous medium using a critical Rayleigh number and a corresponding critical wavenumber a_w to express when natural convection begins. The critical Rayleigh number and the corresponding critical wavenumber a_w are determined from a linear stability analysis of the steady state solution of the equations describing the problem eq. (2.1-2.3). In the general case of a horizontal porous layer heated from below with impermeable and isothermal boundaries, Ra_m and a_w, according to Nield and Bejan [1992], are connected through:

$$Ra_{m,j} = \frac{(j^2\pi^2 + a_w^2)^2}{a_w^2} \qquad j = 1,2,3....... \qquad (2.15)$$

the lowest value of $Ra_{m,j}$ is obtained when $j = 1$ and $a_w = \pi$ which means that the critical Rayleigh number $Ra_{m,cr}$ becomes $4\pi^2$, and the associated critical wavenumber $a_w = \pi$. In case of $Ra_m < 4\pi^2$, heat is transferred in a stable state by conduction and radiation. When Ra_m is above this limit, instability appears as convection in the form of a cellular motion with a horizontal wavenumber equal π. In this way, the linear stability theory predicts the size of the convection cells in a homogeneous material (Nield and Bejan, 1992). The wavenumber and the wavelength of the convection cells are related by $a_w = 2\pi/\lambda_w$. Figure 2.2 illustrates convection cells with the wavelength λ_w.
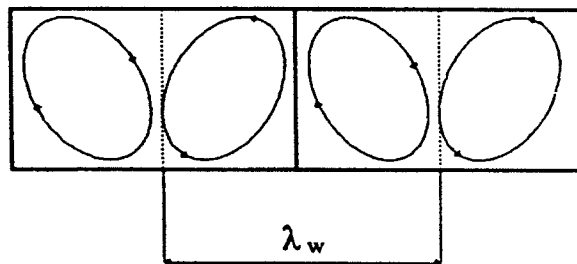
Figure 2.2:   Cross section in convection cells in which the shape is elliptical rolls of wavelength λ_w. Calculated in case a fluid is situated between two impermeable surfaces (reproduced from Serkitjis, 1995).

The onset criteria for convection is tabulated by Nield [1968] for all combinations of impermeable (closed) or permeable (open), and conducting or insulating conditions at the lower and upper horizontal boundaries, shown in table 2.1. The permeable boundary is equivalent to constant pressure whereas the conducting and insulating boundary equals constant temperature and constant heat flux, respectively.

Table 2.1: Value of the critical Rayleigh number $Ra_{m,cr}$ and associated critical wavenumber $a_{w,cr}$ for various boundary conditions according to Nield [1968].

Boundary conditions				$Ra_{m,cr}$	$a_{w,cr}$
of permeability		of conductivity			
lower	upper	lower	upper		
impermeable	impermeable	conducting	conducting	$4 \cdot \pi^2$	π
impermeable	impermeable	conducting	insulating	27,10	2,33
impermeable	impermeable	insulating	insulating	12	0
impermeable	permeable	conducting	conducting	27,10	2,33
impermeable	permeable	insulating	conducting	17,65	1,75
impermeable	permeable	conducting	insulating	π^2	$\pi/2$
impermeable	permeable	insulating	insulating	3	0
permeable	permeable	conducting	conducting	12	0
permeable	permeable	conducting	insulating	3	0
permeable	permeable	insulating	insulating	0	0

Experimental verification of $Ra_{m,cr}$ shows that a deviation from isothermal boundaries will initiate the convection when $Ra_m > 0$, but the convection will not be significant until $Ra_{m,cr}$ has been exceeded (Langlais et al. 1990).

2.3.1 Effects of anisotropy

Castinel and Combarnous [1975] obtained the onset criterion of convection in a porous layer with anisotropic permeability, whereas Epherre [1975] allowed both permeability and thermal conductivity to be anisotropic. The material in this section is based mainly on the review by McKibbin [1985, 1986] in which he discusses, how the part of fluid circulating in the space varies with the cell width, the anisotropy in permeability, and the thermal conductivity when different boundary conditions are applied. When the top is impermeable, the circulation of fluid will be total. In McKibbin [1986] the $Ra_{m,cr}$ and $a_{w,cr}$ concerning anisotropy are also given when the upper boundary is open, either with constant pressure and heat flux or with constant pressure and temperature. Only the case where the boundaries are impermeable and isothermal is described in this section.

A measure of the anisotropy of the porous material is introduced by:

$$\xi = \frac{K_H}{K_V} \quad \text{and} \quad \eta = \frac{\lambda_H}{\lambda_V} \tag{2.16}$$

in which ξ and η express the ratio between the horizontal and the vertical permeabilities and thermal conductivities, respectively. With impermeable, isothermal boundaries Epherre [1975] found the critical Rayleigh number for the onset of two-dimensional convection (rolls) of cell width/depth ratio L to be:

$$Ra_{m,cr} = \frac{\pi^2 (\xi + L^2)(\eta + L^2)}{\xi \cdot L^2} \tag{2.17}$$

As L varies, the minimum value of $Ra_{m,cr}$ is obtained when $L = (\xi \cdot \eta)^{1/4}$:

$$[Ra_{m,cr}; a_{w,cr}] = \left[\pi^2 \left(1 + \sqrt{\frac{\eta}{\xi}} \right)^2 ; \frac{\pi}{(\xi \cdot \eta)^{1/4}} \right]$$

(2.18)

For an isotropic material ($\xi = \eta = 1$) eq. (2.18) equals the conditions in table 2.1:

$$[Ra_{m,cr}; a_{w,cr}] = [4\pi^2; \pi]$$

(2.19)

Several experimental studies with different types of fibrous material have been carried out in order to verify the onset criteria for natural convection e.g. Fournier et al. [1974], Bankvall [1972] and Langlais et al. [1990]. In the main part of the investigations, the fibrous material has been considered a homogeneous material as far as the $Ra_{m,cr}$ is concerned. This seems to be an acceptable approach as the anisotropy ratio ξ/η is in the range of 1.3-1.8 depending on type and density of the fibrous material. Kvernvold and Tyvand [1979] found that for two-dimensional flow, the Nusselt number depends on the ratio ξ/η only as shown in figure 2.3.
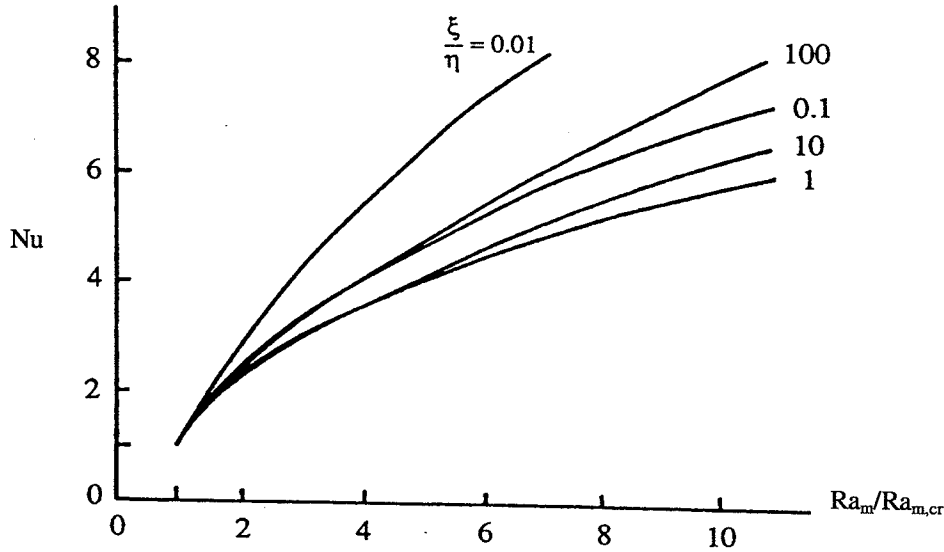
Figure 2.3: Nusselt number versus $Ra_m / Ra_{m,cr}$ for various anisotropy ratios ξ/η (reproduced from Nield and Bejan 1992 after Kvernvold and Tyvand 1979).

Figure 2.4 shows the onset of convection in a horizontal porous layer obtained by experimental and numerical results. The experimental results agree with the numerical results about the onset criteria for convection to take place.

11
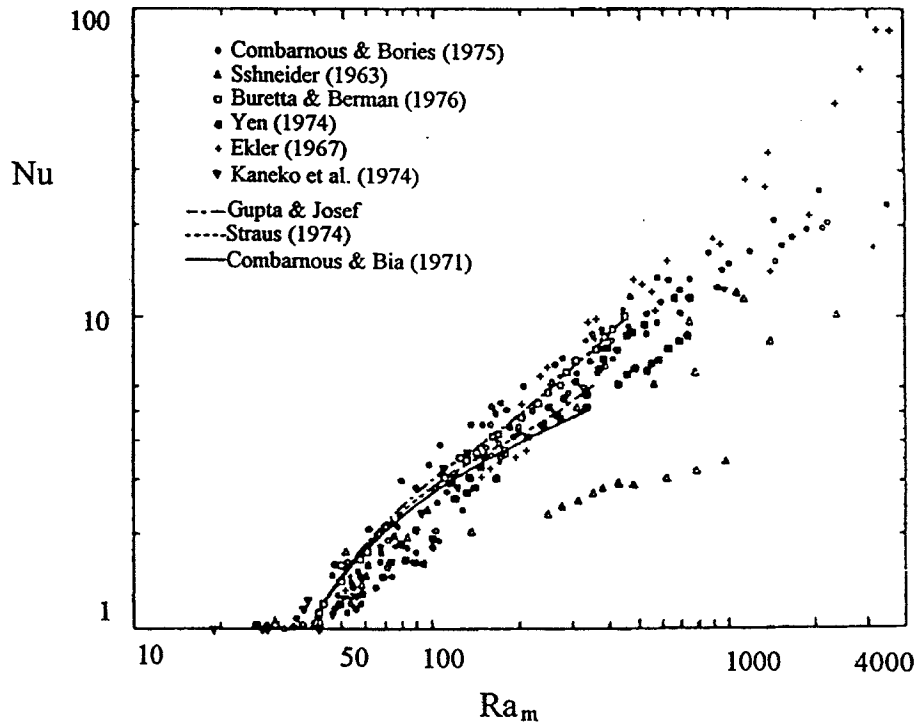
Figure 2.4: Onset criteria for convection in case of a horizontal porous layer. Comparison of experimental and numerical results (P.Cheng, 1978).

2.4 Vertical space: Onset criteria for natural convection

When a vertical space is filled with a homogeneous material and the boundaries are impermeable, the modified Rayleigh number is usually defined as:

$$Ra_m = \frac{g \cdot \beta \cdot (\rho c_p)_f}{\nu} \cdot \frac{h \cdot K_m \cdot \Delta T}{\lambda_m} \tag{2.20}$$

The geometry of the vertical permeable space is shown in figure 2.5.
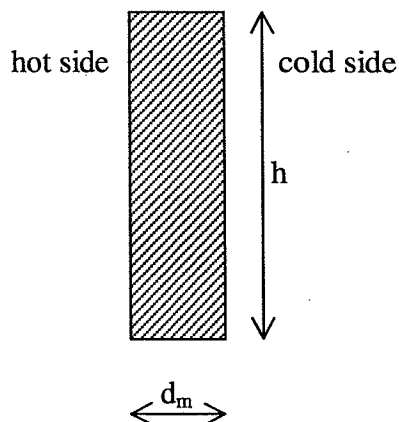
Figure 2.5: Geometry of vertical permeable space.

Bomberg and Klarsfeld [1983] suggest that the modified Rayleigh number is calculated on basis of eq. 2.21 when the heat conduction and permeability depends on the direction in the material.

$$Ra_m = \frac{g \cdot \beta \cdot (\rho c_p)_f}{\nu} \cdot \frac{4 \cdot K_{m,H} \cdot K_{m,V}}{(\sqrt{\lambda_{m,V} \cdot K_{m,H}} + \sqrt{\lambda_{m,H} \cdot K_{m,V}})^2} \cdot h \cdot \Delta T \qquad (2.21)$$

In the vertical space containing a permeable material, the situation is more complicated than in the horizontal space, as the onset of natural convection will be influenced by both the modified Rayleigh number Ra_m (or filtration Rayleigh number), the aspect ratio of the space h/d_m, and the boundary conditions. Bankvall [1977] emphasis that no critical Ra_m values exists in the vertical case. Which agrees with the work by Klarsfeld [1970], and Bomberg and Klarsfeld [1983] in which they emphasis that convective movement in a vertical structure grows gradually with the temperature difference.

Whereas Fornier and Klarsfeld [1974], Bhattacharyya [1980], and Silberstein et al. [1990] report the criterion for the onset of convection in a vertical structure with impermeable and isothermal boundaries to be:

$$Ra_{m,cr} > 4 \cdot \frac{h}{d_m} \qquad (2.22)$$

The Nusselt number for the vertical structure containing a permeable material can be expressed in the general form:

$$Nu = f(Ra_m, h/d_m, \text{boundary conditions}) \qquad (2.23)$$

Nield and Bejan [1992] propose the Nusselt number shown in eq. (2.24) in a porous layer heated from the side after convection has been initiated.

$$Nu = \frac{1}{\sqrt{3}} \cdot \frac{d_m}{h} \cdot \sqrt{Ra_m} \qquad (2.24)$$

Figure 2.6 shows a comparison between eq. (2.24) and experimental data obtained by different researchers.
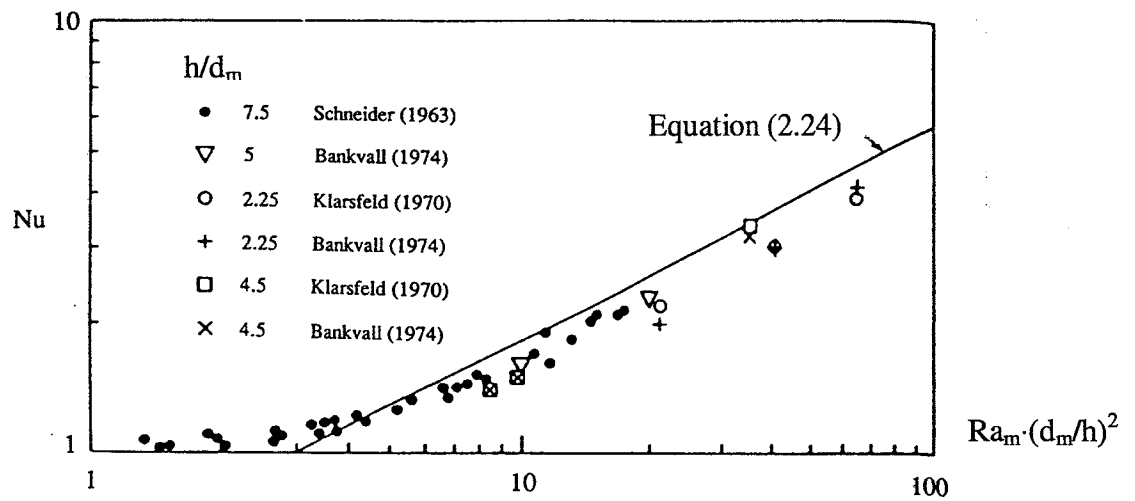
Figure 2.6: Comparison of Nusselt numbers from experimental results with the relation in eq. (2.24) in case of different aspect ratio h/d_m Bejan, [1984] (reproduced from Nield and Bejan, 1992).

3. Numerical calculation of convection by means of the computer program CHConP

The computer program CHConP (Convection Heat Conduction Program) is used to evaluate the effect of convection in fibrous material with directionally homogeneous properties in a vertical structure similar to the test equipment used in the experimental investigation. CHConP is developed by Professor C-E Hagentoft, Chalmers University of Technology, Gothenburg.

3.1 Description of the computer program CHConP

CHConP calculates the temperature distribution and heat flow from combined heat conduction and convection by solving the two-dimensional heat transfer equations shown in eq. (3.4) and (3.5) using the finite difference method FDM and an iterative solution method.

The input data needed to run CHConP are:

- the geometry of the structure
- the thermal conductivity and permeability of the materials in two directions
- the boundary conditions: temperature and thermal resistance, pressure and pressure resistance

The results from the simulations are presented as: heat flow Φ (W/m) through an arbitrary boundary, air flows in two directions at a given position in the porous material q_a (m³/m²·s), and as temperature distribution at an arbitrary level in the construction.

The equations used in CHConP to calculate the two-dimensional coupled convection and conduction in the porous material, in which the properties are anisotropic, are shown in eqs. (3.1-3.6).

The air flow rate vector $\mathbf{q_a} = (q_{ax}, q_{ay})$ (m³/m²·s) is determined from the force balance equation eq. (2.2) in which the Boussinesq approximation is used for the buoyancy forces:

$$q_{ax} = -\frac{K_x}{\eta} \cdot \frac{\partial p}{\partial x} \tag{3.1}$$

$$q_{ay} = -\frac{K_y}{\eta} \cdot \left(\frac{\partial p}{\partial y} + \rho_f \cdot \beta \cdot g(T - T_0) \right) \tag{3.2}$$

in which the y-coordinate is pointing downwards, and p (Pa) is the deviation in air pressure from the hydrostatic air pressure at temperature T_0. It is assumed that all the fluid properties are constant. Only the temperature dependence on the density in the buoyancy term causing the thermal convection is taken into account.

15

The continuity equation describes the conservation of mass. In order to achieve mass conservation the condition in eq. (3.3) must be fulfilled in each control volume.

$$\frac{\partial q_{ax}}{\partial x} + \frac{\partial q_{ay}}{\partial y} = 0 \tag{3.3}$$

The density of heat flow rate $q = (q_x, q_y)$ considering coupled conduction and convection inside the porous material, when steady-state conditions occur, is obtained from eqs. (3.4 - 3.5).

$$q_x = -\lambda_{tot,x} \frac{\partial T}{\partial x} + q_{ax} \cdot (\rho c_p)_f \cdot (T - T_o) \tag{3.4}$$

$$q_y = -\lambda_{tot,y} \frac{\partial T}{\partial y} + q_{ay} \cdot (\rho c_p)_f \cdot (T - T_o) \tag{3.5}$$

At steady-state conditions, the energy equation describes that the amount of energy flowing out of a unit volume equals the heat conducted into it. The energy balance must be maintained everywhere in the material:

$$\frac{\partial q_x}{\partial x} + \frac{\partial q_y}{\partial y} = 0 \tag{3.6}$$

As default the boundaries in CHConP are adiabatic. If the boundaries deviate from the default conditions, the surface temperature and the thermal resistance together with the pressure and pressure resistance must be specified.

For the general case, no exact solution to the above-mentioned equations is available, and a numerical technique must be applied. A description of the iterative solution method used in CHConP can be found in Hagentoft and Serkitjis [1995].

Fryklund [1995] compares simulated heat flows from CHConP with:

- measurements of attic heat flow from the Oak Ridge National Laboratory (ORNL)
- the theory of the onset of convection
- simulated heat flows from a computer program developed by ORNL.

In Fryklunds investigation, the input parameters in the computer simulations were gradually refined until good agreement was obtained between the calculated and the measured heat flow from ORNL. This was necessary because the information available from ORNL was not sufficient to make a complete computer model of the test conditions.

The simulations made with CHConP and the theory of the onset of convection proved to be in good agreement. When using the same aspect ratio in CHConP as in the computer program from ORNL (Wilkes et. al, 1991), they proved the same results.

Hagentoft and Serkitjis [1995] have further developed the computer code to work on a three-dimensional problem concerning a horizontal geometry (CONVBOX) in which all the

16

boundaries are considered air-tight, except for the horizontal top surface of the insulation. The three-dimensional model has been compared with measurements of convection in a horizontal structure filled with a homogeneous, porous material (cylindrical polystyrene pellets) with good accordance (Serkitjis, 1995).

3.2   Description of model

Figure 3.1 shows a sketch of the model applied in the numerical calculations. The geometry of the convection apparatus is used in the model. The height of the apparatus is 3 m, and the calculations were performed on a specimen thickness of 0.2 and 0.5 m i.e. the aspect ratio h/d_m of the vertical structure were 15 and 6, respectively. In the measurements, all the boundaries were impermeable. In the computer calculations, the two vertical boundaries of a height of 3 m were presumed to have a pressure resistance of $1 \cdot 10^{20}$ Pa·s/m^2; which equals a totally air-tight surface and a boundary pressure of $1 \cdot 10^{-20}$ Pa. The two remaining boundaries are adiabatic and impermeable. The heat conductivity and air permeability used in the calculations are shown in table 3.1 together with the family of fibrous materials, which match the thermophysical properties.

Table 3.1:   Input parameters.

Material	Heat conductivity [mW/m·K]		Permeability [·10^{-10} m^2]		Thermal surface resistance [m^2·K/W]	
	λ_x ($\perp$)	λ_y (‖)	K_x ($\perp$)	K_y (‖)	cold	hot
Stone wool (1), $\rho = 30$ kg/m^3	35.7	38.7	17.9	28.7	0.1	0.006
Fibre glass (2), $\rho = 17$ kg/m^3	35.9	39.5	23.6	45.4	0.1	0.006
Fibre glass (3)*, $\rho = 8.6$ kg/m^3	47.0	51.7	107.8	198.0	0.1	0.006

*   This fibre glass contains loose fibres without any binder and does not have a well defined shape which makes it difficult to measure the permeability.

The thermal surface resistance on the hot side equals the resistance of the glass plates which serve as the heating unit in the convection apparatus, and the resistance on the cold side equals the resistance of the plywood cover which forms the impermeable surface against the cold box. The design of the convection apparatus is described more detailed in chapter 4. In the apparatus, the heat flow through the specimen is measured individually in twelve different sections each with a height of 0.25 m. In the model, two materials A and B are used (figure 3.1) in order easily to achieve the result of the heat flow in the different sections of the model. The properties of material A and B are equal, except for the permeability in the x-direction which has been increased by $1 \cdot 10^{-12}$ m^2 in material B.

The applied surface-to-surface temperature differences in both the calculations and the experimental investigation range from 20 to 40°C using the following combinations of surface temperature on the hot and cold side, respectively (20°C; 0°C), (20°C; -10°C), and (30°C; -10°C).
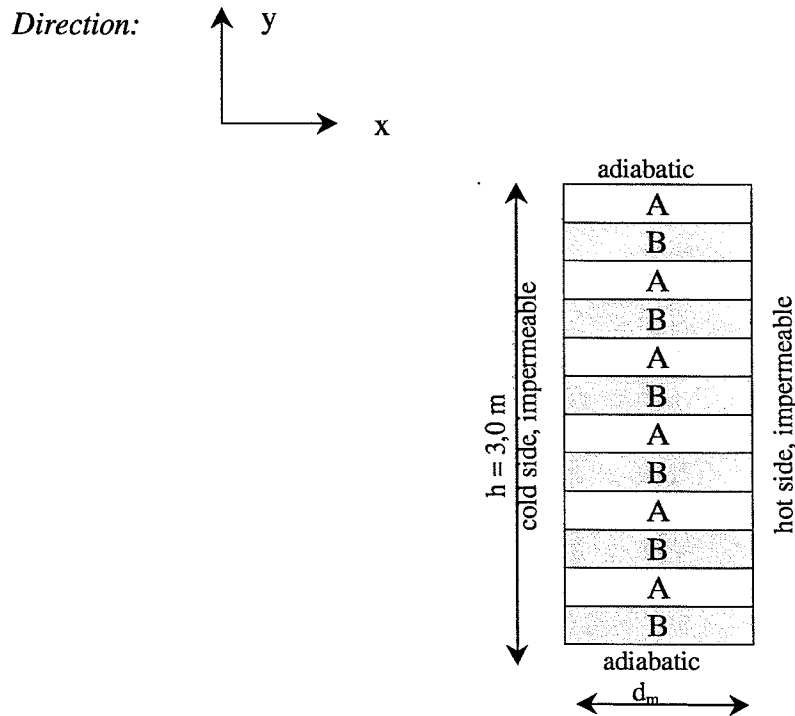
Figure 3.1: Computer model; geometry and boundary conditions when simulating a vertical structure. The calculations have been performed with an aspect ratio of $h/d_m = 6$ and 15.

3.3 Results and discussion

The calculations have been performed on the three materials in table 3.1. The ratio between the average heat flow with convection $\Phi_{with\ cv}$ and the average heat flow without convection Φ_0 (= the Nusselt number) is shown in table 3.2 together with the value of Ra_m calculated according to eq. (2.21).

Table 3.2: Surface temperature difference and calculated Nusselt number.

Material according to table 3.1	Surface temp. difference	Surface temperature		Ra_m according to eq.(2.21)	Average heat flow ratio $Nu = \Phi_{with\ cv}/\Phi_0$		max. air flow $\times 10^{-3}\ m^3/m^2 \cdot s$	
	ΔT [°C]	T_{hot} [°C]	T_{cold} [°C]		h/d_m 6	h/d_m 15	h/d_m 6	h/d_m 15
(1)	20	20	0	11.1	1.00	1.00	0.064	0.063
(1)	30	20	-10	17.8	1.00	1.00	0.096	0.095
(1)	40	30	-10	22.2	1.01	1.00	0.127	0.126
(2)	20	20	0	15.7	1.00	1.00	0.101	0.100
(2)	30	20	-10	25.2	1.01	1.00	0.151	0.150
(2)	40	30	-10	31.4	1.01	1.00	0.201	0.200
(3)	20	20	0	53.6	1.04	1.00	0.438	0.433
(3)	30	20	-10	86.1	1.08	1.00	0.657	0.649
(3)	40	30	-10	107	1.13	1.01	0.875	0.866

18

The critical Rayleigh number $Ra_{m,cr}$ for the calculated structures according to eq.(2.22) is shown in table 3.3.

Table 3.3: Critical Rayleigh number $Ra_{m,cr}$ for the calculated vertical structures according to eq. (2.22).

$Ra_{m,cr}(h/d_m = 15)$	$Ra_{m,cr}(h/d_m = 6)$
60.0	24.0

According to the experimental perception, we would only expect the total heat flow to be influenced by natural convection in the cases where Ra_m exceeds $Ra_{m,cr}$.

In the investigated cases of $h/d_m = 6$ the numerical calculations show an increase in the average heat flow when Ra_m reaches $Ra_{m,cr}$. When $h/d_m = 15$ the numerical calculations only show an insignificant increase in the average heat flow even though the Ra_m has exceeded $Ra_{m,cr}$.

The maximum air velocity is found near the vertical boundaries at $h/2$. The air velocity in the structure seems to be independent of the aspect ratio but increases as the permeability, and the temperature gradient increases. The air movements in the material cause a deviation from linearity in the temperature profile in the material.

For the materials described in table 3.1 the local Nusselt number is calculated for each of the twelve separate sections applying the surface temperature from table 3.2. The results are presented in figures 3.2 - 3.4.

From the figures 3.2 and 3.3, and the result in table 3.2, it is obvious that even if the convective air movement does not affect the total heat flow in the structure, a big difference in the heat flow between the top and bottom sections may exist in the vertical structure. The difference in heat flow between the top and bottom section increases with the permeability, the surface temperature difference, and with the thickness of the specimen i.e. when the aspect ratio decreases.
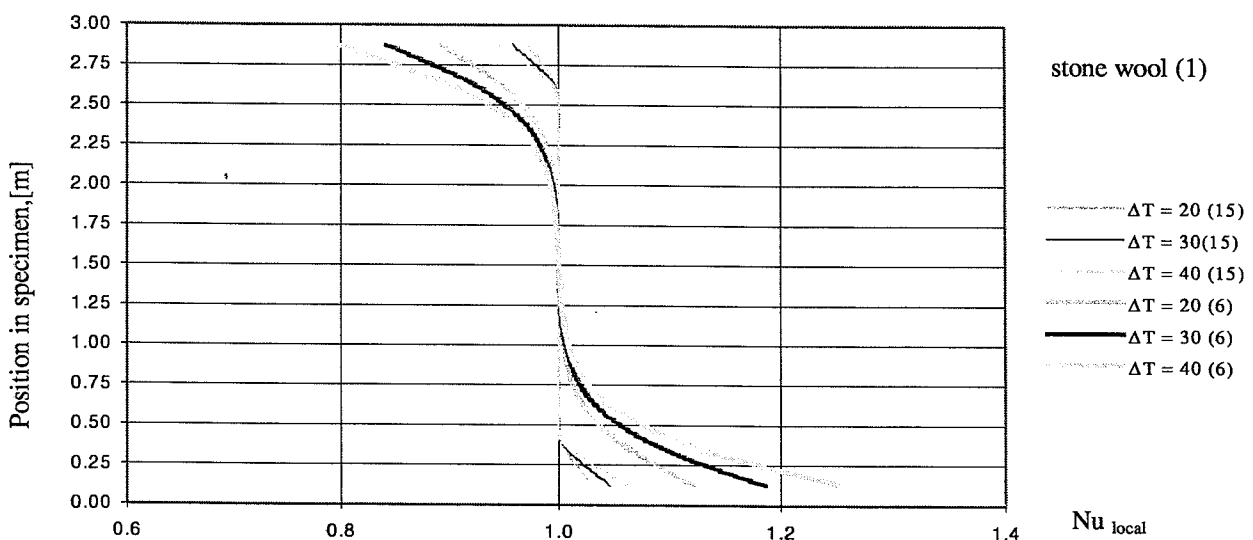
Figure 3.2: Calculated heat flow pattern in stone wool (1) with aspect ratio $h/d_m = 6$ and 15 applying the surface temperatures from table 3.2.
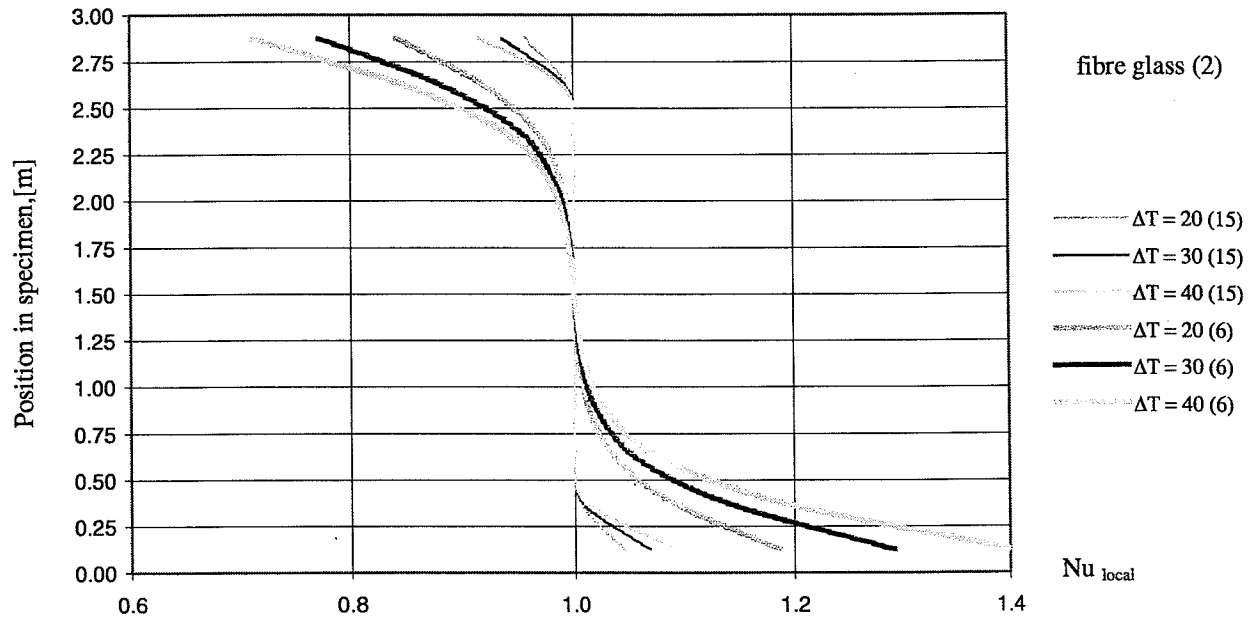
Figure 3.3: Calculated heat flow pattern in fibre glass (2) with aspect ratio $h/d_m = 6$ and 15 applying the surface temperatures from table 3.2.
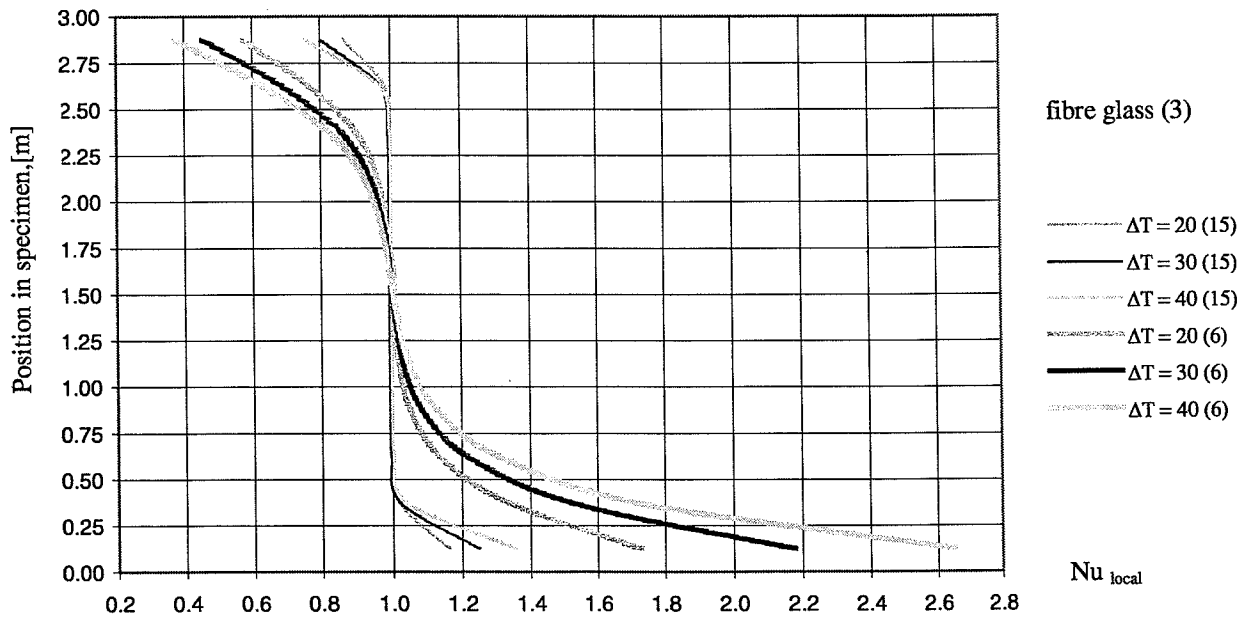
Figure 3.4: Calculated heat flow pattern in fibre glass (3) with aspect ratio $h/d_m = 6$ and 15 applying the surface temperatures from table 3.2.

In stone wool (1) the Nusselt number in the bottom part at $\Delta T = 40°C$ increased from 1.06 to 1.25 when the thickness was increased from 0.2 m to 0.5 m. In fibre glass (2) the Nusselt number in the bottom part increased from 1.09 to 1.40 when the thickness was increased and $\Delta T = 40°C$. While the corresponding increase in the Nusselt number in the bottom part in

20

fibre glass (3) was from 1.35 to 2.65. In fibre glass (3) both the permeability and heat conductivity are high, when $\Delta T = 40°C$ the heat flow in the bottom section becomes approx. seven times the heat flow in the top section.
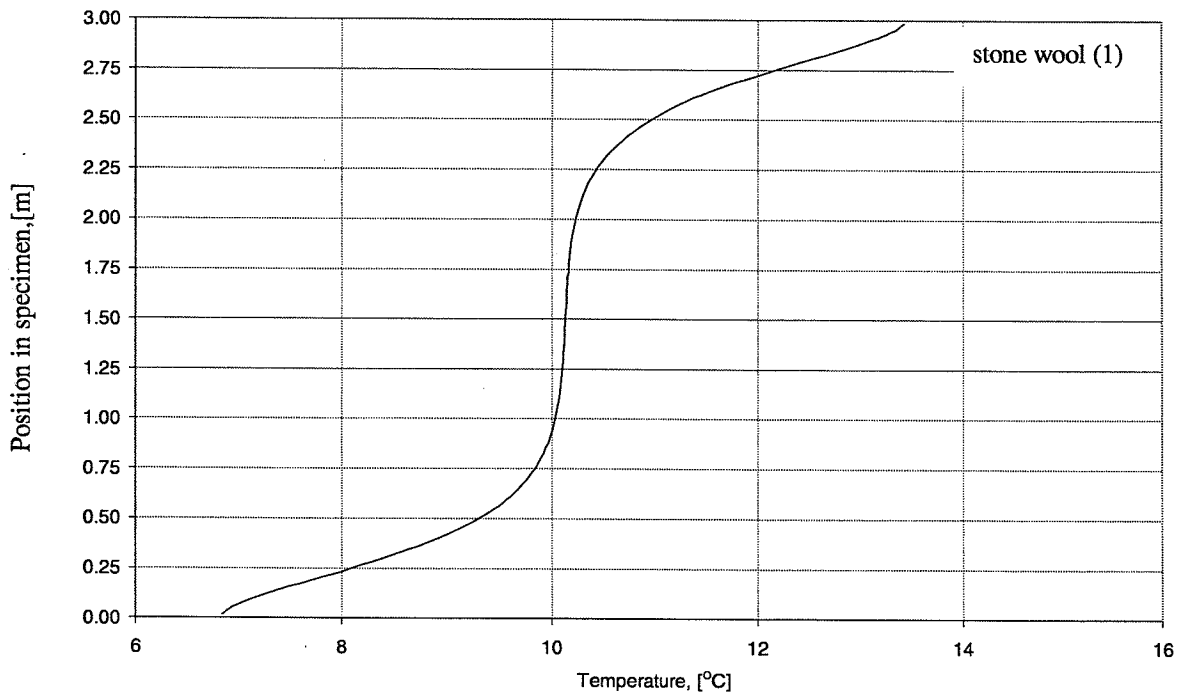
Figure 3.5: Calculated temperature distribution in the centre of stone wool (1) when $h/d_m = 6$ and when the surface temperature difference is 40°C.
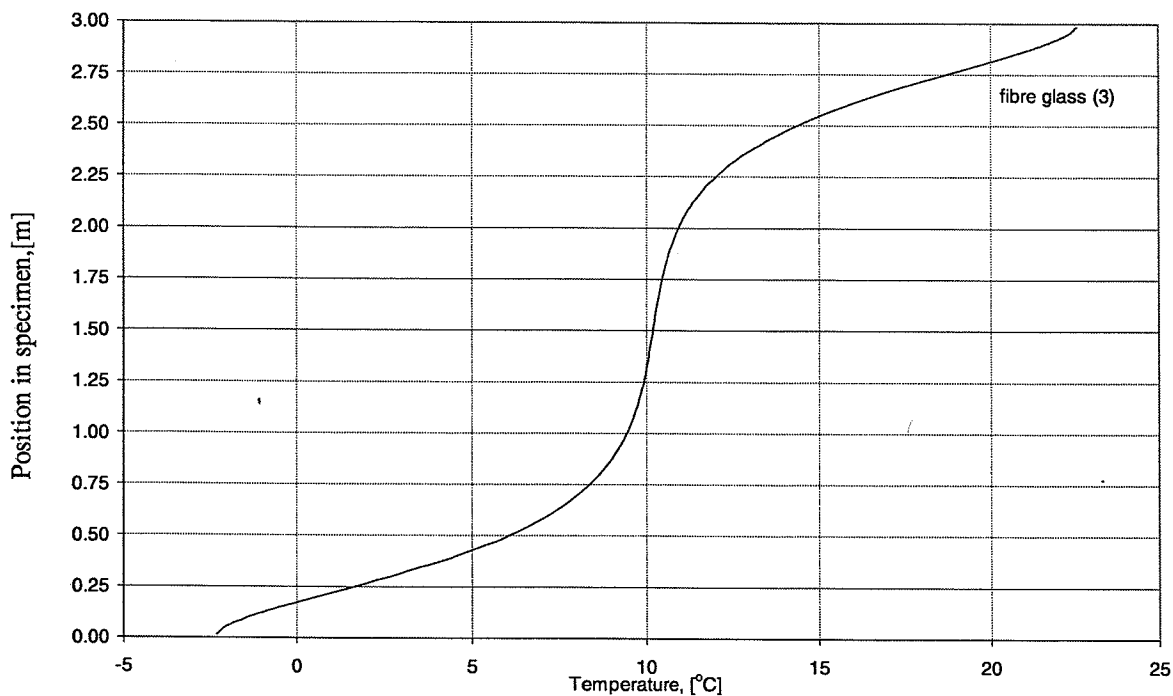
Figure 3.6: Calculated temperature distribution in the middle of fibre glass (3) when $h/d_m = 6$ and when the surface temperature difference is 40°C.

21

Figure 3.5 and 3.6 show the temperature profile in the centre of the materials stone wool (1) and fibre glass (3) when $h/d_m = 6$ and a temperature difference of 40°C is applied. If no convection had occurred, the temperature in the centre would have been 10°C, and uniform due to the thermal conductivity of which temperature dependence is disregarded in the numerical calculations. In stone wool (1), when calculating the temperature profile in the centre, the temperature at the bottom becomes 6.6°C lower than the temperature at the top. In the highly permeable insulation, fibre glass (3), the temperature at the bottom becomes 25°C lower than the temperature at the top.

The calculations have also been performed on the same structure as shown in figure 3.1 when it is turned into a horizontal position with the cold side on top using the properties of the materials stone wool (1) and fibre glass (3) and a temperature difference of 40°C. In these cases the heat flow from all the twelve sections was equal, and the numerical calculations did not show any air movement in the structure.

3.4   Summary

In this section numerical calculations of the effect of natural convection on the heat flow pattern in fibrous materials have been performed on a structure similar to the convection apparatus used in the experimental investigation. The aim of the calculations was theoretically to examine the distortion of the heat flow pattern caused by natural convection in fibrous materials with constant directional-dependent properties without distortions from joints in the specimen, and from uncertainty in the measurement.

The numerical calculations showed that:

- an increase in the total heat flow should only be expected in the highly permeable material, fibre glass (3)

- the difference in heat flow between top and bottom of the specimen increases as the following parameters are increased: the surface temperature difference, the thickness of the specimen, and the permeability

- the distortion in heat flow may also be observed as a similar distortion in the temperature profile in the centre of the specimen.

4. Test equipment - Convection apparatus

In connection with this study, a convection apparatus was built-up at the Dept. of Buildings and Energy. The design of the apparatus was tested in a small-scale prototype apparatus described in Svendsen and Dyrbøl [1995]. The purpose of the apparatus was to measure the difference in heat flow at different sections in porous materials, expressed as local Nusselt numbers, when the apparatus was located in various positions, and when different temperature conditions were applied. The design of the apparatus follows the principle of a guarded hot plate apparatus for measuring thermal conductivity (ISO8302, 1991). This section describes the design of the convection apparatus and the results of the performance test.

4.1 Design of convection apparatus

The convection apparatus has a total measuring area of 1×3 m². The measuring area is divided into 12 individual sections which makes it possible to measure the heat flow throughout the individual sections of the test specimen. The area of each measuring section is 1.0×0.25 m². Figure 4.1 shows the geometry and the guard arrangement in the apparatus.
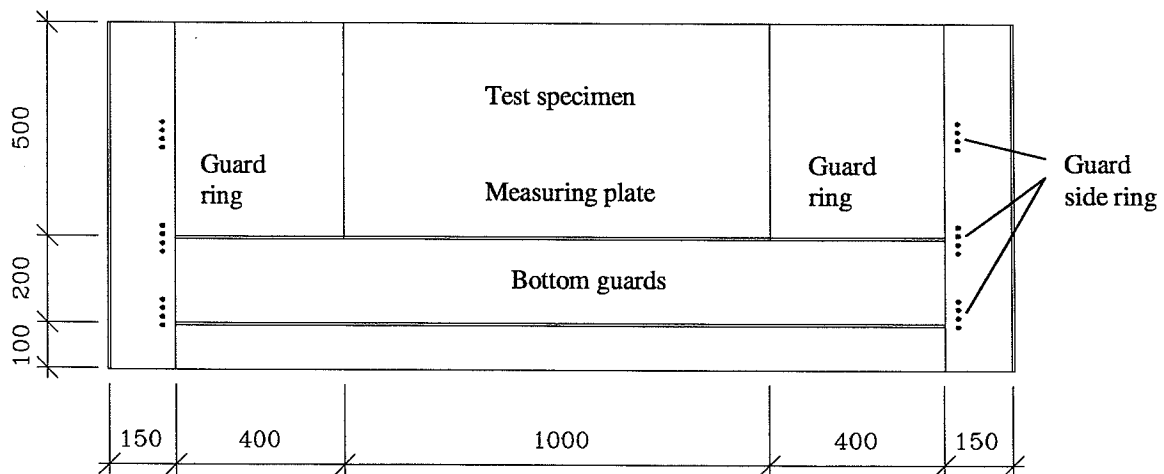
Figure 4.1: Cross section A – A in convection apparatus. The location of the cross section is shown in figure 4.2.

In order to avoid that the measurement is disturbed by air movements in the material covering the guard ring, the test specimen only covers the exact measuring area. The area above the guard ring is covered by an impermeable insulation material (polystyrene). The thickness of the guard insulation is varied with the thickness of the test specimen as the airtight cover for the test specimen rests on the guard insulation. The guard insulation is pressure stable and serves to define the thickness of the test specimen. The apparatus is designed to measure test specimens of a thickness of 100 to 500 mm. When measuring heat flow, the apparatus has a maximum capacity of 51.2 W/m², i.e. 12.8 W/0.25 m².
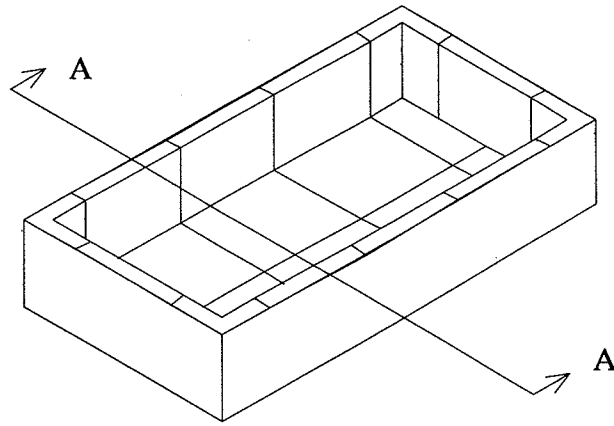
(a) Bottom and side guards
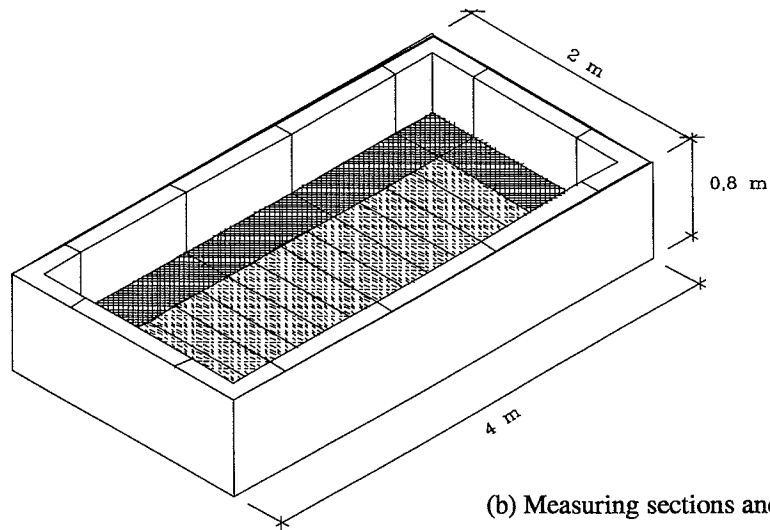
(b) Measuring sections and guard ring

Figure 4.2: Sketches of the test apparatus. (a) shows how the bottom and side guards have been designed, and (b) shows the arrangement of the twelve measuring sections and the guard ring surrounding the measuring area.

The apparatus is placed in a cold box which forms the cold side of the apparatus. The apparatus is suspended by an axis of rotation which allows it to be placed in any random position in order to simulate the conditions in either a ceiling or a wall as shown in figure .

24
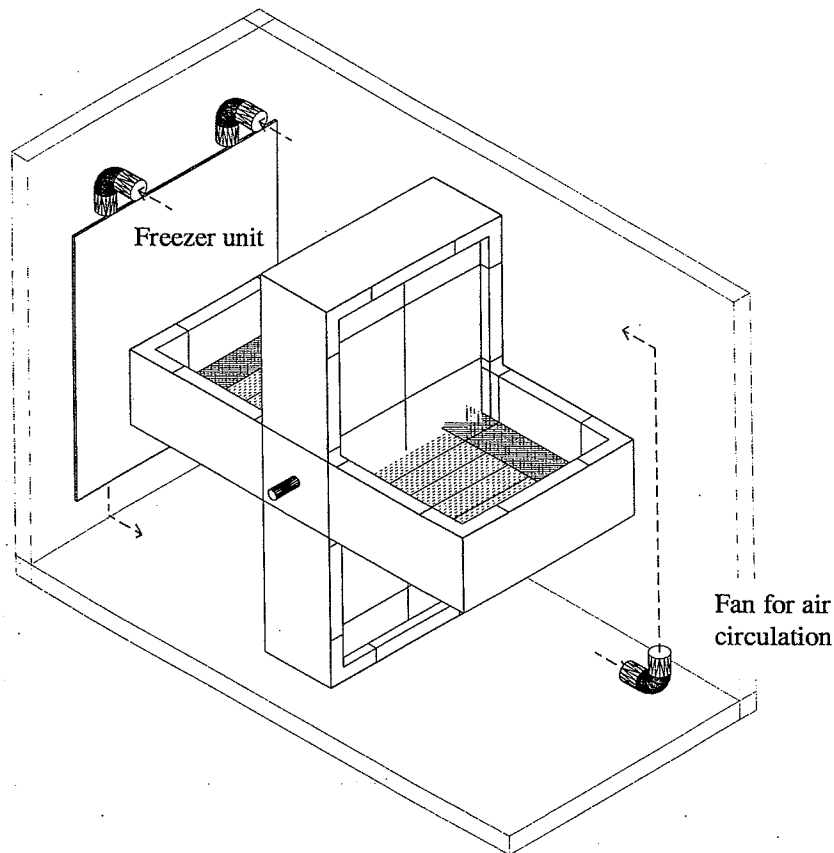
Figure 4.3: Convection apparatus placed in the cold box. The suspension of the apparatus allows it to be rotated 360°, and the measurement to be performed in various positions.

4.1.1   Measuring plates and warm side in the apparatus

The individual measuring sections consist of a glass plate with an electrically conductive coating located on the opposite side of the test specimen. The electrical resistance of the coating is known for each glass plate, and the temperature control of the glass plates is gained from power supplied to the coating. The measuring plates are individually operated at a constant temperature. The temperature set point of the measuring area can be controlled within the limits of the power supplies taking into consideration the temperature stability of the material used in the construction i.e. polystyrene.

The power supplied to the glass coating to control the plate temperature is regulated by a PID-regulator. The temperatures of the glass plates are measured every ten seconds. From the measured temperatures, the power required to maintain a constant temperature on the plates is calculated and supplied to the coating within the next ten seconds. When the electrical resistance of the coatings is known, the heat flow throughout the individual measuring sections can be calculated based on the power supplied to the coatings. The design of the apparatus and the regulation is described in detail in Nielsen [1997] and Dyrbøl [1998].

The arrangement of thermocouple for temperature measurements and thermopile for the control of the guard ring is shown in figure 3.1. The measurements performed show that the

temperature distribution over the total measuring area is uniform within ±0.1°C when no convection occurs. With convection, the air movements in some of the observed cases caused a horizontal temperature gradient which exceeded 1.0°C on single glass plates.

GR 1-10:   Guard Ring 1-10
MP 1-12:   Measuring Plate 1-12
GSR 1-12: Guard Side Ring 1-12

—•   thermopile between measuring plates and guard ring
o   thermopile between measuring plates and bottom guards
×   thermocouple for temperature measurement

Figure 4.4:   Design of warm side in convection apparatus showing the arrangement of thermocouples and thermopiles for the temperature control of the measuring plates and guard ring.

4.1.2   Cold side in the apparatus

The cold side of the apparatus is formed by a 14 mm plywood cover which forms a straight airtight cover for the test specimen. The air temperature in the cold box, in which the apparatus is placed, is used to control the temperature of the cold plate in the apparatus. The temperature in the box is regulated by a PI-regulator, and it is possible to adjust the temperature down to -10°C. In order to get a uniform temperature distribution in the box, which has the internal dimension $5.9 \times 3.1 \times 4.5 \text{ m}^3$ (length×width×height), three fans

circulate the air in the box. The location of the fans and the freezer unit in the cold box is shown in figure . The temperatures on the cold side of the specimen are measured by thermocouples located between the plywood cover and the test specimen, just above the locations where the temperatures are measured on the measuring plates, see figure 3.1. The temperature on the cold side of the test specimen is uniform within 0.5°C.

4.1.3 The guard sections in the apparatus

To ensure a one-dimensional heat flow throughout the test specimen when measuring specimens thicker than 200 mm, the convection apparatus is designed with a three-dimensional guard system. The guard ring sections (GR), which are at the same level as the measuring plates (MP), are made of glass just as the MP. The guard sections at the bottom (GB) behind the measuring plates are made of aluminium with a uniform heating wire. The guard section units on the side are made from stainless steel; each with three heating bands. The high thermal conductivity of the steel helps achieve a linear temperature profile at the edges in the apparatus. The three heating bands are placed at the same level as the bottom guard sections (GSB), the guard ring sections (GSR), and 0.25 m above the measuring plates (GSM), which equals the centre of the specimen when measuring a thickness of 500 mm. Each heating band is balanced against the temperature of the guard in front of it. The heating band GSM, which controls the temperature in the centre of the specimen, is balanced against the temperature in the guard insulation next to the test specimen and approx. 0.2 m above the measuring plates. The location of thermopiles for regulating the guard ring is shown in figure 3.1. The bottom guard section is balanced against the average temperature of the four measuring plates above it; which the guard ensures. The temperature of the individual guard sections deviates by less than 0.1°C from the temperature against which it is balanced.

4. 2 Performance test

The purpose of the apparatus was to measure the relative differences in heat flow rates rather than measuring high-precision absolute values. When performance testing the apparatus, the following was investigated:

- the absolute measurements were compared to measurements performed in a heat flow meter apparatus according to ISO8301[1991]
- the reproducibility when removing and remounting the test specimen
- the ability of the apparatus to measure in vertical as well as in horizontal position
- the steady-state conditions

In order to test the thermocouple wires, 10 elements were compared to a precision measurement by using an extra measurement card at 0°C and 20°C with an average deviation of -0.15°C and -0.06°C, respectively. The reference temperatures in the used measurement cards were checked while the apparatus was in thermal equilibrium with the surroundings.

The results of the performance test are described in detail in Dyrbøl [1998].

The performance test was performed on polystyrene slabs. This material was chosen as it is an impermeable, homogenous material, and when the cells contain air, its thermal conductivity does not change over time. As the total test specimen consists of up to 30 individual slabs dependent on the measured thickness, three slabs, of a density close to the average density of the specimen installed in the apparatus were chosen as reference material. The thermal conductivity of the three reference slabs was measured at least four times on each in a heat flow meter apparatus, in order to obtain the best prediction of the thermal conductivity.

The assigned thickness of the polystyrene slabs was 100 mm. The measurements performed on the reference slabs in the heat flow meter apparatus were made on the 100 mm slabs with one layer of 3 mm soft foam on each side to make the measurement comparable with the measurement in the convection apparatus. The results are shown in figure 3.4. The deviation in the thermal conductivity is due to uncertainty in the measurement.
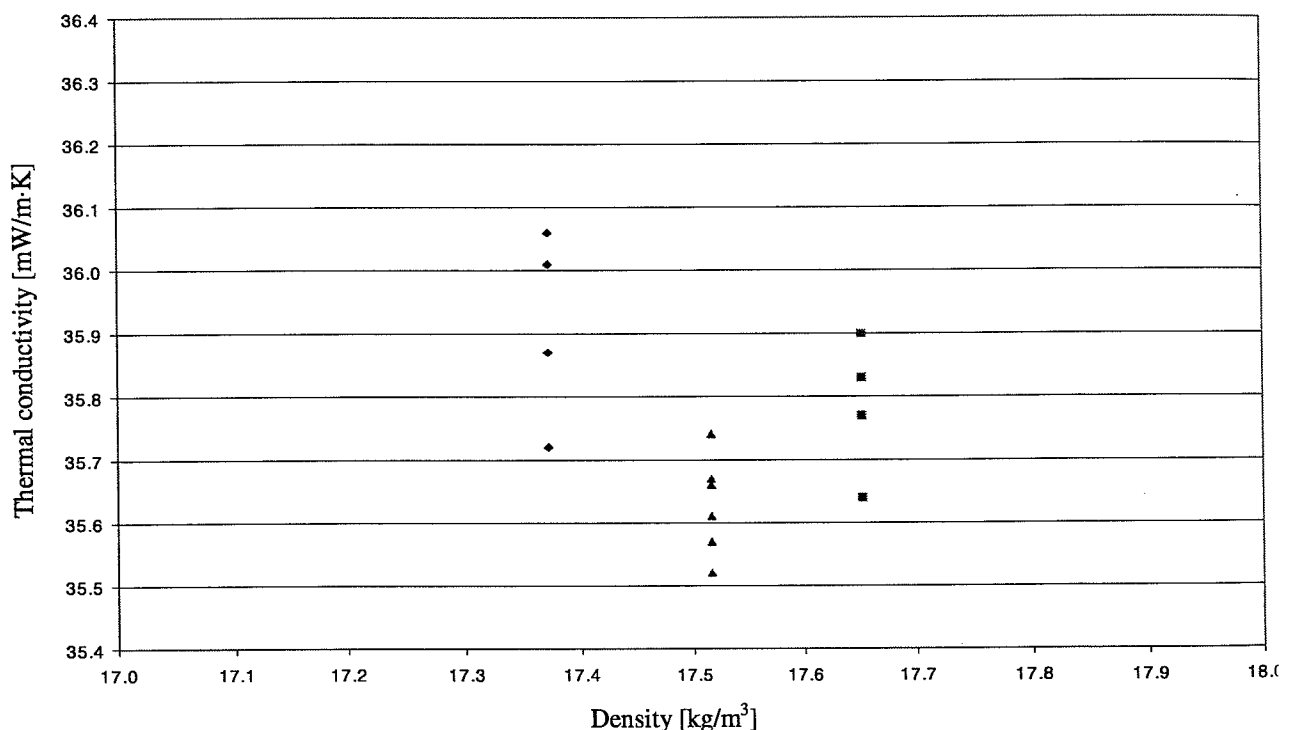
Figure 4.5: Thermal conductivity λ_{10} measured on three polystyrene reference slabs in a heat flow meter apparatus.

When the polystyrene slabs were inserted in the convection apparatus, the density of the individual slabs was considered in order to achieve a uniform density of the entire test specimen. In order to avoid cracks either from the thermocouples placed between the slabs or from the slabs with no plane surface, two layers of 3 mm soft foam were placed between the slabs and one layer at the boundaries. Table 4.1 shows the result of the measurement performed in the convection apparatus on polystyrene.

Table 4.1: Thermal conductivity measured in the convection apparatus on polystyrene.

Measuring plate number	Thermal conductivity λ_{10} [W/m·K]			
	Horizontal position			Vertical position
	(1)♣	(2) ♣	(3)	(4)
	d_m= 212 mm ρ=17.9 kg/m^3	d_m= 212 mm ρ=17.9 kg/m^3	d_m= 530 mm, ρ=18.1kg/m^3	d_m= 530 mm ρ=18.1kg/m^3
1	0.0370	0.036	0.0399	0.0400
2	0.0362	0.0353	0.0346	0.0344
3	0.0366	0.0365	0.0368	0.0366
4	0.0358	0.0348	0.0347	0.0345
5	0.0378	0.0372	0.0379	0.0381
6	0.0365	0.0358	0.0360	0.0361
7	0.0364	0.0360	0.0362	0.0367
8	0.0363	0.0360	0.0365	0.0367
9	0.0361	0.0361	0.0369	0.0369
10	0.0368	0.0363	0.0372	0.0378
11	0.0367	0.0370	0.0375	0.0377
12	0.0358	0.0346	0.0353	0.0353
average	0.0365	0.0360	0.0366	0.0368

♣ the air circulation in the cold box was not satisfactory.

The measurements in the convection apparatus have been performed on an assigned thickness of 212 mm and 530 mm, respectively, and with a boundary temperature of 0°C and 20°C, respectively. When measuring the assigned thickness of 212 mm, the air circulation in the cold box was not sufficient; which was rectified by installing an extra fan in the box.

The average thermal conductivity measured in the heat flow meter apparatus was 0.0358 W/m·K, and the average density of the three slabs was 17.5 kg/m^3. The average of the measurements (3) and (4) in the convection apparatus, which must be regarded as the most representative due to the problem with the temperature in the cold box, deviates by 0.0009 W/m·K when compared to the reference slabs. The number of reference slabs is too little to make a correction for the difference in density. As the density of the specimen inserted in the convection apparatus and the average density of the reference slabs differ by only 0.6 kg/m^3, it is reasonable to use the average measurement as a reference. The deviation from the reference measurement is within 3% in both the horizontal (3) and the vertical positions (4). The deviation from the reference measurement to the individual measuring sections is larger in a few cases; which might indicate a thermal leakage between the individual measuring sections.

The reproducibility when the specimen was removed and reinserted after a short time was within 2% (measurements (1) and (2)), whereas the reproducibility when the specimen was kept in the apparatus was less than 1.2% for all the measuring sections (measurement (3)).

Figure 3.6 shows the measured thermal conductivity in the convection apparatus from table 4.1 and the local Nusselt numbers calculated on basis of measurement (3) and measurement (4).
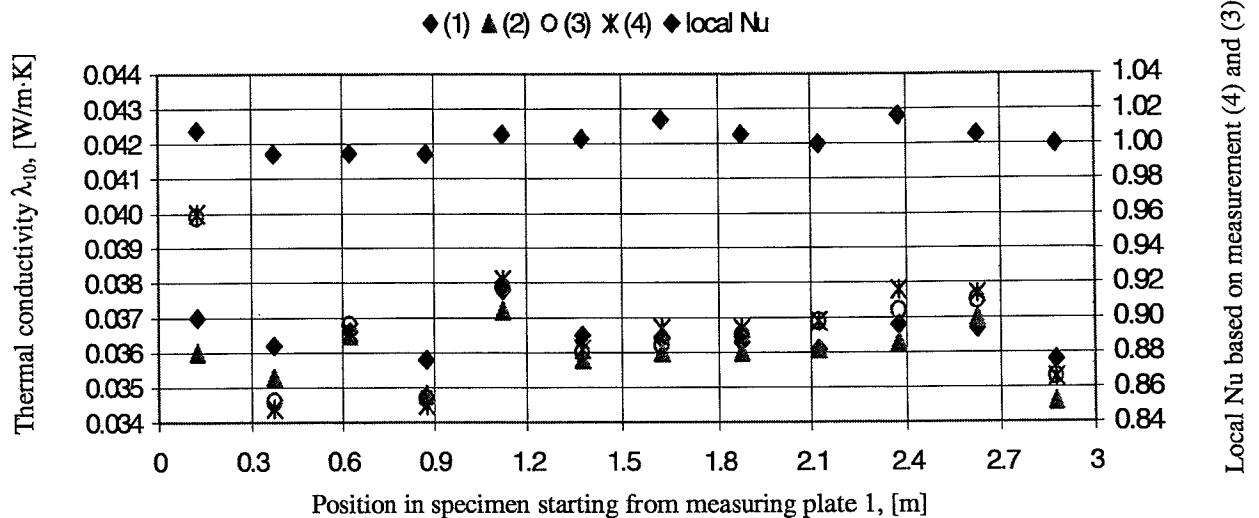
Figure 4.6: Local Nusselt numbers and thermal conductivity measured on polystyrene at an assigned thickness of 212 and 530 mm measured at the different sections of the specimen when $T_{hot} = 20°C$ and $T_{cold} = 0°C$.

As the local Nusselt number approaches unity for all the twelve measuring plates the apparatus is, in spite of possible thermal leakage, able to give a good assessment of the relative differences in heat flow between the individual sections in the specimen.

When measuring the impermeable test specimen, the temperature on the warm side was uniform within 0.3°C. In the centre and on the cold side, the temperature was uniform within 0.5°C. Figure 3.6 shows the temperature profiles in the impermeable specimen measured 0.1 m above the measuring plates when measuring in horizontal and vertical position.
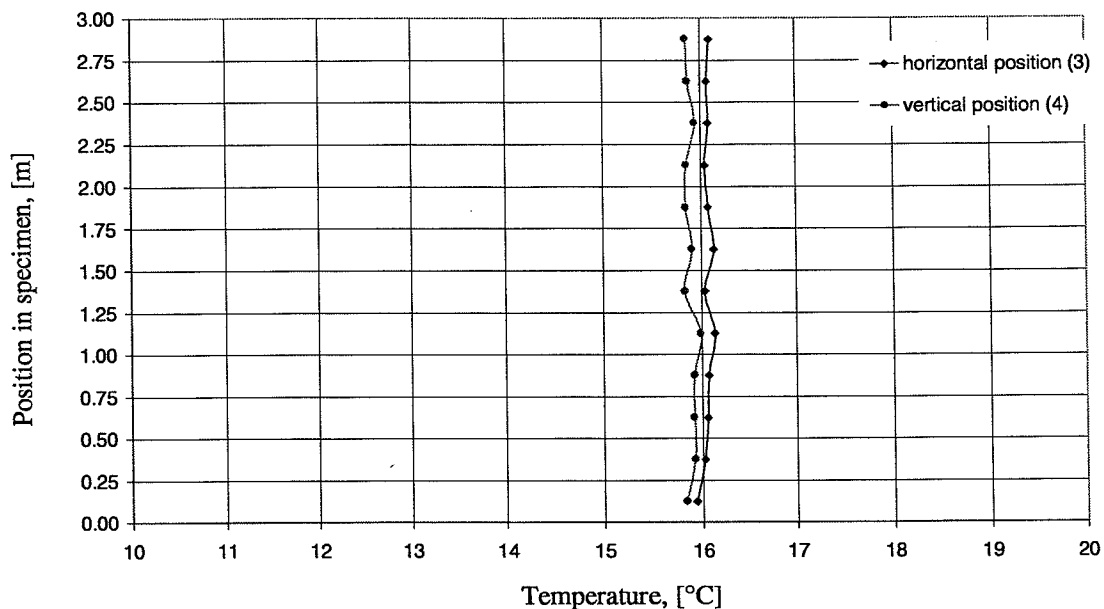
Figure 4.7: Polystyrene: temperature profiles measured 0.1 m above the measuring plates when measuring a surface temperature difference of 20°C in both the horizontal position (3) and the vertical position (4). The specimen thickness was 530 mm.

Due to a minor difference in the cold side temperature, the temperature 0.1 m above the measuring plates in measurement (3) should be 0.12°C warmer than measurement (4). The temperature profiles have an insignificant deviation from being linear. The measured deviation is caused by local deviation in the thermal conductivity of the test specimen and by uncertainty in measuring the temperature.

4.2.1   Steady-state conditions

The measurement runs until steady-state conditions have been obtained i.e. that the heat flow through all twelve measuring sections does no longer change with time. The duration of the transient time and the measuring period are determined by the test specimen and the actual initial temperature conditions.

The criteria used in the test period for defining when steady-state conditions have been reached are as follows:

- the measured thermal resistance averaged over a three hour period no longer changes monotonically
- the measured thermal resistance averaged over a 20 minute period no longer differs by more than 2% from the measured average in the three hour period

A typical transient time progress for one of the twelve measuring plates in the convection apparatus is shown in figure 3.5. In order to ensure that the specimen has reached a stable steady-state condition, the measurement is performed over an extra day, and the result presented is the averaged value from the last day.
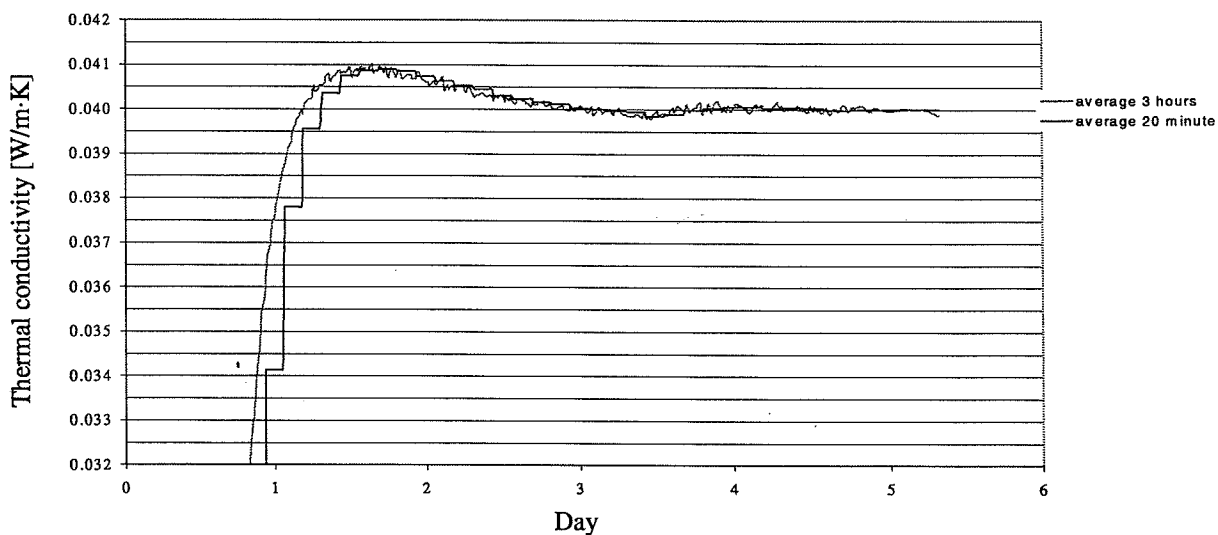
Figure 4.8:   Example of a transient time progress for one of the twelve measuring plates when measuring the thermal conductivity. The figure shows the measurement of polystyrene with an assigned thickness of 530 mm and boundary temperatures 0°C and 20°C.

31

4.3   Error estimation

Errors in measurement can be divided into two types of errors:

- systematic errors
- random errors

A systematic error is the type of error which occurs with the same deviation in all the measurements. The random error is the random variation in the measurements caused by the material, the operator, or other variations in the test conditions.

In relative measurements the systematic error can be ignored as the effect neutralises itself. However, an estimation of the maximum relative error from systematic errors - when measuring the thermal conductivity in the convection apparatus - is described in Appendix A. The maximum systematic error is estimated at ± 6.8%. The relative error decreases as the thickness increases.

When evaluating the systematic error, the error from measuring heat flow to the guard side is also considered. In the measurements performed, the temperature difference, which causes the heat flow to the side guards, mainly occurs when air movements exist in the measurement; i.e. when the measurement is performed with the apparatus in the vertical position. This means that even if the actual work includes relative measurements, the difference in heat loss to the side guard may result in a maximum error of ±1.5% in the relative measurement.

In the performance test of the apparatus, the reproducibility was found to be approx. ±1.2% when the specimen was kept in the apparatus.

From the above evaluation, the uncertainty in the relative measurements performed in the convection apparatus is expected to be within 3%. This means that differences measured in the apparatus of less than 3% should not be considered as significant, as they remain within the uncertainty of the apparatus.

5. Experimental investigation

This section describes the investigations performed to study the influence of convection on the heat transfer through different types of fibrous materials for building use. The measured heat flow patterns and temperature profiles are presented and discussed in section 5.4.

The original measuring plan of the project included five different products of fibrous materials. The products were chosen based on the intention to measure comparable fibre glass and stone wool products in the form of slabs as well as rolls when using various temperature differences. An overview of the products, which were intended for measuring is given in table 5.9. The permeability of the stone wool and the corresponding fibre glass differs, whereas the thermal conductivity is equal, except in the very light rolls of fibre glass.

Table 5.1: Overview - products of fibrous materials, which were planned to be tested in the original measuring plan.

Material	Slabs	Rolls	Density [kg/m^3]	Permeability, $\perp$ [$\cdot 10^{-10}$ m^2]	Thermal conductivity, $\perp$ [W/m·K]
Stone wool (1)	x		~ 33	~18	~ 0.035
Stone wool (1)		x	~ 33	~18	~ 0.035
Fibre glass (2)	x		~ 17-20	~24	~ 0.035
Fibre glass (2)		x	~ 17-20	~24	~ 0.035
Fibre glass (3)		x	~ 8-10	~108	~ 0.045

Due to the limited time for the project, it was not possible to follow the original measuring plan instead measurements have been performed on the two materials which represent the extremity in material properties. An overview of the performed measurements presented in this project is shown in table 5.10. The remaining parts of the measuring plan will be completed after this project have been reported.

Table 5.2: Overview – measurements, which have been performed within the time limit of the project.

Material	Surface temp. diff. ΔT [°C]	Surface temperature		Position of apparatus						
		T_{hot} [°C]	T_{cold} [°C]	Vertical					Horizontal heat flow upwards	
				h/d = 6		h/d=7.5		h/d=15		
				MP1 on top	MP12 on top	MP1 on top	MP12 on top	MP1 on top	d=0.4m	d=0.5 m
Stone wool (1)	20	20	0	x	x			x		x
Stone wool (1)	30	20	-10	x	x			x		x
Stone wool (1)	40	30	-10	x	x					x
Fibre glass (3)	40	30	-10			x	x		x	

33

5.1 Test specimens: Properties

5.1.1 Determination of density

The properties of the fibrous material influencing the convection are the permeability and the thermal conductivity which are both correlated to the density of the material. Although the performed measurements are presented as relative measurements, big variations in density may influence the measurement results. In order to avoid this, the density of the individual slabs or rolls has been taken into consideration when the specimens were installed in the convection apparatus in order to achieve a homogeneous density of the entire test specimen.

Material: Stone wool (1)
This material has a well-defined shape, and the density of the individual slabs was measured in the range of 26.2-34.3 kg/m^3. When inserted into the apparatus, the variation in local density when considering the full thickness of the specimen was calculated to be within 30.0-31.1 kg/m^3, whereas the density of the entire test specimen was 30.5 kg/m^3. When the slabs are placed in the convection apparatus, the connections are alternate in the individual layers as shown in figure 5.5.
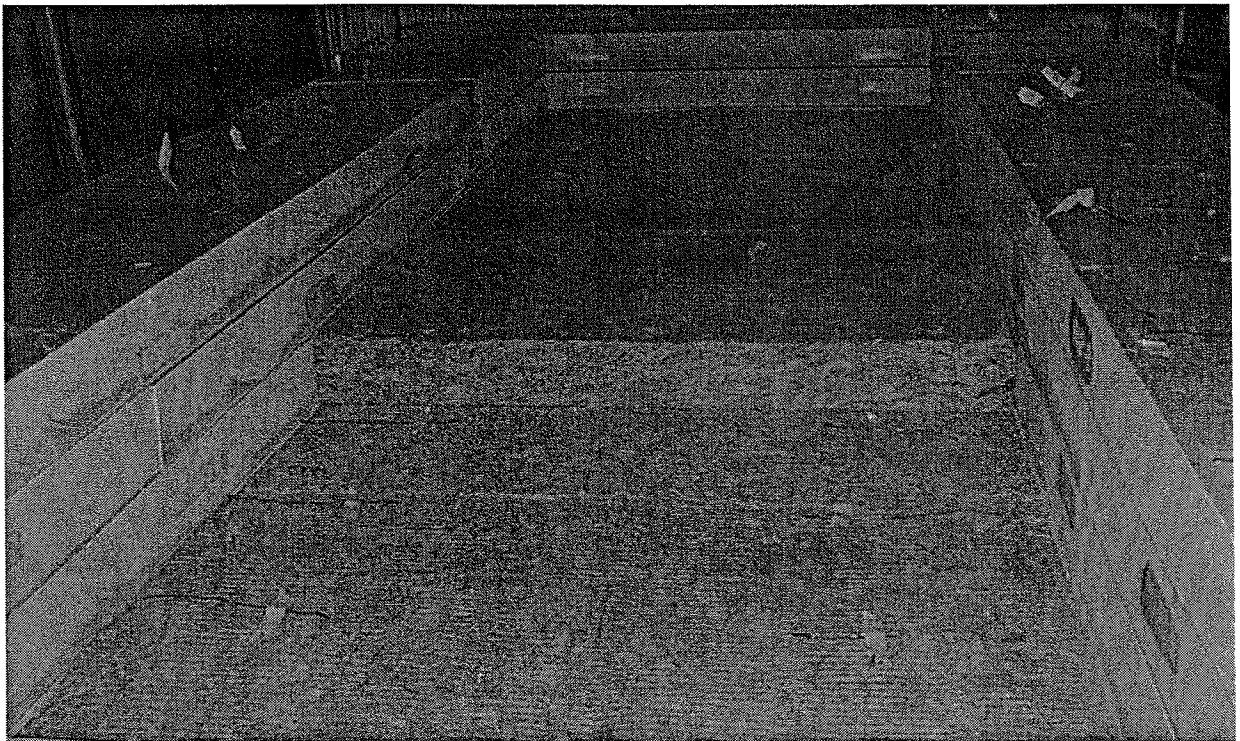
Figure 5.1: Arrangement of individual slabs which make up the test specimen when the material is stone wool (1). The joints between the individual slabs in each layer are shifted in order to avoid joints going through the thickness of the total test specimen.

Material: Fibre glass (3)

This product is in rolls and contains loose fibres without any binder. The rolls are compressed approx. 95% when packed. The average density measured on the unpacked rolls was 8.6 kg/m^3. When placing the rolls in the apparatus, the density of the inserted specimen is calculated to 9.6 kg/m^3. In order to achieve the manufacture-assigned dimension (thickness 0.2 m and width 0.6 m) when the specimen is placed in the apparatus, one roll in each layer has been sliced before unpacking. The fibre glass (3) is enclosed in a plastic cover which is left on when the rolls are placed in the apparatus as shown in figure 5.7. The plastic cover is taped to the inside of the apparatus in order to keep the specimen in the proper position when the apparatus is placed in other positions. Taping the plastic cover to the top and bottom guard insulation may interrupt or inhibit some of the air movements from taking place in the material.

This product is only manufactured for insulation in attics and crawl spaces, and it is only tested here in order to measure a highly permeable product.
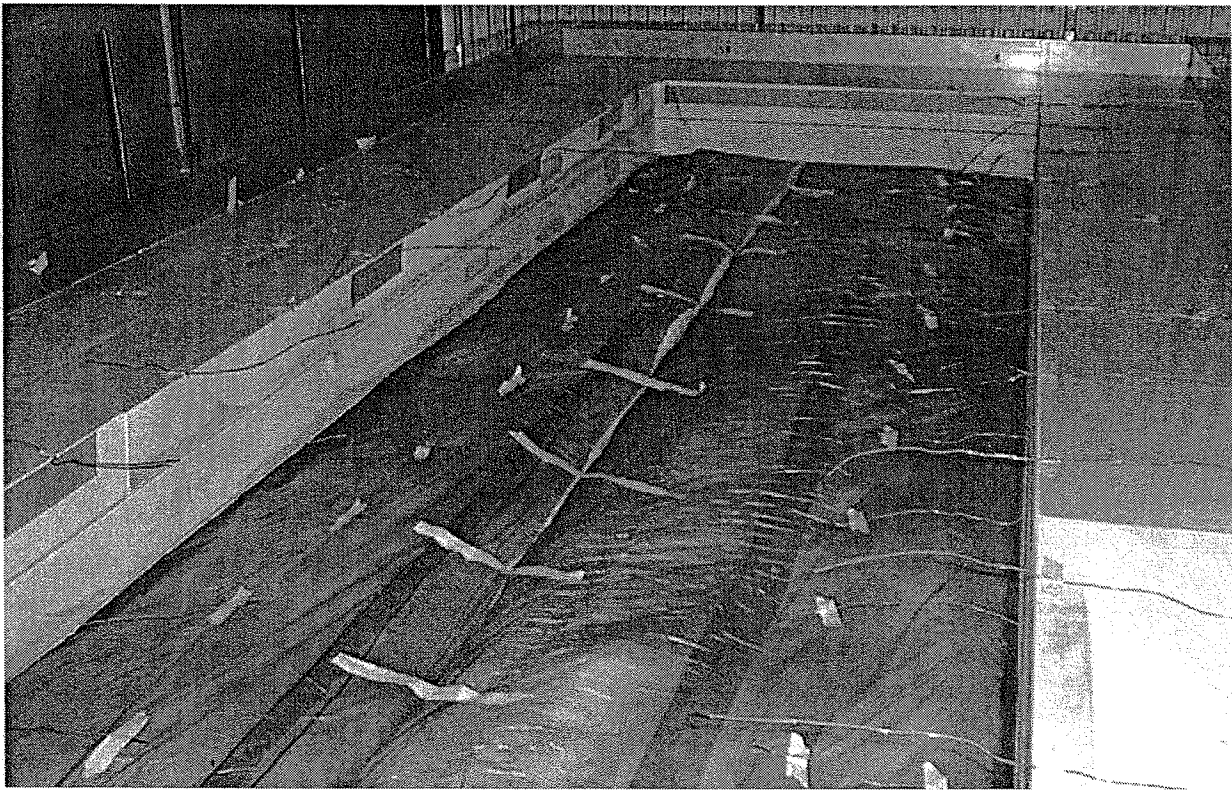
Figure 5.2: Arrangement of individual rolls which make up the test specimen when the material is fibre glass (3).

The different materials, which have been measured in the convection apparatus, are pictured in figure 5.6.

35

Figure 5.3: Picture of measured materials. In front stone wool (1), $\rho = 30$ kg/m^3, and fibre glass (3), $\rho = 8.6$ kg/m^3. In the background the polystyrene slabs, which were used when performance testing the apparatus.

5.1.2   Determination of permeability

The coefficient of specific permeability K of the fibrous material is determined by means of Darcy's law shown in eq. ( )

$$\frac{\dot{m}_a}{\rho_a} = -\frac{K}{\eta_a}\frac{dp}{dx}$$

(5.1)

which states that the mass flow rate per area $\dot{m}_a$ (kg/m$^2\cdot$s) is proportional to the air density ρ_a (kg/m^3), the pressure difference dp (Pa), and inversely proportional to the thickness dx (m). The proportionality coefficient is the factor K/η_a, in which η_a (Pa·s) is the dynamic viscosity of air, and K the specific permeability of the material (m^2). Darcy's law assumes a linear relationship between flow velocity and pressure drop. If this is not the case, the air flow will probably be turbulent, and the measurement should be repeated using a lower pressure gradient. The principle in the measuring method used equals the principle in ISO 9053[1991]. When measuring the pressure drop, a flow velocity of 670 m/h has been used; which is inside the linear relationship between flow velocity and pressure drop for the measured materials. The measurements on fibre glass (3) are performed with the specimen compressed to a higher density due to the shape of the specimen which is very difficult to control and then extrapolated to the density inserted in the apparatus. Due to the loose shape of the product, the measured permeability on fibre glass (3) has a very high uncertainty. Furthermore, it was not possible to control the placement of the specimen sufficiently when the direction (II) was measured which means that K$_y$ (II) of fibre glass (3) should only be regarded as a rough estimate.

5.1.3   Determination of thermal conductivity

The directionally dependent thermal conductivity of the test specimens has been measured without convection in the heat flow meter (HFM) apparatus. The measuring area of the HFM apparatus is 0.3·0.3 m². The temperature on the hot side is 20°C and on the cold side 0°C. The thermal conductivity of the materials tested in the convection apparatus is measured on a selection of specimens with a density close to the average density when installed in the convection apparatus.

In the HFM apparatus, the thermal conductivity of the slabs of stone wool (1) is measured at a thickness of 100 mm. The thermal conductivity of fibre glass (3) is measured when the specimen is compressed to a thickness of 200, 175, 150, and 125 mm due to a greater uncertainty when measuring specimens of a thickness greater than 125 mm in the HFM apparatus. A two-dimensional heat transfer analysis of the HFM apparatus shows that when measuring a thickness of 200 mm the error in the measured heat flow is increased by 1.5% due to increased boundary loss compared to the situation when measuring a specimen thickness of 100 mm.

From the measurements, a relation between density and thermal conductivity similar to eq. (1.3) has been determined. Figure 5.10 shows the actual properties measured in the heat flow meter apparatus and the estimated relations between thermal conductivity and density.
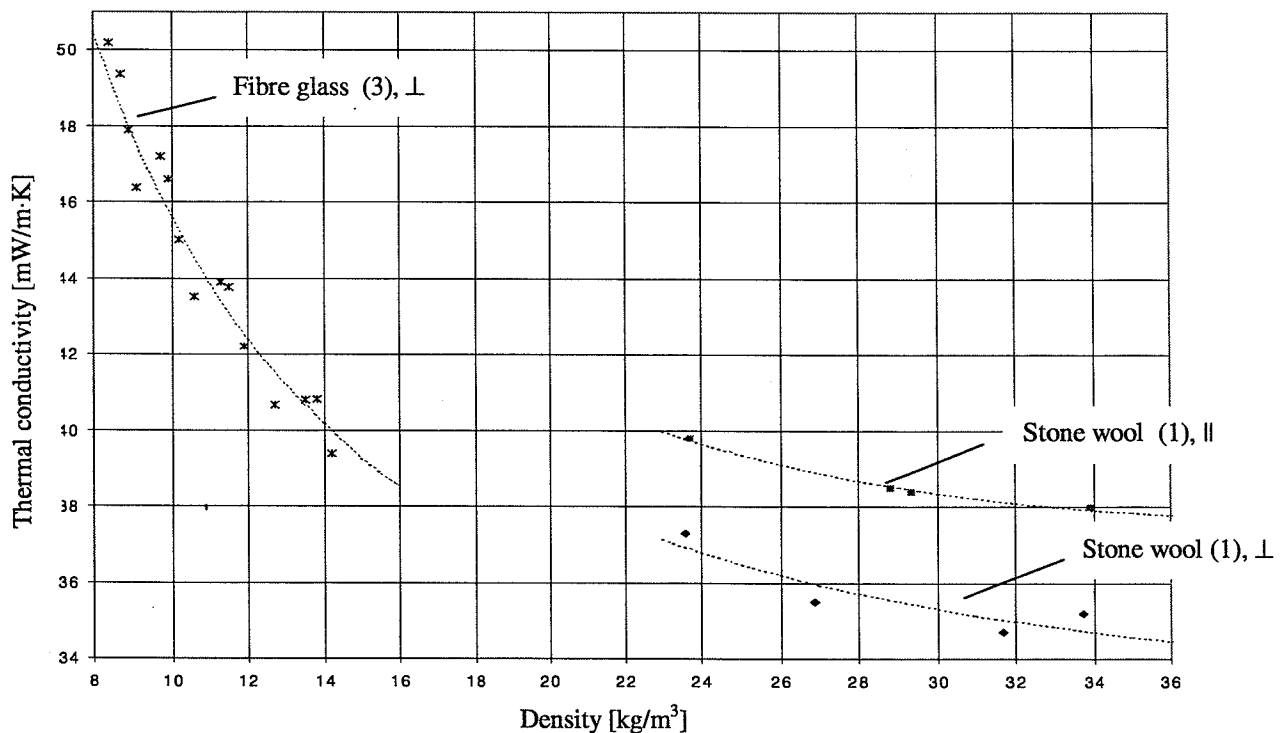
Figure 5.4:   Directionally dependent thermal conductivity, λ_{10} measured in the heat flow meter apparatus on stone wool (1) and fibre glass (3). The dotted lines show the estimated relations on the form of eq. (1.3) determined on basis of the actually measured properties.

Table 5.11 shows the properties corresponding to the density inserted in the convection apparatus determined from the estimated relations between density and thermal conductivity.

Table 5.3: Material properties measured on a selection of specimens. "♣": Each specimen has been measured at a thickness of 200, 175, 150 and 125mm. "♣♣": The thermal conductivity parallel to the fibre direction has not been measured. Instead, the value was assessed from corresponding measurements and an empirical correlation between the two directions.

Material	Number of specimens	Mean density [kg/m³]	Thermal conductivity at 10°C [W/m·K]		Air permeability [10⁻¹⁰ m²]	
			λ_x ($\perp$)	λ_y (||)	K_x ($\perp$)	K_y (||)
Stone wool (1)	4	30.5	0.0352	0.0383	17.4	28.0
Fibre glass (3)	4♣	9.6	0.0464	0.0517♣♣	~ 68	> 95

5.2 Test methods - convection apparatus

The aim of the convection measurements performed was to examine:

- the distribution of heat flow over the height of the structure;

- if the average heat flow through the total specimen is increased compared to the horizontal reference position without convection;

when different products of fibrous material are examined and different surface temperatures are applied.

In a complete measuring series, the measurements have been performed with the apparatus placed in the four positions illustrated in figure 5.11:.
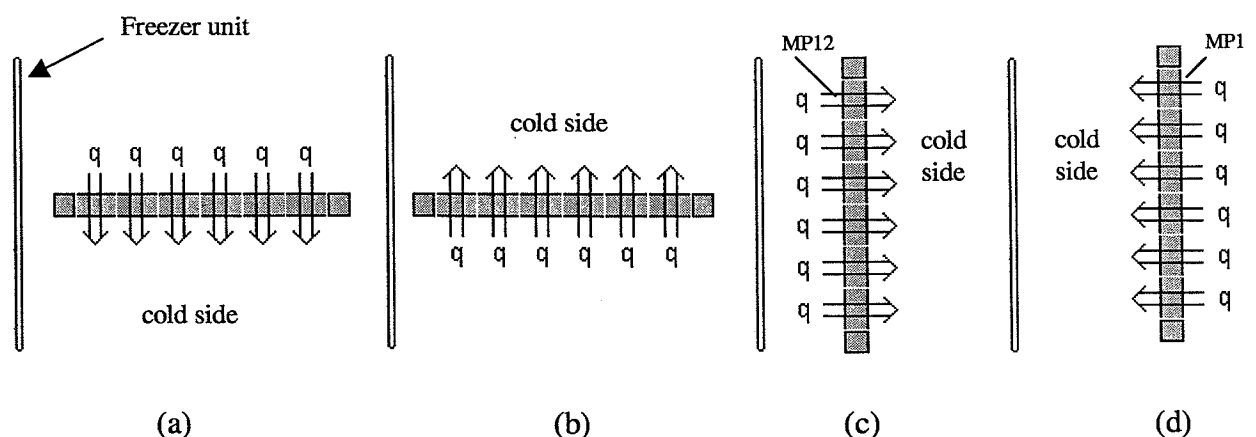
Figure 5.5: Positions of the convection apparatus used in the measurements. Position (a) is the horizontal reference position where no convection occurs. In (b) the apparatus has been turned 180° and the cold side is on top. In this position, convection is possible but not probable with the boundary conditions and materials used. Position (c) and (d) show the two vertical positions. In (c) measuring plate 12 (MP12) is located on top whereas measuring plate 1 (MP1) is located on top in (d). In a complete measuring series, all four positions have been measured.

Position (a) shows the horizontal reference position without convection as the cold side is at the bottom and no driving forces will initiate convection. In position (b) convection is theoretically possible depending on the material properties and thickness. The theoretically calculated convection in this position is insignificant for all the temperature conditions and material properties applied in the measurements. However, the measurement in this position is performed in order to compare the measurement with the theory, as well as to get an impression of the ability of the apparatus when measuring in different positions. The two vertical positions (c) and (d) equal the conditions in a typical wall with perfectly installed insulation. Both positions are measured in order to detect the effect from inhomogenities in the test specimen or from internal apparatus error disturbing the measurement of the heat flow.

The specimen is placed in the apparatus as shown in figure 5.5 and 5.7. The thickness of the inserted specimen is fixed by the impermeable insulation above the guard ring and the plywood cover. To avoid air space between the plywood cover and the test specimen, layers of 3 mm soft foam are placed on top of the test specimen until the thickness of the test specimen and the soft foam exceed the thickness of the guard ring insulation. The thermocouples, which measure the temperature on the cold side of the specimen, are taped on top of the soft foam in each measurement. The thermocouples, which measure the temperature on the hot side, are permanently taped to the measuring plates. In order to measure the temperature field inside the material, 24 thermocouples are placed in the joints between the slabs or rolls as close to the centre as possible.

On stone wool (1) the measurements have been performed with an assigned specimen thickness of 200 mm and 500 mm which equals an aspect ratio of 15 and 6, respectively. Fibre glass (3) is measured at an assigned thickness of 400 mm which equals an aspect ratio of 7.5. The thickness of fibre glass (3) is chosen based on the manufacturer-specified thickness (210 mm). Due to the time limit for the project, a complete measurement series (position a-d) has been performed on stone wool (1), only at a thickness of 500 mm. The rest of the measurements performed within the time limit of the project have been chosen in order to collect an impression of how convection takes place in different materials when different conditions are applied.

According to literature, natural convection in a vertical structure with isothermal and impermeable boundaries should not be considered when $Ra_m < Ra_{m,cr}$.

Ra_m calculated according to eq. (2.21) for the measured structures is shown in table 5.8 together with the corresponding critical values $Ra_{m,cr}$. The values of Ra_m show that, according to the experimental experience, we should not expect the average heat flow to be increased by natural convection when measuring on the low permeable material stone wool (1) which corresponds to the calculations performed by CHConP in chapter 3.

Whereas, in the highly permeable material fibre glass (3) an increase in the average heat flow is expected due to natural convection. When applying the conditions used when measuring fibre glass (3), the CHConP calculation shows an increase in the average heat flow of 7%. This degree of disturbance in the heat flow due to convection should be detectable in the convection apparatus.

Table 5.4: Ra_m calculated according to eq. (2.21) in the performed vertical measurements based on the material properties in table 5.11.

Material	Temp. difference	Surface temperature		Ra_m according to eq.(2.21)	$Ra_{m,cr}$ according to eq.(2.22)		
	ΔT [°C]	T_{hot} [°C]	T_{cold} [°C]		$h/d_m=6$	$h/d_m=7.5$	$h/d_m=15$
Stone wool (1)	20	20	0	11.0	24		60
Stone wool (1)	30	20	-10	17.6			
Stone wool (1)	40	30	-10	21.9			
Fibre glass (3)	40	30	-10	~ 60		30	

The temperature differences and the corresponding surface temperature used in the measurements are shown in table 5.8. Two of the measuring series were performed with a mean temperature of 10°C, and one of the series was performed with a mean temperature of 5°C. The contribution of radiation and conduction to the total heat transfer differs in accordance with the mean temperature however, it is kept at a constant level within the individual measuring series.

Due to a minor vertical temperature gradient in the cold box, the surface temperature difference of the individual measuring sections may differ slightly within the measurements. When calculating the local Nusselt number Nu_i at the twelve measuring sections, differences in surface temperature are taken into account according to eq. ( ):

$$Nu_i = \frac{\dfrac{\Phi_{with\,convection,i}}{\Delta T_{with\,convection,i}}}{\dfrac{\Phi_{without\,convection,i}}{\Delta T_{without\,convection,i}}} \quad , \quad i = 1,..,12 \tag{5.2}$$

The average Nusselt number of the measurement is obtained by eq. (5.):

$$Nu = \frac{\displaystyle\sum_{i=1}^{12} \dfrac{\Phi_{with\,convection,i}}{\Delta T_{with\,convection,i}}}{\displaystyle\sum_{i=1}^{12} \dfrac{\Phi_{without\,convection,i}}{\Delta T_{without\,convection,i}}} \tag{5.3}$$

5.3 Measurements performed in the convection apparatus

In all the measured structures on stone wool (1) the actual modified Rayleigh number, Ra_m, is less than or close to the corresponding critical Rayleigh number whereas the Ra_m in the measured structures on fibre glass (3) exceeds $Ra_{m,cr}$. The calculations performed by CHConP on fibre glass (3) show that natural convection increases the average heat flow by 7% when the aspect ratio is 7.5 and the surface temperature difference 40°C.

In table 5.5 the average Nusselt numbers measured in the convection apparatus are presented according to eq. (5.3).

Table 5.5: Measured influence on average heat flow of performed measurements. "-" signifies that the measurement has not been performed with the apparatus in this position. MP1 and MP12 denote measure plates 1 and 12, respectively.

Material	Surface temp. diff. ΔT [°C]	Surface temperature T_{hot} [°C]		Measured average Nusselt numbers according to eq. (5.3)						
			T_{cold} [°C]	Vertical position					Horizontal "heat flow upwards"	
				h/d = 6		h/d=7.5		h/d=15		
				MP1 on top	MP12 on top	MP1 on top	MP12 on top	MP1 on top	d=0.4m	d=0.5 m
Stone wool (1)	20	20	0	1.01	0.99	-	-	1.01	-	0.98
Stone wool (1)	30	20	-10	1.02	1.00	-	-	1.01	-	0.97
Stone wool (1)	40	30	-10	1.01	0.99	-	-	-	-	0.95
Fibre glass (3)	40	30	-10	-	-	1.07	1.17	-	0.99	-

When regarding the measurements made in the vertical positions on stone wool (1), the average Nusselt numbers fluctuates around "1.00" which is the exact value if no convection occurs. The deviations from unity correspond to the reproducibility found when performance testing the apparatus which was approx. 1.2% when keeping the specimen in place. This means that the measurements performed on stone wool (1) show no significant increase in the overall average heat flow caused by natural convection; which concurs with the theoretical considerations. However, considering the distribution of heat flow over the height of the specimen, we find that natural convection occurs in the material even if the surface temperature difference is only 20°C. The measured distribution of heat flows and temperatures is presented in section 5.4.

The measurement on fibre glass (3) in the vertical position with MP1 on top shows an increase in the average heat flow of 7%, whereas the increase becomes 17% when Mp12 is located on top. As there is no known asymmetry built in the specimen or in the apparatus to cause this big difference between the two positions, a probable slide movement of the inserted specimen, which also may have caused minor air gaps inside the specimen, may explain the big difference when the apparatus was turned. The lowest measured increase in the average Nusselt number corresponds to the calculations performed by CHConP.

In table 5.5 also the measured average Nusselt numbers in the horizontal position with heat flow upwards are presented. When regarding the measurements on stone wool (1), all the Nusselt numbers are less than one and seem to decrease with the surface temperature

difference throughout the specimen. To clear up this discrepancy, disturbances from the guard sections in the horizontal measurements have been examined in the following paragraphs.

5.3.1   Examination of disturbance in horizontal measurements

All the guard sections in the convection apparatus are controlled by thermopiles. When performance testing the apparatus, five of the thermopiles were found unstable. The five guard sections, which had unstable thermopiles, were: GR1, GB2, GSR2, GSB2 and GSR12. The location of the individual guards is shown in Appendix B. When attempting to check the thermopile it was either not possible to change it, as most of the parts in the apparatus are glued together, or it was not possible to detect the soldering flaw in the thermopile. The regulation of the apparatus was designed with a security system, which switches off all the power supplies if just one of the measured temperatures in the apparatus exceeds a critical limit. To prevent the unstable thermopiles from interrupting the measurements, the affected guard sections have been regulated according to the other guard sections with the same position in the apparatus. The most important guards affected by the defective thermopiles are the guard ring (GR1) which serves measuring plate 1 (MP1), and the bottom guard (GB2) which serves to prevent heat loss throughout the bottom at the right side of measuring plate 1- 4.

To examine if the poor regulation of GR1 has been able to cause the Nusselt numbers in the horizontal position to become less than "1.00" in all the measurements, the measured temperature difference between GR1 and MP1 has been simulated by use of HEAT2. HEAT2 is a computer program for calculating two-dimensional heat transfer, Blomberg [1996]. The HEAT2 model includes half of the convection apparatus. The distance between GR1 and MP1 is calculated at 0.005 m, and the material properties of stone wool (1) are used at a specimen thickness of 0.5 m. Figure 5.6 shows a sketch of the HEAT2 model.
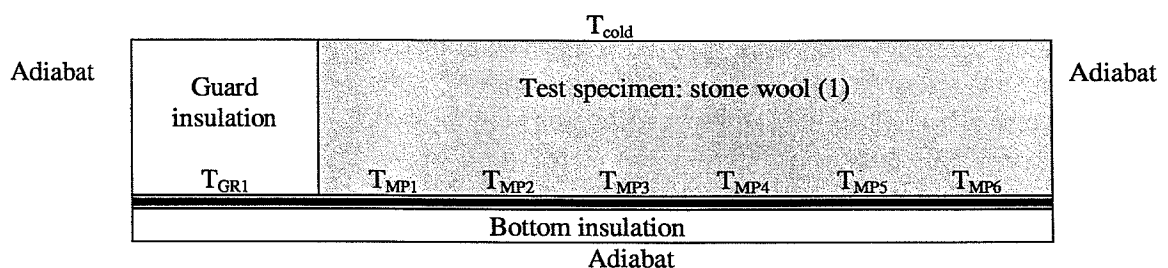
Figure 5.6:   Sketch of HEAT2 model modelling half of the convection apparatus. The boundary conditions applied in the model are given in the figure. T_{GR1} is the temperature of guard ring 1 and T_{MP} is the temperature of the corresponding measuring plate.

Table 5.6 shows the simulated temperatures of GR1, the measuring plates and the cold side temperature, together with the calculated heat flow ratio of MP1. Table 5.6 also shows the calculated error in the absolute measurements performed by MP1 caused by the measured temperature difference between MP1 and GR1 when compared to the situation of equal temperature on MP1 and GR1.

Table 5.6: Calculated disturbance caused by temperature difference measured between GR1 and MP1 on the heat flow ratio measured by MP1 in horizontal position with heat flow upward. The last column shows the calculated error in the absolute measurement of the heat flow performed by MP1 caused by the existing temperature difference between MP1 and GR1 compared to the situation of equal temperature of MP1 and GR1.

Apparatus position	Internal temperatures		Boundary temperature	Heat flow ratio	Error in MP1 due to temp. diff. between MP1 and GR1
	T_{GR1} [°C]	T_{MP1-6} [°C]	T_{cold} [°C]	MP1	
Heat flow upwards	19.80	20	0	0.973	5.6%
Reference	19.69	20	0		8.6%
Heat flow upwards	19.75	20	-10	0.967	4.7%
Reference position	19.55	20	-10		8.2%
Heat flow upwards	29.69	30	-10	0.972	4.3%
Reference position	29.47	30	-10		7.3%

Table 5.6 shows that the temperature difference between GR1 and MP1 in all the measurements was greater in the horizontal reference position than in the horizontal position with heat flow upward. The table also shows that this results in a greater heat flow in the reference position than in the horizontal position with an upward heat flow. In both cases the temperature difference between GR1 and MP1 will cause an error in the measured heat flow performed by MP1 which in the reference position exceeds 8%. The error in the absolute measurement decreases as the heat flow increases with the surface temperature difference.

In the apparatus GR1 is regulated according to GR5 which is placed in the opposite direction on the apparatus meaning that when GR1 is close to the freezer unit, GR5 is at the opposite end and vice versa. The heat losses from GR1 and GR5 have not been equal contrary to our expectations, and a better regulation of GR1 could probably have been achieved by regulating GR1 according to GR2 or GR8.

Figure 5.7 shows the calculated disturbance caused by the too low temperature of GR1 on the heat flow ratio in horizontal positions with heat flow upwards on the six simulated measuring plates.

The heat flow ratio calculated for measuring plates 2 - 6 exceeds 0.999 in all the calculations which means that the temperature of GR1 mainly affects the measured heat flow from measuring plate 1.
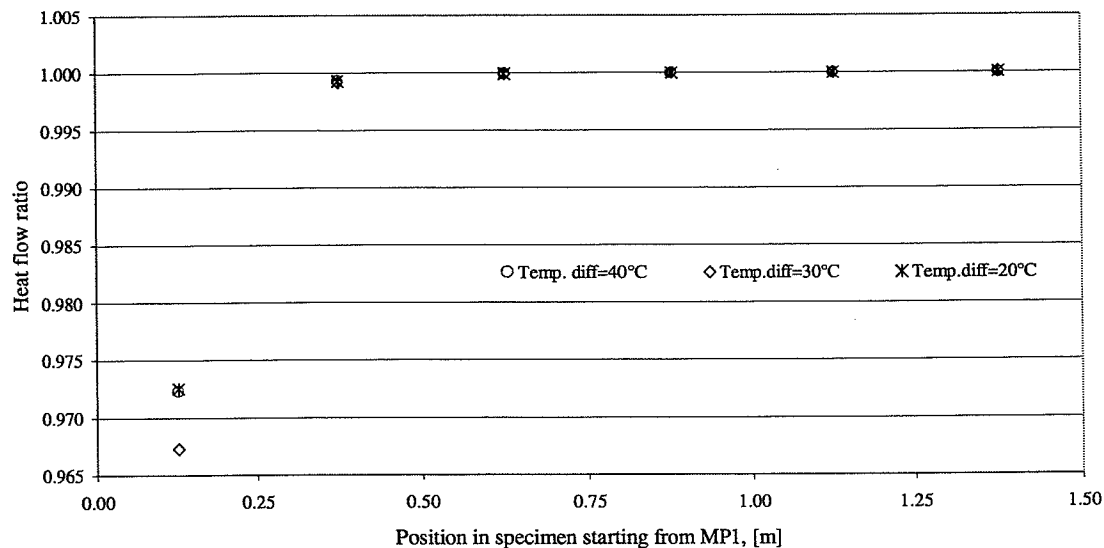
Figure 5.7: Calculated heat flow ratio in horizontal position with heat flow upwards, based on the actual measured temperature differences between MP1 and GR1 when measuring stone wool (1) of a thickness of 500 mm.

The other important guard section, in which the thermopile was unstable, was the one on the bottom guard which covers the right side of measuring plates 1 – 4. Instead, this guard was regulated according to the bottom guard, which covers the left side of measuring plates 1 – 4. In table 5.7 the measured heat flow is corrected according to the measured temperature differences between the measuring plates and the bottom guards before calculating the average Nusselt numbers.

Table 5.7: Average Nusselt numbers in horizontal position when the measured heat flows are corrected to the measured temperature difference between the measuring plates and the bottom guards. "♣" This measurement has been repeated in order to verify the significance of the average Nusselt numbers measured.

Material	Surface temperature		Average Nusselt numbers of horizontal position with heat flow upwards and a specimen thickness at 500 mm	
	T_{hot} [°C]	T_{cold} [°C]	measured	corrected
Stone wool (1)	20	0	0.98	0.97
Stone wool (1)	20	-10	0.96	0.96
Stone wool (1)♣	20	-10	0.98	0.96
Stone wool (1)	30	-10	0.95	0.97

The concern was that the measured Nusselt numbers in the convection apparatus decreased with increasing surface temperature difference, and that the Nusselt numbers consistently became less than "1.00". As table 5.7 shows, the average Nusselt numbers in the horizontal position remains less than "1.00" when the heat flows are adjusted according to the measured temperature differences between the measuring plates and the bottom guards. But now the Nusselt numbers no longer decreases with the surface temperature difference.

This result, - together with the previous investigation of the disturbance from the temperature difference between the guard ring and the measuring plates, - indicates that the measured average Nusselt numbers in the horizontal position are less than "1.00" due to the error in guard regulations which prevents some of the guards from compensating for small deviations in temperature conditions in the cold box. As the heat flows become very small as the specimen thickness increases, the measurement becomes very sensitive even to small temperature differences between the measuring plates and the guard sections.

Another probable circumstance is that cracks have occurred between the individual layers of soft foam placed between the specimen and the plywood cover, and that the net weight of the specimen will make the cracks disappear when the specimen is placed above the soft foam. In that case an air gap between the specimen and the measuring plates will only occur in the reference position. As the temperatures are measured on the measuring plates, an air-gap between the specimen surface and the measuring plates will cause a surface resistance to become part of the measurement. The value of the surface resistance depends on whether there are air-movements in the crack and on the temperature difference between the measuring plates and the specimen surface. The conduction/convection in the air crack, the unknown change in specimen thickness when measuring, and the surface resistance will all influence the measured heat flow in the horizontal reference position, in which the various contributions are inseparable due to the used measuring principle. This problem could probably have been avoided by using thicker layers of soft foam and by avoiding joints in the soft foam - this will be controlled in the further work.

In Table 5.8 the measured thermal conductivities in the convection apparatus are compared to the measurement performed in the heat flow meter apparatus. The measurements performed with heat flow upwards concur within 1%, whereas the deviation in the reference position reaches 5% and seems to increase with the temperature of the measuring plates.

Table 5.8: Average thermal conductivity λ_{10} of stone wool (1) measured in convection apparatus (thickness = 500 mm) compared to measurement in heat flow meter apparatus (thickness = 100 mm).

	Surface temperature difference	λ_{10} [W/m·K]	Deviation compared to heat flow meter
Heat flow meter	20°C	0.0352	
Convection apparatus:			
Reference position	20°C	0.0364	3.4%
Heat flow upwards	20°C	0.0355	1%
Reference position	40°C	0.0370	5%
Heat flow upwards	40°C	0.0352	0%

In this section different factors which could disturb the measured heat flow in the convection apparatus have been considered, and it is reasonable to think that the observed distortion is caused by a combination of the factors considered above. From the investigation it is obvious that the measurement performed in the horizontal position with heat flow upwards is less disturbed by errors. However, in the heat flow patterns presented in section 5.4 the measurement from the reference position has been used as reference in order not to over-

interpret the results. Using the measurement from the position with heat flow upwards as reference would cause the deviation from unity in the heat flow pattern to increase further.

5.4 Measured heat flow pattern and temperature profiles

This section presents the heat flow patterns and temperature profiles of the measurements performed which have been investigated in order to detect the potential effect of natural convection in the measured structures. The average Nusselt number in the vertical position was only found to increase in the measurement on fibre glass (3). In the rest of the measurements no significant increase in the overall heat flow was observed due to natural convection.

In the section the measurements are presented as relative measurements; the absolute values expressed as thermal conductivity can be found in appendix C.

5.4.1 Stone wool (1) in vertical position (h/d$_m$ =15)

Stone wool (1) with an aspect ratio of h/d$_m$ = 15 has only been measured in one vertical position together with the corresponding horizontal reference position. The measurements have been performed with two surface temperature differences: 20°C and 30°C. In figure 5.8 the measured heat flow patterns are presented as the local Nusselt numbers calculated according to eq. (5.2).
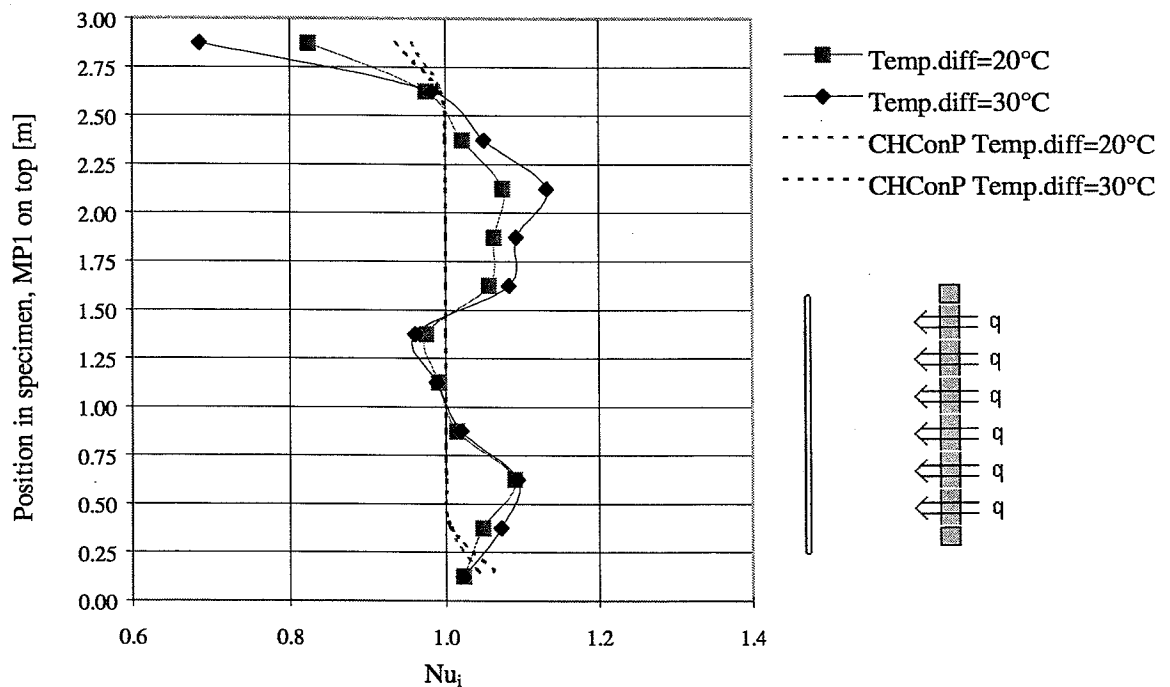
Figure 5.8: Heat flow pattern – stone wool (1): local Nusselt numbers when measuring in vertical position with the aspect ratio h/d = 15 and the surface temperature differences 20°C and 30°C, respectively. The dotted lines show the heat flow pattern calculated by CHConP. The vertical position of the apparatus is shown at the right-hand corner.

The temperature profiles measured in the middle of stone wool (1) are shown in figure 5.9 when measuring the heat flow with the apparatus placed in both the horizontal reference position and the vertical position with MP1 on top.

Local variations exist in the temperature profiles which, in the horizontal positions, should be linear if no convection occurs, and the thermal properties within the specimen were homogeneous. The local variations are presumed to be caused by local variations in the thermal conductivity of the test specimen and uncertainty in the temperature measurement. The expected variation in temperature, calculated on basis of the density variation measured on the slabs and assuming the thermal conductivity to be temperature independent, is shown together with the measured temperature profiles in figure 5.9.

When considering the temperature profile in the horizontal position when a surface temperature difference of 30°C is measured, it is obvious that the upper temperature is influenced by GR1, which was too cold. The temperature differences between MP1 and GR1 and MP12 and GR5 are shown in table 5.9. A positive difference signifies that the measuring plate is warmer than the guard ring section.

47

As it is obvious that MP1 in the different measurements is disturbed in various ways by the poor regulation of GR1, the measurement performed by MP1 should not be considered very significant. The analysis made in section 5.3.1 showed that the distortion of MP1 not is going to disturb the measurements of the rest of the measuring plates.
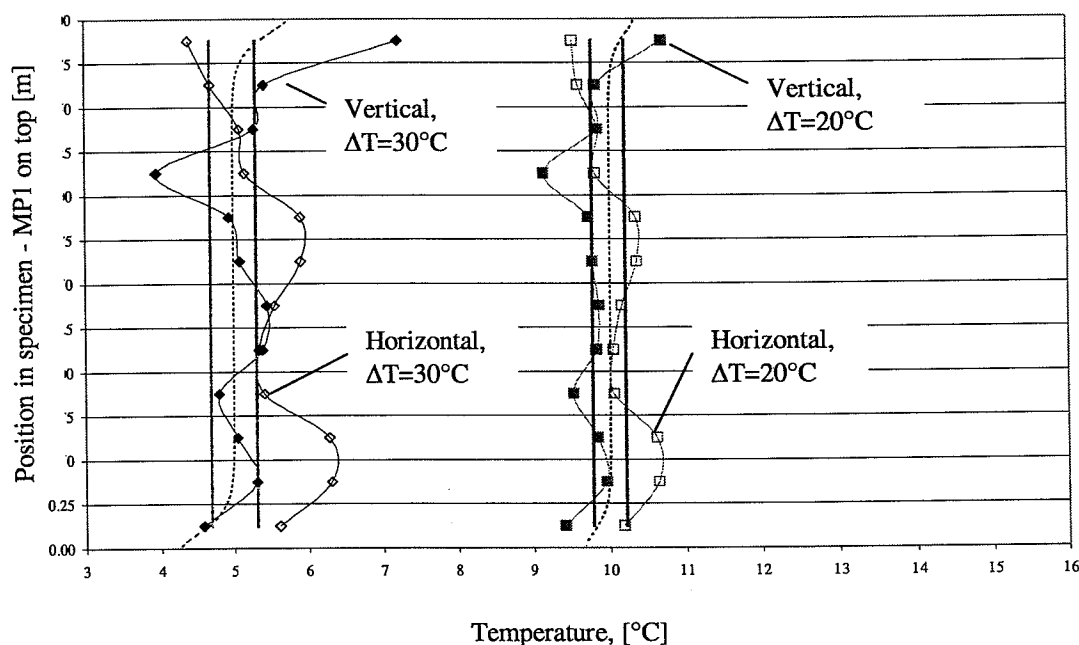
Temperature, [°C]

Figure 5.9: Stone wool (1): temperature profiles 0.1 m above the measuring plates when measuring a surface temperature difference of 20°C and 30°C in both the horizontal reference position and in the vertical position with MP1 on top. The dotted curves show the corresponding temperature profiles calculated by CHConP in the same position. The vertical lines show the temperature ranges within the temperatures are expected to vary due to inhomogenities in the specimen properties.

Table 5.9: Temperature differences between the measuring plate and the guard ring supporting the measuring plate. If the guard ring becomes colder than its measuring plate, the temperature difference becomes positive and vice versa. The regulation of GR5 works as intended.

Material	Apparatus position h/d = 15	Surface temperature difference, [°C]	Temperature difference between MP1 and GR1	Temperature difference between MP12 and GR5
Stone wool (1)	MP1 on top	20	0.053	-0.012
Stone wool (1)	Horizontal	20	-0.019	-0.022
Stone wool (1)	MP1 on top	30	-0.170	-0.025
Stone wool (1)	Horizontal	30	0.877	-0.010

Comments on results

Both the heat flow patterns and the change in the temperature profiles from the reference position to the vertical position indicate the occurrence of natural convection in the specimen when compared to the measurements performed on the impermeable material in the performance test of the apparatus. The occurrence of natural convection concurs with the result obtained by CHConP.

In contrast to the CHConP calculations, which only show little distortion at the top and bottom due to one convection cell, both the heat flow pattern and the temperature profiles seem to indicate that there is more than one convection cell in the specimen. In the CHConP calculations the material properties are assumed to be constant in each direction. However, this is not the case in real materials in which there will be local variations in the individual slabs and overall variations as the total test specimen consists of several slabs.

The fluctuations in the temperature profiles measured in the horizontal positions indicate local variations in the thermal conductivity as the fluctuations increase with the temperature difference. The measured fluctuations seem to be reasonable when comparing to the expected variation in thermal conductivity from variation in the measured density and also when remembering the temperature profiles measured in the polystyrene specimen in which the thermal conductivity is expected to be more homogeneous.

Furthermore, the existence of joints between the individual slabs - especially in the height of the specimen - may cause some local changes in permeability; which again may have the effect that the convection cell is divided into several mixed cells.

5.4.2 Stone wool (1) in vertical position (h/d$_m$ = 6)

Stone wool (1) with an aspect ratio h/d$_m$ = 6 is measured with the apparatus placed in the two vertical positions. The upper chart in figure 5.10 shows the heat flow pattern when the apparatus is placed with measuring plate 1 located at the top, and the bottom chart shows the heat flow pattern when the apparatus has been turned around 180° and measuring plate 12 is located at the top.
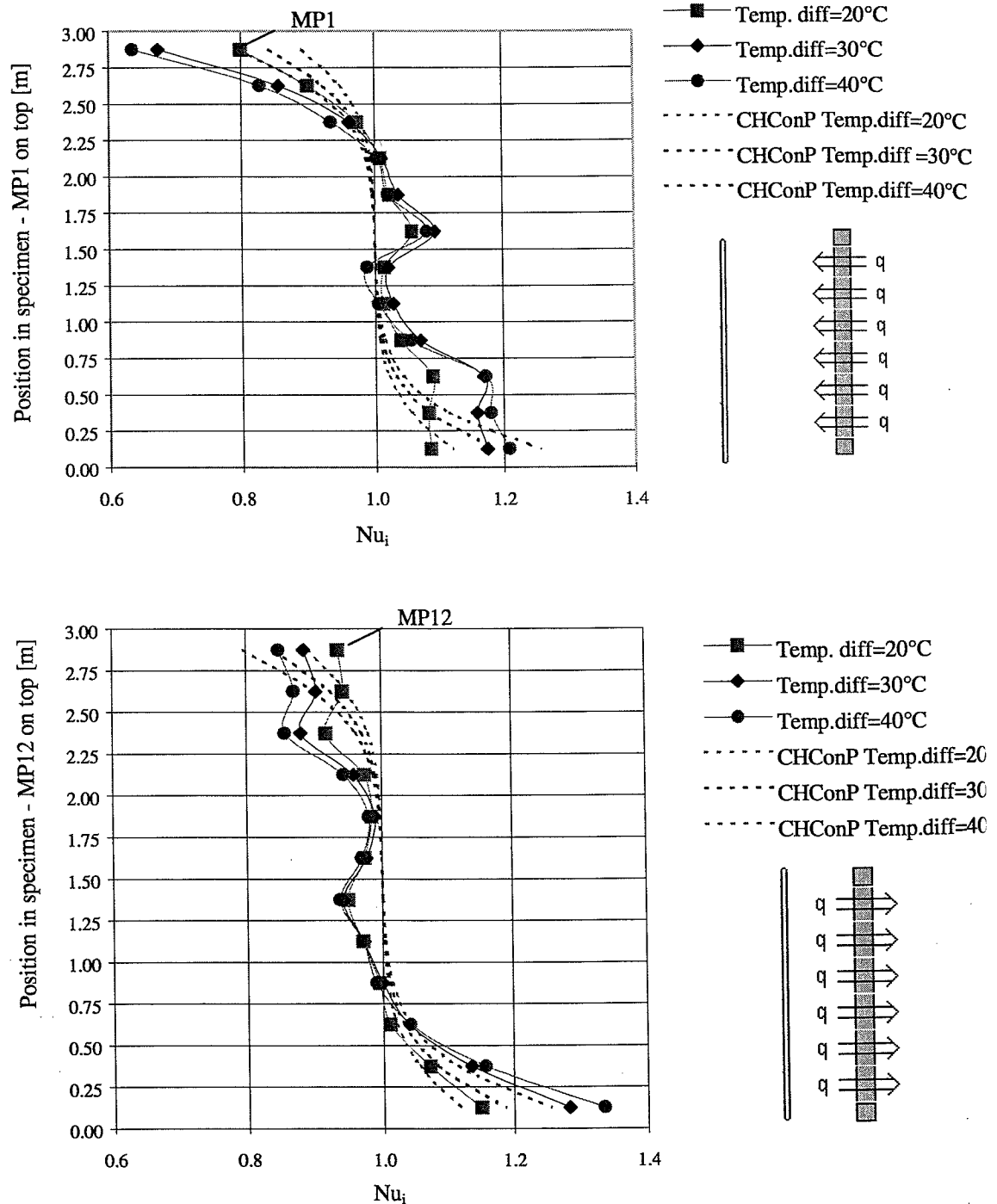
Figure 5.10: Heat flow pattern - stone wool (1): calculated and measured local Nusselt numbers in the vertical positions with aspect ratio h/d$_m$ = 6, and surface temperature differences of 20°C, 30°C, and 40°C, respectively. The upper chart shows MP1 located on top and the lower chart shows MP12 located on top. In both charts the vertical position of the apparatus is shown in the right-hand corner.
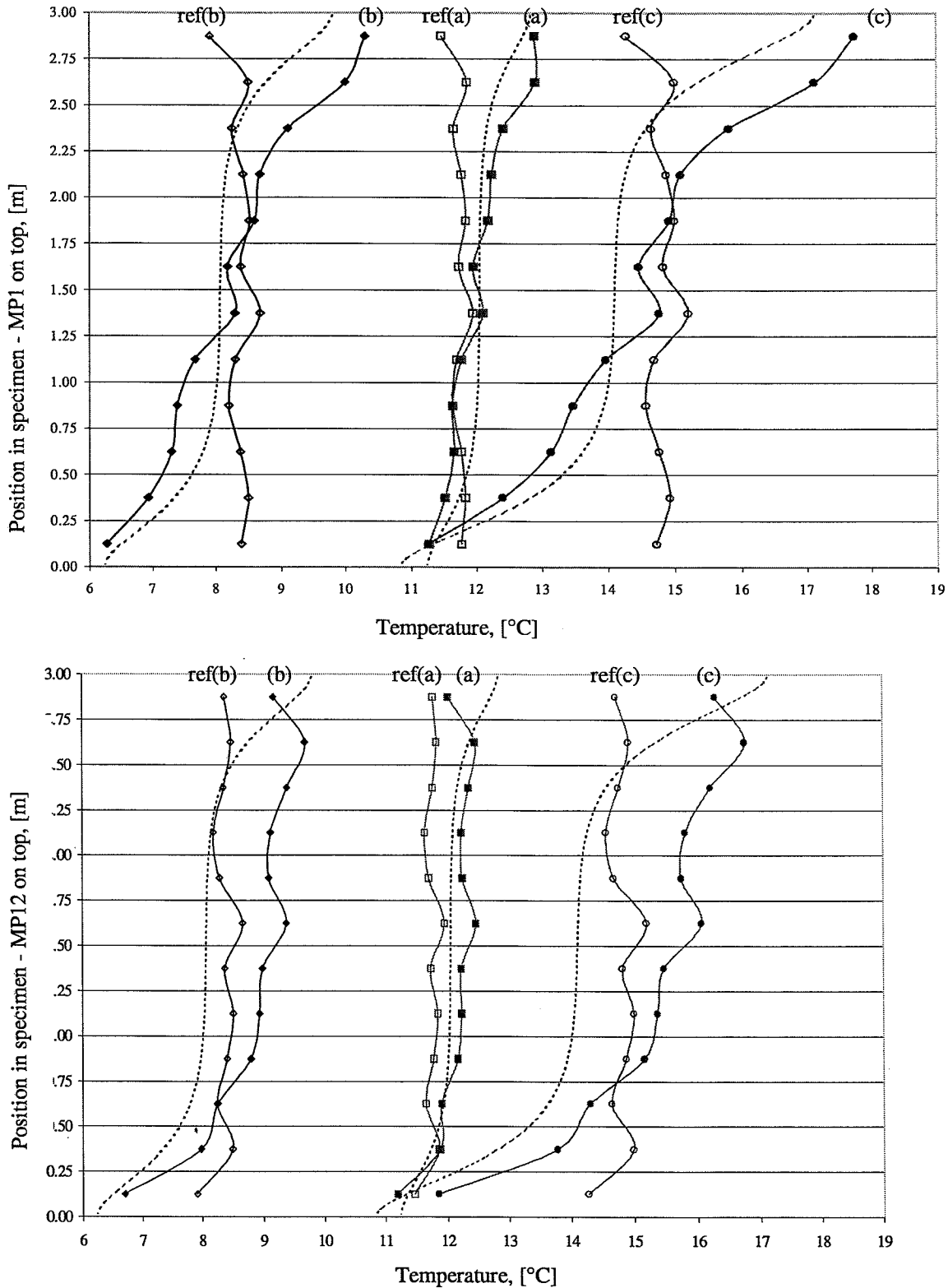
Figure 5.11: Stone wool (1): temperature profile 0.2 m above the measuring plates when measuring an aspect ratio h/d_m = 6, and a surface temperature difference of (a) = 20°C, (b) = 30°C, and (c) = 40°C. "ref" signifies the measurement made in the horizontal reference position. The upper chart shows MP1 located on top, whereas the lower chart shows MP12 located on top. The dotted line shows the temperature profile 0.2 m above the measuring plates calculated by CHConP when natural convection occurs. In the CHConP calculations the temperature dependence of the thermal conductivity is not included which causes the difference between the measured and the calculated temperature level to increase when the temperature difference increases.

51

Figure 5.11 shows the temperature profiles at a distance of 0.2 m above the measuring plates. In this figure the corresponding temperature profiles calculated by CHConP are shown as dotted lines. The upper part of the figure shows the temperatures when MP1 is located on top and the lower part when MP12 is located on top. The temperatures are measured at both the right and the left side of the specimen, the temperature profiles shown in figure 5.11 are the average of the two measured temperatures above each measuring plate. The distortion from the poor regulation of GR1 is clearly affecting the measurement of MP1 in both vertical positions of the apparatus. An overview of the measured temperature difference between GR1 and MP1 is shown in table 5.10 together with the similar temperature difference when measuring the horizontal reference position.

Table 5.10: Measured temperature difference between MP1 and GR1 when the convection apparatus is placed in the two vertical positions and in the horizontal reference position. A positive temperature difference means that the measuring plate has been warmer than the guard ring.

Material	Apparatus position	Surface temperature difference [°C]	Temperature difference between MP1 and GR1 [°C]	Temperature difference between MP1 and GR1 in horizontal reference position, [°C]
Stone wool (1)	MP1 on top	20	-0.034	0.313
Stone wool (1)	MP1 on top	30	-0.312	0.449
Stone wool (1)	MP1 on top	40	-0.571	0.532
Stone wool (1)	MP12 on top	20	0.443	0.313
Stone wool (1)	MP12 on top	30	0.863	0.449
Stone wool (1)	MP12 on top	40	1.323	0.532

Table 5.10 shows that when MP1 is located on top the measured heat flow becomes too small due to the heat flow contribution from GR1 to MP1 which increases as the surface temperature difference increases. The opposite occurs when measuring the horizontal reference position; the measured heat flow from MP1 becomes too large as a heat flow is contributed from MP1 to GR1. Both occurrences cause the measured local Nusselt number of MP1 to become less than if GR1 had worked properly. When MP12 is located on top, GR1 becomes colder than MP1 which causes a heat flow contribution from MP1 to GR1 which is greater in the vertical position than in the horizontal position. Here, this circumstance causes the local Nusselt number of MP1 to become greater than if GR1 had worked properly.

Comments on results

When the specimen thickness is increased to 0.5 m, the variations in the heat flow pattern become more significant than when the specimen thickness was 0.2 m. Two maxima/minima dominate the heat flow pattern when the conditions at the top and bottom are ignored. At a specimen thickness of 0.5 m the local maxima/minima follow the measuring plates when the apparatus is turned 180°. When comparing the heat flow pattern with the specimen thickness of 0.2 m, the local deviation still exists, but not at the exact same locations. This leads to the conclusion that the heat flow patterns stem from the inserted specimen and not from the apparatus. Although the shape of the heat flow pattern indicates the existence of more than one convection cell, this can not be confirmed by the average temperature profile as the

temperature profile in the vertical position only has one point of intersection with the temperature profile in the horizontal reference position.

From these temperature profiles it is obvious that the numerical change in temperature increases as the surface temperature difference increases, and that the temperature in the upper part of the specimen becomes higher, whereas the temperature in the bottom part becomes lower than the horizontal reference position. However, the temperature on top when measuring with MP12 on top seems to become lower than expected.

The deviations from a linear temperature profile in the horizontal reference positions caused by inhomogenities in the test specimen increase with the surface temperature difference as expected. The effect from the inhomogenities reoccurs in the vertical measurements. The shape of the measured temperature profiles matches the calculated profiles quite well considering the distortion from the guard regulation and the inhomogenities in the test specimen. The calculated profile only includes one convection cell and does not consider the temperature dependence of the thermal conductivity of the specimen.

5.4.3   Stone wool (1) in horizontal position with heat flow upwards ($d_m = 0.5$ m)

The heat flow patterns in the horizontal position with the heat flow upwards have been measured on stone wool (1) with a specimen thickness of 0.5 m. Figure 5.12 shows the measured heat flow pattern, and figure 5.13 shows the temperature profiles 0.2 m above the measuring plates in both the horizontal reference position and the horizontal position with heat flow upwards.
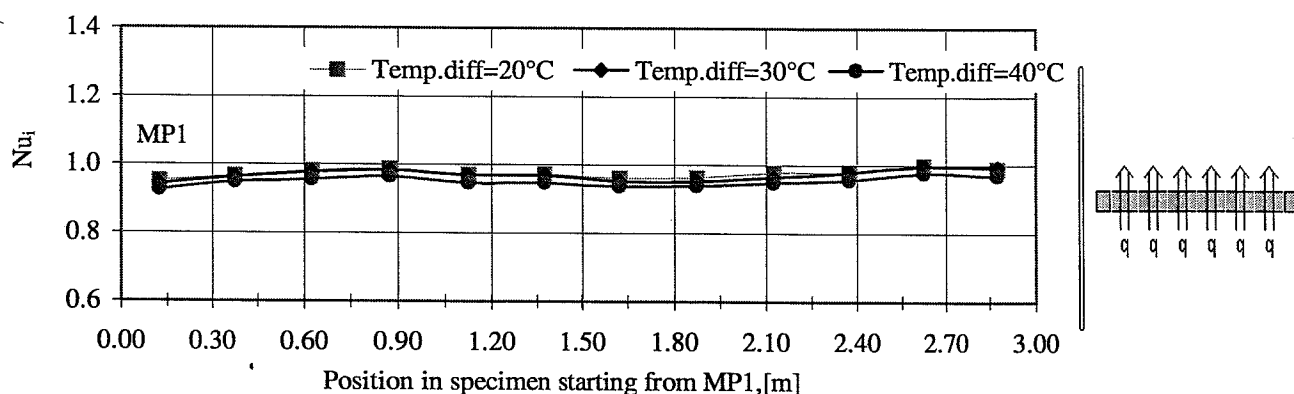
Figure 5.12: Heat flow pattern - stone wool (1): local Nusselt numbers measured in the horizontal position with heat flow upwards when the thickness is 0.5 m and the surface temperature differences 20°C, 30°C, and 40°C, respectively.
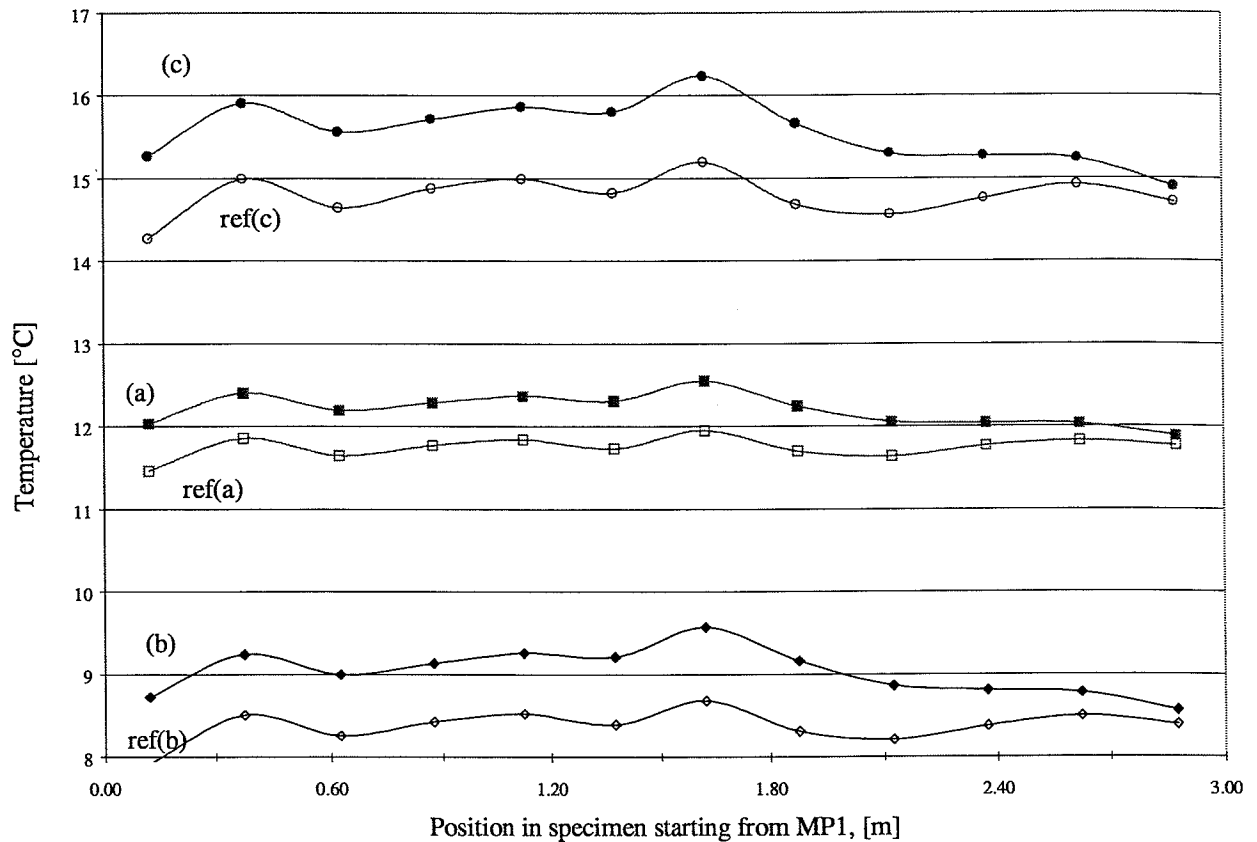
Figure 5.13: Stone wool(1): temperature profile 0.2 m above the measuring plates when measuring a thickness of 0.5 m in the horizontal position with heat flow upwards and a surface temperature difference of (a) = 20°C, (b) = 30°C, and (c) = 40°C. "ref" signifies the measurement made in the horizontal reference position.

Comments on results

If no convection occurred and the ability of the apparatus to measure in both horizontal positions was equal, then the local Nusselt numbers should be unity. The local Nusselt numbers in the horizontal position with heat flow upwards are measured to be within 0.96 and 1.0. As discussed in section 5.3.1, the measurements are influenced by the poor regulation of some of the important guard sections which caused the heat flow in the horizontal reference position to become less than in the horizontal position with heat flow upwards, and probably influenced by air cracks which have exists between the soft foam layers.

Regarding the temperature profiles in figure 5.13, the temperatures measured in the reference positions are consistently lower than the corresponding temperatures measured in the position with heat flow upwards. Due to a small, vertical temperature gradient in the cold box, the temperature on the cold side of the convection apparatus changes with the position of the apparatus. Thus the cold side temperature is lower when measuring in the horizontal reference position than in the position with heat flow upwards. For instance, when measuring a surface temperature difference of 40°C, the actual surface temperature difference in the horizontal reference position was 40.2°C, whereas it was only 39.5°C when measuring with heat flow upwards. A minor part of the difference in the measured temperatures is caused by the fact that the surface temperature difference is not equal in the two positions. When approximating

54

the temperature profile throughout the specimen as linear and correcting according to the actual surface temperatures, the remaining difference in temperature at "$x = 0.2$ m" corresponds to the distance from the measuring plates to the thermocouples having been increased by 6-7 mm in the reference position. Based on this observation, it is reasonable to think that the net weight of the specimen compresses the air cracks in the soft foam layers and causes the specimen to sink against the cold side when the apparatus is turned into the horizontal reference position, and that this will cause an increase in the distance between the thermocouples and the measuring plates.

5.4.4   Fibre glass (3) in vertical position ($h/d_m = 7.5$)

The measurements on fibre glass (3) have been performed with a surface temperature difference of 40°C only. Figure 5.14 shows the heat flow pattern measured in the two vertical positions together with the heat flow pattern calculated by CHConP. Figure 5.15 shows the corresponding temperature profiles measured on the cold side, in the centre, and on the hot side in each side of the apparatus.
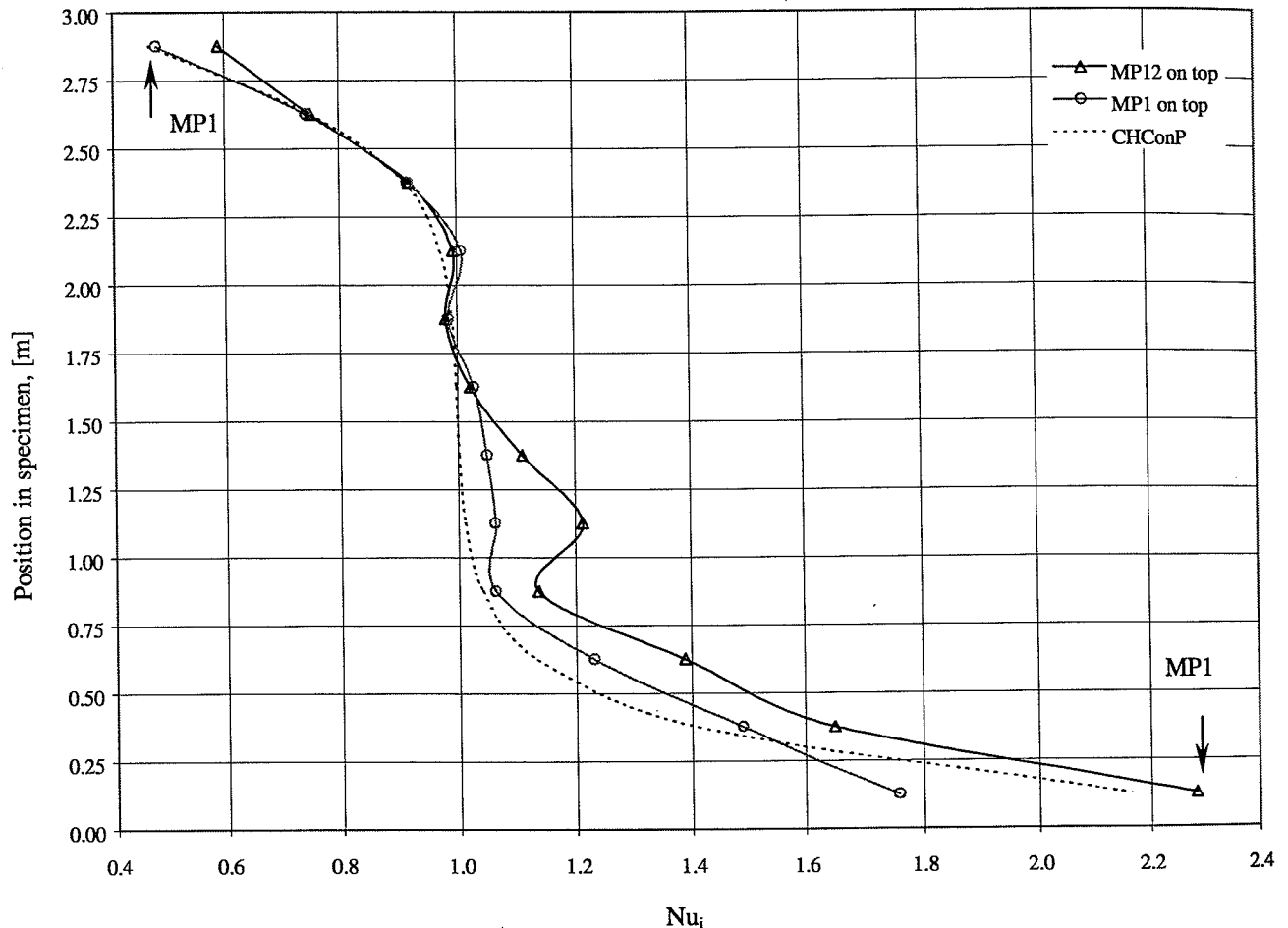
Figure 5.14: Heat flow pattern - fibre glass (3): calculated and measured local Nusselt numbers in the two vertical positions with an aspect ratio $h/d_m = 7.5$ and a surface temperature difference of 40°C. The dotted curve shows the heat flow pattern calculated by CHConP when using the permeabilities from table 3.1.

In the measurement with MP1 located on top, GR1 became 3°C too warm; which means that GR1 has helped MP1 in this position and the measurement by MP1 has become "too good". With MP1 located at the bottom GR1 was 3.7°C too cold; which means that MP1 in this position has had extra edge losses and the measurement by MP1 was "too poor".

However, as the measured heat flow increases, the measurement becomes less sensible to balance error between the measuring plates and the guards.

56
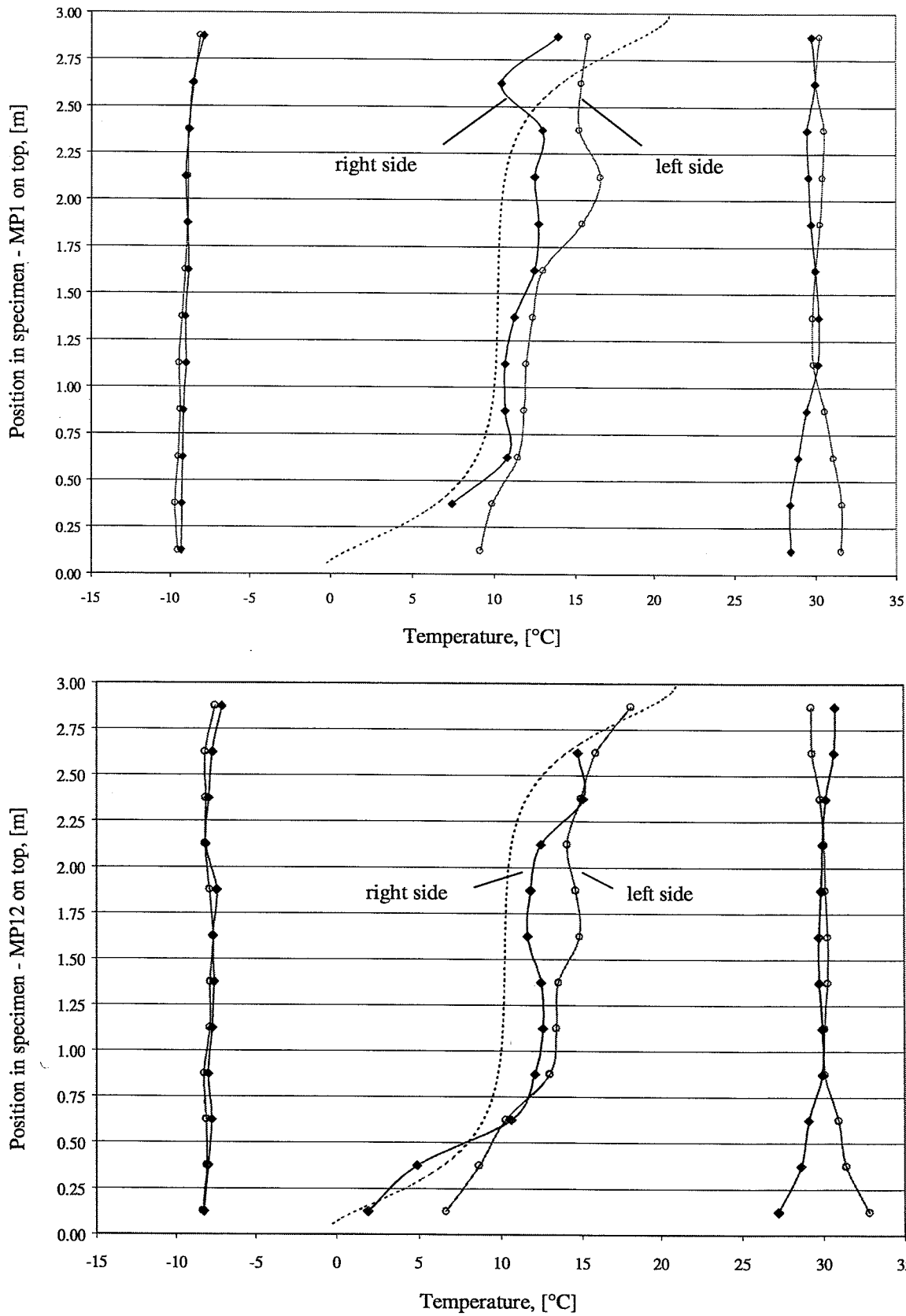
Figure 5.15: Fibre glass (3): temperature profiles measured at the right and left sides in the specimen on the cold side, in the middle, and on the hot side with a surface temperature difference of 40°C and an aspect ratio of $h/d_m = 7.5$. The dotted curves show the temperature in the middle calculated by CHConP. The upper chart shows the temperature when MP1 is located on top and the lower chart shows the temperature when MP12 is located on top.

57

Comments on results

The heat flow pattern in fibre glass (3) is much more influenced by convection at the upper and lower parts of the specimen in comparison to the measurement made on stone wool (1). If only the measurement at the edge made by MP12 is considered, the maximum distortion at the edge seems to become lower than calculated by CHConP. The plastic cover in which fibre glass (3) was enclosed was taped to the inside of the apparatus, taping the plastic cover to the top and bottom may have reduced the effect of convection in the specimen compared to the situation without impermeable layers in the specimen.

The local Nusselt numbers in the lower half of the specimen in both vertical positions become greater than expected. With MP12 at the top, an increase in the local Nusselt number appears at a distance of 1.125 m from the bottom. However, this distortion cannot be related to the measured temperature profile in the centre of the specimen.

The increase in the total measured heat flow is 7% when MP1 is positioned on top; which matches the increase calculated by CHConP. However, when MP12 is positioned on top, the total heat flow increases by 17% compared to the horizontal reference position. The difference in the total heat flow between the two vertical positions is probably due to the arrangement of the specimen in the apparatus. Even though the specimen was fixed very carefully to the guard insulation when it was fitted into the apparatus, the measurements performed indicate that the specimen or parts of the specimen may have changed position in the apparatus when the position of the apparatus was changed.

With regard to the temperature profiles in the centre of the specimen, it should also here be remembered that the plastic cover may have interrupted some of the air movements in the material, and that the thermocouples were placed between the plastic covers. The measurements made in the centre of the specimen show a temperature difference of up to 5°C across the specimen. As equal differences in temperatures across the specimen in the centre also are apparent when the two horizontal positions are measured, the main part of the temperature difference across the specimen is assumed to be caused by difference in thermal conductivity in the inserted specimen.

The great temperature difference across the specimen affects the temperature distribution on the measuring plates. The temperature in the cold box keeps the temperature on the cold side of the apparatus constant, whereas the temperature of each measuring plate is regulated according to the mean temperature of two measuring points on each plate. If a big variation exists in the thermal conductivity of the inserted specimen across the measuring plates, the measuring plate itself is not able to maintain a uniform temperature distribution. When measuring stone wool (1), a maximum difference of 1.5°C was observed between the two temperatures measured on the measuring plates, whereas the difference reaches 5.7°C when measuring fibre glass (3).

5.4.5　　　Fibre glass (3) in horizontal position with heat flow upwards (d_m = 0.4 m)

The heat flow pattern in the horizontal position with heat flow upwards has been measured on fibre glass (3) with a specimen thickness of 0.4 m. Figure 5.16 shows the measured heat flow pattern, and figure 5.17 shows the temperature profile in the middle of the specimen measured at the right and left side in both the horizontal reference position and the horizontal position with heat flow upwards.
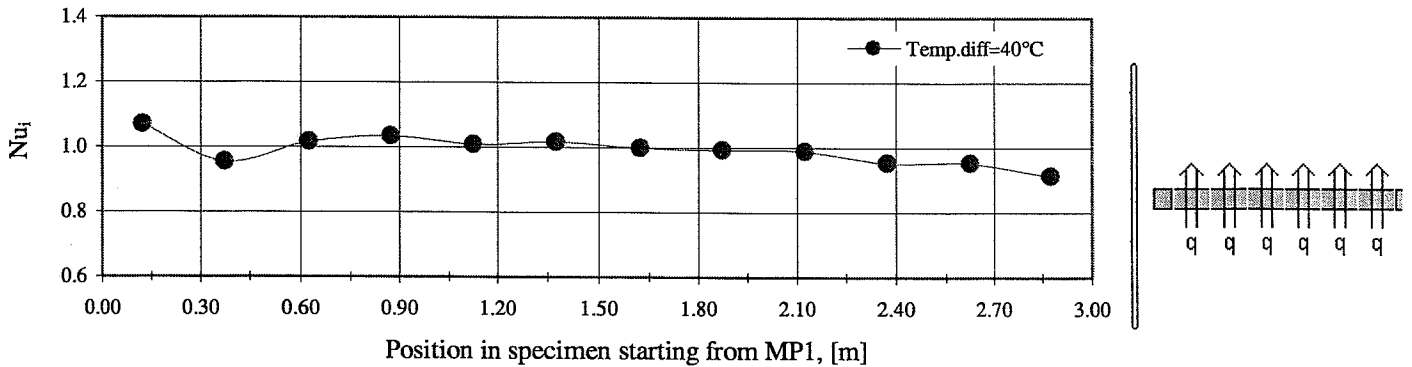
Figure 5.16: Heat flow pattern - fibre glass (3): local Nusselt numbers measured in the horizontal position with heat flow upwards with a specimen thickness of 0.4 m and a surface temperature difference of 40°C.
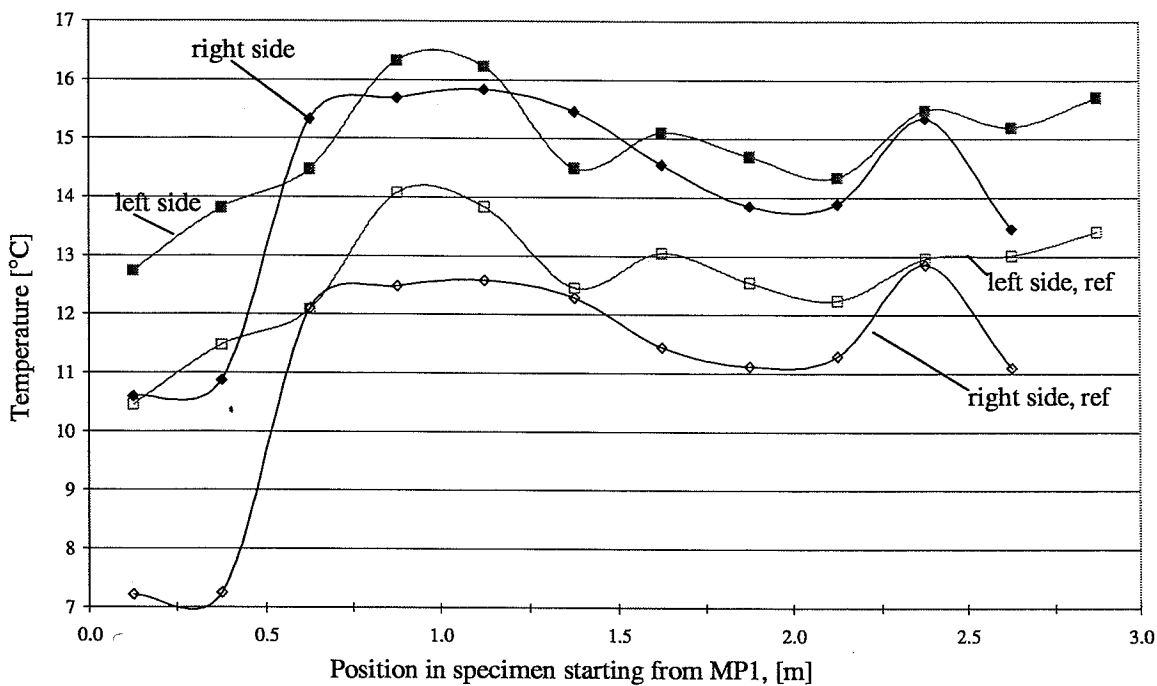
Figure 5.17: Fibre glass (3): temperature profiles in the right and left sides of the specimen 0.2 m above the measuring plates with a specimen thickness of 0.4 m and a surface temperature difference of 40°C. "ref" signifies the measurement made in the horizontal reference position.

59

Comments on results

The average Nusselt number in the position with heat flow upwards becomes 0.99 which concurs with the theory even though the measured heat flow pattern differs notably from unity near the edges. When regarding the temperature profile in the centre of the specimen, it is apparent that big variations have occurred in the thermal conductivity in both directions of the inserted specimen, and that the biggest deviations exist near the edges. The variations in thermal conductivity are caused by density variations in the inserted specimen. As the specimen contains loose fibres without any binder, it is difficult to ensure a homogeneous density when the specimen is located in the apparatus. Furthermore, the specimen, or part of it, may have moved in the apparatus when the position was changed. This may also explain the big deviation from unity at the edges in the heat flow pattern as the guard regulation of GR1 has worked quite appropriately in the horizontal measurements on fibre glass (3). When measuring stone wool (1) in the horizontal positions, the maximum observed difference in temperature across the specimen was 0.8°C, whereas the maximum difference in fibre glass (3) reached 4.2°C 0.2 m above the measuring plates.

Comparing the temperature profiles in the two horizontal positions, the temperatures in the reference position are consistently lower than the temperature in the position with heat flow upwards. The surface temperature difference was 38.8°C when the reference position was measured. When measuring the position with heat flow upwards, the surface temperature difference was reduced to 36.3°C in order to achieve stable temperature conditions in the cold box in spite of other activities in the laboratory. Correcting the temperatures according to the difference in surface temperature, and assuming that the average temperature profile is linear, the remaining difference in temperatures between the two horizontal positions at x=0.2 m becomes 1.35°C and signifies that the distance between the thermocouples and the measuring plates has been increased by 16 mm when changing the position from measuring with heat flow upwards to the reference position. When measuring stone wool (1), the displacement of the thermocouples was assessed to be within 6-7 mm.

5.5   Summary

In this chapter the result of the experimental investigation is presented. The convection measurements have been performed on two fibrous materials one with a high and one with a low permeability. The results are presented as relative values obtained by comparing the measurements in the different positions to the measurements in the horizontal reference positions.

The regulation of a few guards sections has not worked as expected in the measurements, and has caused the measurements on single measuring plates to be disturbed in a different way in different measurements. The distortion from the poor regulation of the guards has been commented in relation to the actual measurements.

In spite of the poor regulation, the measured heat flow pattern in the vertical positions corresponds to the calculated heat flow pattern using numerical calculations. Minor deviations exist which are probably due to either anisotropy in the material properties and/or joints between the individual samples. In all the vertical positions measured, it was possible to detect distortion in the heat flow pattern similarly to the calculated distortion due to natural convection in the material even in the low permeable material and with a surface temperature

difference of 20°C only. However, the total heat flow throughout the specimen was only affected in the highly permeable material which also agrees with the result obtained by numerical calculations. Though, the measured increase in the total heat flow differs significantly in the two corresponding vertical positions. This leads to the concern that the specimen may have undertaken slide movements in the apparatus mainly in the measurement with the largest heat flow.

The measured temperature profiles in the material indicate that the way of ensuring contact between the specimen and the plywood cover has not been sufficient and may have caused a slide movement of the specimen in some of the measurements.

Even though, the measurements may have been disturbed by error in the apparatus or by the insufficient contact between the specimen and the plywood cover the main conclusions from the measurements seem to be reliable as the measured heat flow pattern and the calculated heat flow patterns corresponds quite well.

6.   Conclusion

The significance of natural convection to the total heat transfer has experimentally been examined on two fibrous materials with different permeability and thermal conductivity. The performed measurements are supported by numerical calculations.

The project was limited to investigating the effect of natural convection under the following conditions:

- "perfectly" installed material
- impermeable and isothermal boundaries
- measurements when the specimen is placed in both horizontal and vertical positions and in dimensions for building use.

For this purpose a newly designed convection apparatus has been built. The measuring area in the apparatus is 1·3 m², and a specimen thickness of 0.1 – 0.5 m can be measured. The boundary conditions are achieved by way of the apparatus design. Great attention has been paid to the placement of the specimens in the apparatus in order to perform measurements only on perfectly installed materials.

Both the measurements and the corresponding numerical calculations show a distinct convection-induced redistribution of the heat flow in the form of an increase in heat flow primarily through the lower part of the structure, and a decrease in heat flow primarily through the upper part of the structure. The redistribution of heat flows is obvious even at a specimen thickness of 0.2 m and a temperature difference of only 20°C. In the low-permeable material the redistribution of heat flow does not affect the average heat flow throughout the specimen. Whereas, in the highly permeable material a convection-induced increase in the total heat flow of 7% and 17% was measured in two measurements presumed to be equal. Realising that convection occurs even in "perfectly" installed materials with low permeability, impermeable boundaries and even at low temperature differences means that the precondition applied for practical use, neglecting natural convection, is not fulfilled even when the most favourable conditions are applied.

In the performed numerical calculations it is possible to presuppose a perfectly installed material with constant direction-dependent properties. Thus, the numerical calculations compared with the measurements performed give a good impression of how variations in the material properties influence the distribution of heat flows in the material.

The measuring principle in the convection apparatus using a three-dimensional guard system was found suitable for measuring one-dimensional heat flow on large material dimension. The performance of the convection apparatus has been verified on an impermeable material; when measuring a specimen thickness of 0.5 m a good correlation was found to measurements carried out in a heat flow meter apparatus on specimens of 0.1 m thickness.

When performance testing the apparatus, problems in controlling a few guard sections were found. The method chosen for solving this problem proved not to be optimal during the measurements. The significance of the problem in relation to the performed measurements has been analysed and discussed in the report.

The measurements performed indicate that it is very difficult to obtain "perfection" when installing the specimen in the convection apparatus due to the material itself and the specimen volume measured. The measurements in some cases indicate differences in density and permeability within the specimen, which are partly caused by variations in the material itself, and partly by the way the specimen is arranged in the apparatus. When measuring in the horizontal reference position there are signs of the underlying material being compressed, which means that the existence of minor air cracks within the specimen cannot be rejected.

6.1 Recommendations for further work

On the basis of the performed investigation it must be recommended to include convection in the building legislation and in the international standards. The effect of convection in building structures is more significant than the results found in this project, due to the fact that "perfectly" installed insulation materials do not exist in building structures. Convection could be taken into consideration by correcting the design value of the thermal conductivity of the insulation materials with respect to; the permeability of the material, the applied material thickness, the design temperatures, and the family of insulation material used – the family of insulation material influence the risk of creating gaps in the insulated structure.

The agreement between the measurement performed in this project and the numerical calculations shows that theoretically it is possible to calculate a correction factor concerning the material properties, dimensions and temperatures. However, the influence of convection when the materials contain gaps and the material-dependent risk of gaps in the insulated structure need to be investigated further.

In this project the attention has been focused on how natural convection influences the heat flow distribution in fibrous materials. A further investigation should go further into how interrelated conditions might influence materials and structures, such as moisture which is transferred within the structure together with air movements, how the big temperature differences affect the comfort, and how thermal bridges affects the conditions for convection to take place.

6.2 Commercial perspective

Behind this project were four commercial perspectives:

- to strengthen the Danish research in the area of buildings physics

- to create new collaboration contacts for future projects – national as well as international

- to investigate the effect of natural convection when the material properties approach the limits

- to acquire knowledge of the different heat transport mechanisms to be used in future research for improving the thermal properties of fibrous materials used in the building sector.

The research in the area of natural convection has been initiated in Denmark through this project. At the Department of Building and Energy a new apparatus has been built which will be used in future projects to assess the effects of natural convection in different types of insulation products.

In the project a valuable collaboration has been established with other universities - mainly in the Nordic countries. This will continue after the project.

The results gained in the scientific part of the project are described in the main conclusions in part I and part II, respectively. The knowledge gained through this project will be used by the companies involved in the project in their future research concerning the thermal properties of fibrous materials.

Bibliography – Part I

Bankvall C., "Natural Convective Heat Transfer in Insulated Structures". Report 38, University of Lund, 1972.

Bankvall C., "Natural convective heat transfer in permeable insulation". SP-Report 1977:16, Swedish National Testing and Research Institute.

Bhattacharyya R. K., " Heat-Transfer Model for Fibrous Insulation", Thermal Insulation Performance, ASTM STP 718, American Society for Testing and Materials, pp. 272-286, 1980.

Blomberg T., "Heat Conduction in Two and Three Dimensions, Computer Modelling of Building Physics Applications". Report TVBH-1008, Dept. of Building Physics, University of Lund, May 1996.

Bomberg M. and Klarsfeld S., "Semi-Empirical Model of Heat Transfer in Dry Mineral Fiber Insulations". *Jour. of THERMAL INSULATION*, Vol. 6, 1983.

Castinel G., Combarnous, M.,"Natural convection in an anisotropic porous layer". *Rev. Gén. Therm.* 168, pp. 937-947, 1975. English translation, *Int. Chem. Eng.* Vol. 17, pp. 605-614, 1977.

Claesson J., Hagentoft C. E., "*Basic Building Physics. Mathematical Modelling*". Dept. of Building Physics, University of Lund, June 94.

Cheng P., "Heat Transfer in Geothermal Systems". Advances in Heat Transfer, Vol. 14, pp. 1-105, 1978.

Dyrbøl S., "Convection apparatus - documentation". Report SR-9814, Dept. of Buildings and Energy, Technical University of Denmark, 1998. (only available in Danish)

Epherre J. F., "Critère d'apparition de la convection naturelle dans une couche poreuse anisotrope". *Revue Génerale de Termique* No.14, pp. 949-950, 1975.

Fryklund P., "Computer Investigations on Heat Transfer in Loose-Fill Attic Insulation". Report 870 R-95:5, Dept. of Building Physics, Chalmers University of Technology, Göteborg 1995.

Fournier D. Klarsfeld S., "Heat Transmission Measurements in Thermal Insualtions". ASTM STP 544, American Society for Testing and Materials, pp. 223-242, 1974.

Hagentoft C. E., Serkitjis M., " Simplified Simulation Models for Natural and Forced Convection in Porous Media". Int. symposium on moisture problems in building walls, Porto - Portugal, pp. 339-350. R-95:8, CTH, Department of Building Physics, Göteborg, Sweden, 1995.

Horton C. W., Rogers F.T., "Convection currents in a porous medium". *Jour. of Appl. Physics*, Vol. 16, No. 6, pp. 367-369, 1945.

65

ISO 8301:1991(E), "*Thermal Insulation – Determination of steady-state thermal resistance and related properties – Heat flow meter apparatus*". International Standard.

ISO 8302:1991(E), "*Thermal Insulation – Determination of steady-state thermal resistance and related properties – Guarded hot plate apparatus*". International Standard.

ISO 9053:1991(E), "*Acoustics – Materials for acoustical applications – Determination of airflow resistance*". International Standard.

ISO, 1995, "*Guide to the expression of uncertainty in measurement*". International Organization for Standardization.

Johansson I., "*Mätvärdesanalys, del 1, Mätteknikens principer*". Chalmers Tekniska Högskola, Göteborg, 1988.

Karsfeld S. M., "Champs de température associés aux mouvements de convection naturelle dans un milieu poreux limité". *Revue Général de Termique*, No. 108, pp.1403-1423, 1970.

Kumaran M. K., "Heat, Air and Moisture Transfer in Insulated Envelope Parts", Final Report, Volume 3, Task 3: Material Properties. Energy Conservation in Buildings and Community Systems Programme, 1996.

Kvernvold O., Tyvand P. A.,"Nonlinear thermal convection in anisotropic porous media". *J. Fluid Mech.* 90, pp. 609-624,1979.

Langlais C., Arquis E., McCaa D. J., "A theoretical and Experimental Study of Convective Effects in Loose-Fill Thermal Insulation". Insulation Materials, Testing and Applications, ASTM STP 1030, American Society for Testing and Materials, pp. 290-318, 1990.

Lapwood, E.R., "Convection of a fluid in a porous medium". Proceedings, Chambridge Philosophical Society, Vol. 14 (McKibbin angiver vol. 44), pp. 508-521,1948.

McKibbin R., " Thermal Convection in layered and anisotropic porous media: a review". Convective Flows in Porous Media. Dept. Sci. Indust. Res., Wellington, New Zealand pp. 113-127, 1985.

McKibbin R., " Thermal Convection in a Porous Layer: Effects of Anisotropy and Surface Boundary Conditions". *Transport in Porous Media* 1, pp.271-292, 1986.

Nield D. A.,"Onset of thermohaline convection in a porous medium". *Water Resources Res.* 11, pp. 553-560, 1968.

Nield D. A., Bejan A., "*Convection in Posous Media*". Springer-Verlag New York Inc, 1992.

Nielsen T. R., "Apparat til måling af konvektion i isolering". Department of Buildings and Energy, Technical University of Denmark, 1997. (only available in Danish)

Serkitjis M., " Natural convection heat transfer in a horizontal thermal insulation layer underlying an air layer". Ph.d.- thesis, Dept. of Building Physics, Chalmers University of Technology, Sweden 1995.

Silberstein A., Langlais C., Arquis E., "Natural Convection in Light Fibrous Insulating Materials with Permeable Interfaces: Onset Criteria and Its Effect on the Thermal Performances of the Product". *Journal of Thermal Insulation.* Vol. 14, pp. 22-42, July 1990.

Svendsen S.A., and Dyrbøl S., "Facility for measuring the apparent thermal conductivity of mineral wool insulation under conditions typical for use in buildings", Eurotherm seminar N° 44, Portugal, 1995.

Wilkes K.E., Wendt R. L., Delmas A. Childs P.W., " Thermal Performance of One Loose-Fill Fiberglass Attic Insulation". Insulation materials: Testing and Applications, 2nd Volume. ASTM STP 1116, American Society for Testing and Materials, pp. 275-291, 1991.

Wolf S., "A Theory for the Effects of Convective Air Flow through Fibrous Thermal Insulation". Presented at ASHRAE 73rd Annual Meeting Toronto, 1966.

Appendix A

Error analysis of convection apparatus

Error in measurement can be divided into systematic errors and random errors. Systematic error is the type of error which occurs with the same size and in the same direction in all the measurements e.g. if the balance shows 1% too little, the same error will occur in all the measurements. The "random" dispersion in measurements depends on the type of measurement and on the way that the reproducibility is performed. The "random" dispersion can either be an expression of real fluctuations in the materials, or a random error in the measurement. In the actual study relative measurements have been performed, and effects of systematic error can be ignored. The maximum systematic error is considered in the following in order to get an impression of the ability of the apparatus to perform absolute measurements.

The estimated maximum error can be expressed according to eq. (5.5), (ISO, 1995 and Johansson, 1988):

$$\Delta F_{max} = \sum_{i=1}^{n} \left| \frac{\partial F}{\partial x_i} \cdot \Delta x_i \right| \tag{a.1}$$

in which Δx_i is the error in determining the parameter x_i in the expression of the measured value. The maximum relative error in the measurement of thermal conductivity can then be found as the sum of the relative errors in each parameter eq. (5.6).

$$\frac{\Delta \lambda_{max}}{\lambda} = \left| \frac{\partial (\frac{\Phi \cdot d}{A \cdot \Delta T})}{\partial \Phi} \cdot \frac{\Delta \Phi}{\lambda} \right| + \ldots\ldots\ldots = \left| \frac{\Delta \Phi}{\Phi} \right| + \left| \frac{\Delta d}{d} \right| + \left| \frac{\Delta A}{A} \right| + \left| \frac{\Delta (\Delta T)}{\Delta T} \right| \tag{a.2}$$

in which

$\Delta \Phi$	= error in measuring the heat flow
Δd	= error in the measured thickness
ΔA	= error in measuring the measuring area
$\Delta (\Delta T)$	= error in measured temperature difference between the warm and cold side of the apparatus

As discussed by Serkitjis [1995], the term above contains different types of error and uncertainties, and a complete error analysis is very complex. The analysis presented below is based on certain simplifying assumptions, but it is still able to give a fairly good impression of the measuring accuracy of the apparatus.

68

A.1 Error in heat flow, $\Delta\Phi$

Error in the heat flow, which is recorded during a measuring period, can be caused by:

- direct error in measuring the power supplied to the heating plates ($\Delta\Phi_1$)
- error from measuring heat flow to the guard side (($\Delta\Phi_{2a}$)) or to the bottom guard caused by a balance error ($\Delta\Phi_{2b}$)
- error from measuring boundary losses from the edge of the specimen ($\Delta\Phi_3$)
- disturbance from other activities in the laboratory or the surroundings ($\Delta\Phi_4$)

The four types of error, which may cause error in the heat flow, are considered as independent, and the summated error in the heat flow can be determined according to eq. (5.11:).

$$\Delta\Phi = \Delta\Phi_1 + \Delta\Phi_2 + \Delta\Phi_3 + \Delta\Phi_4 \qquad (a.3)$$

$\Delta\Phi_1$: Direct error in measuring the heat flow

Figure 5.7 shows a sketch of the principle of how the power supplied to the measuring plates is measured. Each measuring plate is connected with a known precision resistance $R_{resistance} = 1\Omega$ in order to achieve a high precision when measuring the current. The contributed effect on the measuring plates can be calculated from the relation in eq. (5.7).

$$\Phi = R_{MP} \cdot I_{meas}^2 = \left(\frac{U_{meas}}{I_{meas}} - R_{wire} - R_{resis\,tan\,ce} \right) \cdot I_{meas}^2 \qquad (a.4)$$

in which

|	
R_{MP}	= resistance of the coating on the measuring plate [Ω]
R_{wire}	= resistance of wire [Ω]
$R_{resistance}$	= resistance of precision resistance (1Ω)
U_{MP}	= potential difference across the measuring plate [V]
$U_{resistance}$	= potential difference across the precision resistance [V]
$U_{measured}$	= potential difference across the measuring plate, the precision resistance, and the wire [V]
I_{meas}	= current in the circuit [A]
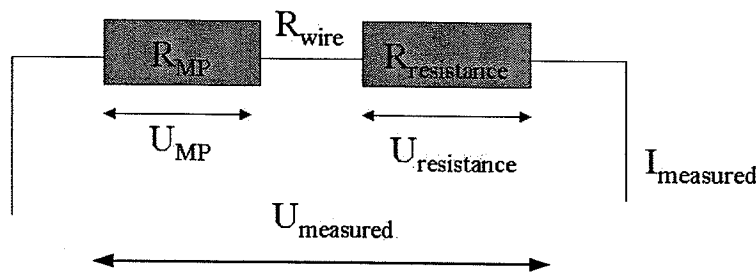
Figure A.1: Principle in measuring the power supplied to the measuring plates MP.

The resistance of the wire and the 1Ω resistance are measured within 1‰ at room temperature, the voltage is measured by the same measurement cards as the temperature with an error dependent on the signal of the voltage. The error of the current and the direct error in the measurement of the power have been evaluated using eq. (5.5). The error in measuring the power was found to be $\Delta\Phi_1 < \pm 0.1\%$.

$\Delta\Phi_{2a}$: Error due to measured heat flow to guard sides:

The main parts of the guard sides are balanced against four measuring plates as shown in chapter 4, figure 4.4. The measured temperature difference between the guard sides and the average of the corresponding measuring plates is usually within 0.1°C in a test period. In measurements without disturbance from air movements, the temperature distribution of the measuring plates is uniform within 0.1°C. With disturbance from air movements in the specimen, the temperature deviation in some cases reaches approx. $\pm$ 0.5°C from a uniform temperature distribution between four adjoining measuring plates. In this situation, the heat flow to the guard sides has been analysed by using HEAT2, which is a computer program for calculating two-dimensional heat transfer, Blomberg [1996].

The maximum relative error from the measured heat flow to the side guard occurs when the total heat flow throughout the specimen is small i.e. when the thickness is large and the temperature difference small. If the specimen is 0.5m thick; if the temperature on the hot side is 20°C and 0°C on the cold side; and if the temperature difference between the measuring plate and the balancing guard side is assumed to be 0.6°C, then the relative error from measuring the heat flow to the guard side becomes $\Delta\Phi_{2a} = \pm$ 1.5%. This equals the maximum deviation from the mean temperature of the four measuring plates and the maximum observed divergence in balance temperature. In this model, the distance between the measuring plate and the guard ring is assumed to be 0.005m and filled with stagnant air.

$\Delta\Phi_{2b}$: Error due to measured heat flow to the bottom guard:

When calculating the heat flow throughout the specimen, the heat flow from each measuring plate is compared with the calculated heat loss throughout the corresponding bottom guard section due to the temperature difference measured by the thermopile. If the temperature difference causes a heat loss throughout the bottom guard which exceeds $\pm$ 1% of the direct measured heat flow from the measuring plate, the measured heat flow is corrected in the calculation. This means that the maximum relative error from measuring heat flow to the bottom guard will not exceed $\Delta\Phi_{2b} = \pm$ 1%.

$\Delta\Phi_3$: Error due to boundary loss from the edge of the specimen:

To avoid boundary loss from the side of the specimen when thick specimens are measured, the apparatus has been constructed with side guards as shown in figure 4.7, so that it is possible to control the temperature at a distance of 0.25 m above the measuring plates. When the thickness of the specimen exceeds 200 mm, the side guards ensure a linear temperature distribution at the edges of the apparatus. When the specimen is 200 mm thick, or less, only the material of the side guards itself, which are made of 1 mm stainless steel with a thermal

conductivity of 15W/mK, will help achieving a linear temperature distribution around the edges of the apparatus. The boundary loss when measuring a 200 mm specimen with a temperature on the hot side of 20°C and of -10°C on the cold side has been analysed by HEAT2. The maximum error from measuring the boundary loss becomes $\Delta\Phi_3 = \pm\,0.2\%$.

$\Delta\Phi_4$: Disturbance from other activities

The cooling capacity of the cold box is influenced by other experimental arrangements using the cooling system. If the set point in the cold box is close to the limit temperature, the temperature control of the box is very sensitive to other activities.

In a few cases, disturbance in the measured power has been observed and it has not been possible to identify the reason. This is a known phenomenon in experimental arrangements if the electrical part of the arrangement has not been isolated from the rest of the laboratory. This type of error is not included in the systematic error.

A.2   Error in the measured thickness

The thickness of the specimen installed in the apparatus is measured by using a thickness gauge with fixed reference points as an average over 24 points evenly distributed over the surface of the total measuring area. The error in the thickness measurement can fluctuate with the apparatus, the measurement, and the specimen. The planeness of the measuring plates installed in the apparatus affects the error in measuring the thickness, as a few plates differ by up to 1 mm. When determining the maximum error, the error from the fluctuation across the surface including the error from the planeness of the measuring plates has been considered, as this is found to be the main factor. In the performed measurements, the maximum error caused by the uncertainty in the measured thickness was found to be within $\Delta d/d = \pm\,2\%$. The relative error decreases with the thickness of the inserted specimen.

A.3   Error in measuring the measuring area

The area of the measuring plates is only measured once, and this error remains the same regardless of test run and specimen. Assuming the observation error to be within $\pm\,0.5$ mm, the relative error in eq. (5.6) of determining the measuring area become:

$$\frac{\Delta A}{A} = \frac{\Delta l}{l} + \frac{\Delta b}{b} = \frac{0.0005}{1} + \frac{0.0005}{0.25} = \pm 0.25\%$$

A.4   Error in measured temperature difference

The temperature difference between the warm and cold side of the apparatus is calculated on basis of the surface temperatures measured on each side of the specimen. The surface temperatures are recorded by thermocouples (Cu/Cu-Ni) which are arranged as illustrated in figure 4.4. In the apparatus, the thermocouples on the warm side are taped to the glass plates and on the cold side to the test specimen, which is covered with impermeable plywood, in both cases along an isotherm. The location of the thermocouples ensures that neither the

surface resistance nor the conductivity of the thermocouple wire will disturb the measurement.

The possible errors remaining when determining the surface temperatures could either be an erroneous reference temperature in the used measurement cards (Schlumberger), or minor fluctuations in the thermocouples. In order to eliminate fluctuations between the thermocouples, all the thermocouples have been produced from the same wire. The temperature measurements from all the thermocouples were checked while the apparatus was in thermal equilibrium with the surroundings, and there was no sign of error in the reference temperature of the measurement cards.

The thermocouple wires (10 elements) were calibrated with an extra measurement card at 0°C and 20°C with an average deviation of -0.15°C and -0.06°C, respectively. On basis of the performed investigation, the error in the averaged value of the two temperatures used for measuring the hot and cold side of the specimen is considered to be within ± 0.15°C each i.e. the error in measuring the temperature difference becomes ± 0.3°C. If a temperature difference of 20°C is applied, the maximum relative error in determining the temperature difference in eq.(5.6 becomes $\Delta T/T = \pm 1.5\%$.

The estimated maximum error:

From the evaluation above, the maximum error in measuring the thermal conductivity in the convection apparatus becomes:

$$\frac{\Delta\lambda_{max}}{\lambda} = (0.1\% + 1.5\% + 1.0\% + 0.2\%) + 2\% + 0.5\% + 1.5\% = \pm 6.8\% \qquad (a.5)$$

Appendix B

Placement of guard sections in convection apparatus:

Left diagram labels:

Top: GSR9   GSR1   GSR10

GR4	GR1	GR10
GR8	MP1 / MP2 / MP3 / MP4	GR2
GR7	MP5 / MP6 / MP7 / MP8	GR3
GR6	MP9 / MP10 / MP11 / MP12	GR4
GR12	GR5	GR11

Left side (top to bottom): GSR8, GSR7, GSR6
Right side (top to bottom): GSR2, GSR3, GSR4

Bottom: GSR12   GSR5   GSR11

Right diagram labels:

Top: GSB9   GSB1   GSB10

GB9	GB8
GB18	GB2
GB3	GB4
GB5	GB6
GB9	GB10

Left side (top to bottom): GSB8, GSB7, GSB6
Right side (top to bottom): GSB2, GSB3, GSB4

Bottom: GSB12   GSB5   GSB11

Figure B.1: Plane section in convection apparatus.

MP1-12   = Measuring plate 1-12

GR1-12   = Guard ring 1-12

GSR1-12 = Guard side ring 1-12
(Heating bands which are balanced
against the guard ring)

GB1-10 = Guard bottom 1-10

GSB1-12 = Guard side bottom
(Heating bands which are
balanced against the bottom
guards)

73

Placement of the heating bands:
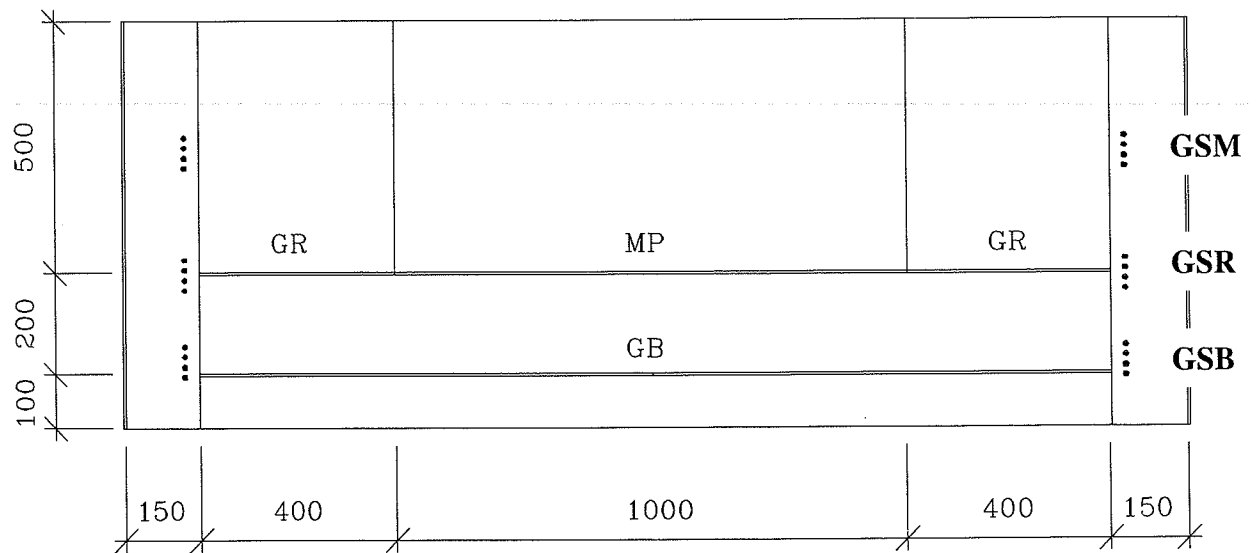
Figure B.2: Cross section in convection apparatus.

GSM = Guard side middle - this heating band is placed 0.25 m above the measuring plates.
GSR = Guard side ring
GSB = Guard side bottom

Appendix C

Results of convection measurement performed

This appendix contains the results of the measurements performed in the convection apparatus. The results are presented as thermal conductivity measured at the individual sections within the apparatus, together with the local Nusselt numbers calculated on the basis of the measurements performed according to eq. (5.2).

An overview of the results given on the following pages is shown in the table below. The numbers in the bracket signifies the page number on which the result can be found.

Table C.1: Overview – measurements, which have been performed within the time limit of the project. The numbers in () signifies the page number on which the result can be found.

Material	Surface temp. diff.	Surface temperature		Position of apparatus						
				Vertical					Horizontal heat flow upwards	
				h/d = 6		h/d=7.5		h/d=15		
	ΔT [°C]	T_{hot} [°C]	T_{cold} [°C]	MP1 on top	MP12 on top	MP1 on top	MP12 on top	MP1 on top	d=0.4m	d=0.5 m
Stone wool (1)	20	20	0	x (76)	x (76)			x (79)		x (76)
Stone wool (1)	30	20	-10	x (77)	x (77)			x (80)		x (77)
Stone wool (1)	40	30	-10	x (78)	x (78)					x (78)
Fibre glass (3)	40	30	-10			x (81)	x (81)		x (81)	

Product: stone wool (1)
h/d = 6 (specimen thickness = 0.5 m)
Surface temperature difference = 20 °C

Thermal conductivity, λ_{10}

Position	Horizontal reference $\lambda_{9.4}$ (20)	Horizontal heat flow upwards $\lambda_{9.6}$ (22)	Local Nu_i (22)	Vertical MP1 on top $\lambda_{9.7}$ (19)	Local Nu_i (19)	Vertical MP12 on top $\lambda_{9.8}$ (21)	Local Nu_i (21)
	W/m·K	W/m·K		W/m·K		W/m·K	
MP1	0.0404	0.0385	0.95	0.0323	0.80	0.0465	1.15
MP2	0.0343	0.0332	0.97	0.0308	0.90	0.0368	1.07
MP3	0.0371	0.0364	0.98	0.0361	0.97	0.0375	1.01
MP4	0.0343	0.0338	0.99	0.0346	1.01	0.0341	0.99
MP5	0.0374	0.0364	0.97	0.0383	1.02	0.0363	0.97
MP6	0.0359	0.0350	0.97	0.0381	1.06	0.0341	0.95
MP7	0.0363	0.0349	0.96	0.0368	1.01	0.0353	0.97
MP8	0.0363	0.0350	0.96	0.0367	1.01	0.0357	0.98
MP9	0.0360	0.0352	0.98	0.0375	1.04	0.0351	0.97
MP10	0.0373	0.0366	0.98	0.0407	1.09	0.0342	0.92
MP11	0.0365	0.0364	1.00	0.0395	1.08	0.0343	0.94
MP12	0.0353	0.0349	0.99	0.0384	1.09	0.0331	0.94
Mean	0.0364	0.0355	0.98*	0.0366	1.01*	0.0361	0.99*

Measured mean temperatures, [°C]

Thot	20.0	20.0		20.0		20.0	
Tcold	-1.3	-0.8		-0.5		-0.5	

* calculated according to eq. (5.3)

Product: stone wool (1)
h/d = 6 (specimen thickness = 0.5 m)
Surface temperature difference = 30°C

Thermal conductivity, λ_5

Position	Horizontal reference		Horizontal heat flow upwards		Local Nu_i average	Vertical MP1 on top	Local Nu_i	Vertical MP12 on top	Local Nu_i
	$\lambda_{4.9}$ (11)	$\lambda_{4.9}$ (13)	$\lambda_{5.2}$ (9)	$\lambda_{5.1}$ (14)	(9,14)	$\lambda_{4.7}$ (10)	(10)	$\lambda_{5.3}$ (12)	(12)
	W/m·K		W/m·K			W/m·K		W/m·K	
MP1	0.0393	0.0401	0.0378	0.0371	0.94	0.0268	0.68	0.0509	1.28
MP2	0.0337	0.0340	0.0328	0.0324	0.96	0.0290	0.86	0.0385	1.14
MP3	0.0360	0.0364	0.0356	0.0353	0.98	0.0348	0.96	0.0377	1.04
MP4	0.0335	0.0338	0.0333	0.0330	0.98	0.0341	1.01	0.0337	1.00
MP5	0.0364	0.0367	0.0355	0.0352	0.97	0.0379	1.04	0.0355	0.97
MP6	0.0349	0.0352	0.0341	0.0338	0.97	0.0384	1.10	0.0330	0.94
MP7	0.0353	0.0356	0.0339	0.0336	0.95	0.0362	1.02	0.0346	0.98
MP8	0.0355	0.0358	0.0341	0.0338	0.95	0.0367	1.03	0.0353	0.99
MP9	0.0351	0.0355	0.0342	0.0340	0.97	0.0379	1.07	0.0338	0.96
MP10	0.0361	0.0365	0.0356	0.0354	0.98	0.0425	1.17	0.0319	0.88
MP11	0.0353	0.0356	0.0355	0.0353	1.00	0.0412	1.16	0.0320	0.90
MP12	0.0345	0.0350	0.0346	0.0344	0.99	0.0408	1.17	0.0307	0.89
Mean	0.0355	0.0358	0.0348	0.0345	0.97*	0.0363	1.02*	0.0356	1.00*

Measured mean temperatures, [°C]

	$\lambda_{4.9}$ (11)	$\lambda_{4.9}$ (13)	$\lambda_{5.2}$ (9)	$\lambda_{5.1}$ (14)		$\lambda_{4.7}$ (10)		$\lambda_{5.3}$ (12)	
T_{hot}	20.0	20.0	20.0	20.0		20.0		20.0	
T_{cold}	-10.3	-10.3	-9.7	-9.7		-10.6		-9.5	

* calculated according to eq. (5.3)

77

Product: stone wool (1)
h/d = 6 (specimen thickness = 0.5 m)
Surface temperature difference = 40°C

Thermal conductivity, λ_{10}

Position	Horizontal reference $\lambda_{9,9}$ (17)	Horizontal heat flow upwards $\lambda_{10,3}$ (15)	Local Nu_i (15)	Vertical MP1 on top $\lambda_{9,7}$ (18)	Local Nu_i (18)	Vertical MP12 on top $\lambda_{10,3}$ (16)	Local Nu_i (16)
	W/m·K	W/m·K		W/m·K		W/m·K	
MP1	0.0409	0.0378	0.93	0.0260	0.64	0.0546	1.34
MP2	0.0352	0.0334	0.95	0.0292	0.83	0.0408	1.16
MP3	0.0376	0.0359	0.96	0.0351	0.93	0.0392	1.04
MP4	0.0351	0.0338	0.96	0.0352	1.00	0.0347	0.99
MP5	0.0379	0.0359	0.95	0.0387	1.02	0.0368	0.97
MP6	0.0364	0.0344	0.95	0.0394	1.08	0.0341	0.94
MP7	0.0368	0.0345	0.94	0.0363	0.99	0.0357	0.97
MP8	0.0370	0.0347	0.94	0.0372	1.01	0.0363	0.98
MP9	0.0368	0.0349	0.95	0.0389	1.06	0.0347	0.94
MP10	0.0376	0.0359	0.96	0.0441	1.17	0.0322	0.86
MP11	0.0368	0.0360	0.98	0.0435	1.18	0.0320	0.87
MP12	0.0364	0.0352	0.97	0.0439	1.21	0.0309	0.85
Mean	0.0370	0.0352	0.95*	0.0373	1.01*	0.0368	0.99*

Measured mean temperatures, [°C]

T_{hot}	30.0	30.0		30.0		30.0	
T_{cold}	-10.2	-9.5		-10.6		-9.4	

*calculated according to eq. (5.3)

Product: stone wool (1)
h/d = 15 (specimen thickness = 0.2 m)
Surface temperature difference = 20°C

Thermal conductivity, λ_{10}

Position	Horizontal reference λ_{10} (5)	Local Nu_i	Heat flow ratio	Vertical MP1 on top $\lambda_{9,8}$ (6)	Local Nu_i (6)	Vertical MP12 on top	Local Nu_i
	W/m·K	W/m·K		W/m·K		W/m·K	
MP1	0.0368			0.0303	0.82		
MP2	0.0354			0.0345	0.97		
MP3	0.0369			0.0377	1.02		
MP4	0.0349			0.0375	1.07		
MP5	0.0365			0.0388	1.06		
MP6	0.0358			0.0378	1.06		
MP7	0.0361			0.0352	0.98		
MP8	0.0356			0.0353	0.99		
MP9	0.0354			0.0359	1.01		
MP10	0.0357			0.0389	1.09		
MP11	0.0354			0.0371	1.05		
MP12	0.0351			0.0359	1.02		
Mean	0.0358			0.0362	1.01*		

Measured mean temperatures, [°C]

T_{hot}	20.0	20.0
T_{cold}	0.0	-0.5

* calculated according to eq. (5.3)

Product: stone wool (1)
h/d = 15 (thickness = 0.2 m)
Surface temperature difference = 30°C

Thermal conductivity, λ_5

Position	Horizontal reference $\lambda_{5,2}$ (8)	Horizontal heat flow upwards	Local Nu_i	Vertical MP1 on top $\lambda_{5,1}$ (7)	Local Nu_i (7)	Vertical MP12 on top	Local Nu_i
	W/m·K	W/m·K		W/m·K		W/m·K	
MP1	0.0396			0.0272	0.69		
MP2	0.0348			0.0342	0.98		
MP3	0.0362			0.0380	1.05		
MP4	0.0339			0.0384	1.13		
MP5	0.0358			0.0391	1.09		
MP6	0.0351			0.0380	1.08		
MP7	0.0357			0.0343	0.96		
MP8	0.0353			0.0349	0.99		
MP9	0.0350			0.0357	1.02		
MP10	0.0352			0.0385	1.09		
MP11	0.0348			0.0373	1.07		
MP12	0.0349			0.0357	1.02		
Mean	0.0355			0.0359	1.01*		

Measured mean temperatures, [°C]

T_{hot}	20.0	20.0
T_{cold}	-9.6	-9.9

* calculated according to eq.(5.3)

Product: fibre glass (3)
h/d = 7.5 (specimen thickness = 0.4 m)
Surface temperature difference = 40°C

Thermal conductivity, λ_{10}

Position	Horizontal reference $\lambda_{10.6}$ (32)	Horizontal heat flow upwards $\lambda_{11.8}$ (30)	Local Nu_i (30)	Vertical MP1 on top $\lambda_{10.5}$ (34)	Local Nu_i (34)	Vertical MP12 on top $\lambda_{11.1}$ (33)	Local Nu_i (33)
	W/m·K	W/m·K		W/m·K		W/m·K	
MP1	0.0483	0.0516	1.07	0.0231	0.48	0.1102	2.28
MP2	0.0409	0.0391	0.95	0.0305	0.74	0.0676	1.65
MP3	0.0469	0.0476	1.01	0.0430	0.92	0.0652	1.39
MP4	0.0442	0.0457	1.03	0.0445	1.01	0.0502	1.14
MP5	0.0479	0.0483	1.01	0.0472	0.99	0.0581	1.21
MP6	0.0481	0.0489	1.02	0.0495	1.03	0.0534	1.11
MP7	0.0463	0.0462	1.00	0.0487	1.05	0.0473	1.02
MP8	0.0469	0.0466	0.99	0.0500	1.06	0.0461	0.98
MP9	0.0475	0.0469	0.99	0.0505	1.06	0.0472	0.99
MP10	0.0504	0.0480	0.95	0.0621	1.23	0.0463	0.92
MP11	0.0469	0.0447	0.95	0.0698	1.49	0.0353	0.75
MP12	0.0469	0.0428	0.91	0.0825	1.76	0.0276	0.59
Mean	0.0468	0.0464	0.99*	0.0501	1.07*	0.0546	1.17*

Measured mean temperatures, [°C]

T_{hot}	30.0	30.0		30.0		30	
T_{cold}	-8.8	-6.3		-9.0		-7.9	

* calculated according to eq.(5.3)

INSTITUT FOR BYGNINGER OG ENERGI

DANMARKS TEKNISKE UNIVERSITET

IBE